International Journal of Rock Mechanics & Mining Sciences 61 (2013) 31–42

Contents lists available at SciVerse ScienceDirect

International Journal of
Rock Mechanics & Mining Sciences

journal homepage: www.elsevier.com/locate/ijrmms

Empirical investigation and characterization of surface subsidence related to block cave mining

Kyu-Seok Woo [a,*], Erik Eberhardt [a], Davide Elmo [b], Doug Stead [c]

[a] Geological Engineering, University of British Columbia, Vancouver, Canada
[b] Golder Associates Ltd, Burnaby, Canada
[c] Department of Earth Science, Simon Fraser University, Burnaby, Canada

ARTICLE INFO

Article history:
Received 20 January 2012
Received in revised form
5 January 2013
Accepted 15 January 2013

Keywords:
Block caving
Empirical database
Subsidence
Undercut depth
Asymmetrical deformation

ABSTRACT

For guidance on relationships between caving depth and surface subsidence, a comprehensive database was developed after an exhaustive search of published data from cave mining operations from around the world. The distribution of data was found to largely focus on caving angles and macro deformations; very little empirical data exists on the extent and magnitudes of smaller surface displacements. The data clearly show that caving-induced surface deformations tend to be discontinuous and asymmetric due to large movements around the cave controlled by geologic structures, rock mass heterogeneity and topographic effects. The data also show that as undercut depth increases for a given extraction volume, the magnitude and extent of the caved zone on surface decreases. However, numerical modeling indicates that this is only the case for macro deformations and the extent of smaller displacements actually increases as a function of undercut depth. The results presented caution against relying on existing empirical design charts for estimates of caving-induced subsidence where small strain subsidence is of concern, as the data being relied upon does not properly extrapolate beyond the macro deformations (i.e., caving angles) that make up the majority of the observations. The findings also suggest that the extent and magnitudes of subsidence may be underestimated if the analysis adopted neglects the influence of geological structures and assumes symmetrical surface displacements above the undercut.

1. Introduction

Block caving is increasingly being favored as a mining method for maximizing net present value (NPV) from large, lower grade ore bodies, especially as companies target deeper resources or transition underground from open pits that have reached the end of their mine life. As a mass mining method, block caving results in significant ground collapse and extensive surface deformations. Yet despite having been in use for more than 100 years, there has been limited research conducted regarding the impact of caving on surface subsidence. Of concern is the locating of mine infrastructure on surface or the impact ground deformations may have on protected areas neighboring the mine property. Damage of surface infrastructure, together with increased dilution due to larger than expected caving angles, is often the cause for additional capital and operation expenditures.

To better understand and assess these potential geo-risks, a database has been developed based on a thorough review of public domain sources reporting subsidence values related to both historic and present-day cave mining operations (including block, panel and sub-level caving). Empirical databases provide a means to learn from case histories, discover causal relationships between different contributing factors, establish guidelines for design, and to help provide a starting point to undertake more sophisticated analyses like numerical modeling. One of the most commonly cited is Laubscher's method [1]. Laubscher proposed a design chart (Fig. 1) that relates the predicted cave angle to the rock mass quality (defined using the mining rock mass rating, or MRMR), density of the caved rock, height of the mined block and mine geometry (minimum and maximum span of a footprint). The resulting prediction by default assumes symmetry; i.e., the caving angle is equally projected from all points around the perimeter of the undercut. The application of Laubscher's method requires sound engineering judgment and a full consideration of the geological and geotechnical setting in which it is being applied.

The caving angle referred to by Laubscher is defined by Van As et al. [2] as the angle of the line extending from the edge of the

* Correspondence to: AMC Mining Consultants (Canada) Ltd., Suite 1330, 200 Granville Street, Vancouver, BC, Canada, V6C 1S4. Tel.: +1 778 228 2919; fax: +1 604 669 1120.
E-mail addresses: kyuseokwoo@gmail.com, kwoo@amcconsultants.com (K.-S. Woo).

1365-1609/$ - see front matter © 2013 Elsevier Ltd. All rights reserved.
http://dx.doi.org/10.1016/j.ijrmms.2013.01.015

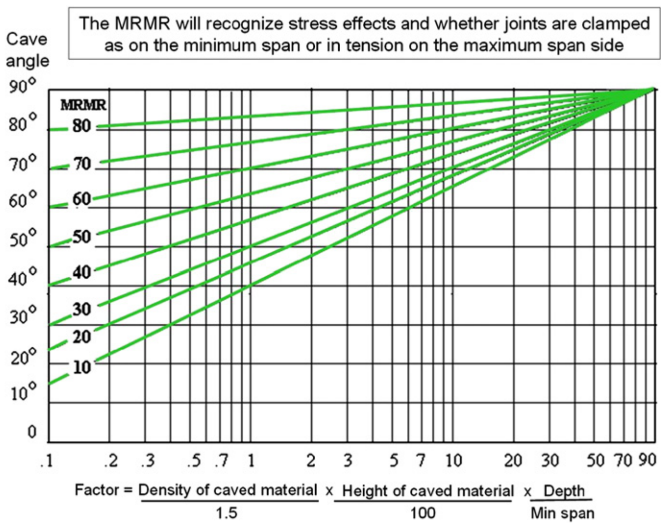

Fig. 1. Laubscher's empirical design chart for assessing cave angle (angle of break) as a function of mining rock mass rating (MRMR) value and the height and depth of the caved block (after [1]).

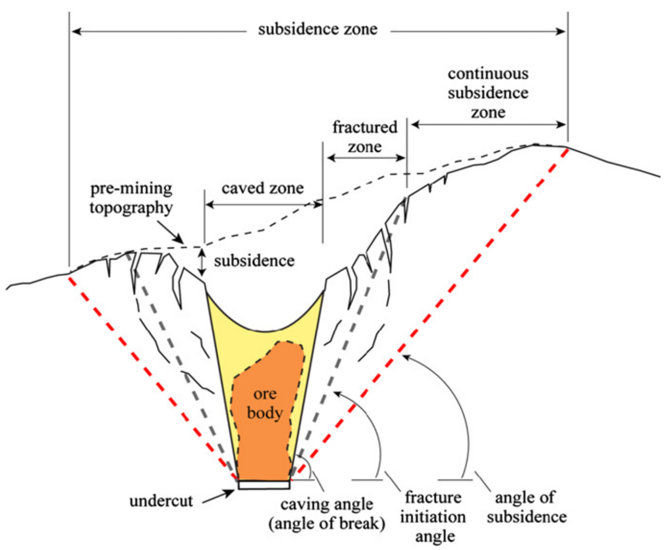

Fig. 2. Definition of block caving deformation zones as defined in [2].

extraction level to the edge of the zone of active caving (Fig. 2). The caved zone is usually located directly above the undercut footprint and thus is characterized as having the greatest surface disturbance, usually manifested as a crater filled with broken, irregular blocks. Van As et al. [2] also defined two further subsidence zones and corresponding angles: the fracture initiation angle and subsidence angle (Fig. 2). The fracture initiation angle is the angle measured from horizontal of the line extending from the edge of the extraction level to the edge of the zone of fracture (or zone of active movement). This zone encompasses all obvious surface deformations adjacent to the caved zone, typically characterized by large radial cracks and rotated and toppling blocks. The angle of subsidence marks the outer most zone and the limits of measurable surface deformations on surface. These are generally described as elastic or continuous non-elastic strains, with vertical displacements greater than 2 mm.

The empirical database presented here was developed to more fully examine the relationships between these zones of surface subsidence and depth of undercut, together with the key factors that influence them. Data relating to geology, topography, orebody type and undercut geometry were specifically targeted to analyze their effects in promoting asymmetry and discontinuous caving-induced subsidence. Where key relationships are revealed, illustrative numerical models are used to help draw conclusions to guide preliminary assessments during the planning stages of future new mining projects where surface subsidence is of concern.

2. The UBC block caving subsidence database

A thorough search of the published literature, university theses, and government reports (e.g., U.S. Bureau of Mines) [15–69] was carried out leading to a cave mine database for empirical analysis and characterization of caving-induced surface subsidence. The database is populated by more than 100 cave mining operations throughout the world including both historic mines that have ceased to operate and those still producing. A tabular format adopted for the database is designed to systematically display diverse basic information on a mine including its location, undercut depth and geology, combined with measurements related to macro-and micro-surface displacements. Although the study was primarily directed towards block and panel caving operations, data from sub-level caving operations were also collected.

2.1. General trends

Fig. 3 shows the breakdown of cave mines by continent, mining method, and resource mined. The majority of operations reported are North American (Fig. 3a), although these are mostly historic involving the iron mines of Michigan where the method was first developed, the copper mines of Arizona, and asbestos mines of Quebec. Currently developing or operating cave mines are more globally distributed between South America, Asia, Australia, Africa and North America. With respect to mining method, 62% of the cases involve block caving, with 19% using sub-level caving to adapt to steeply dipping orebodies of narrower width (Fig. 3b). Grouped with sub-level caving are mines that combined sub-level caving with similar methods like top slicing and shrinkage stoping. The reported use of two caving methods in tandem – block caving plus sub-level caving for example–were found where it was advantageous to optimize the operations relative to variations in the shape of the orebody. As for minerals produced by these mines (Fig. 3c), copper and gold form the majority at 29% and 15%, respectively, followed by asbestos (9%) and diamond (9%). The large number of copper-based caving operations reflects the favorability of block and panel caving for mining low-grade copper porphyry ore deposits.

Based on these data, two interesting trends are evident. Fig. 4 shows the changing trend in block heights being caved. Before 1950, block caving was typically applied to block heights between 20 and 100 m, employing multiple lifts of increasing depth where the height of the ore column was greater. However, this trend has transitioned to larger block heights exceeding 100 m to reduce development costs as confidence has been gained in draw sequencing practices that help minimize dilution by steering and maintaining cave propagation within the ore column. In step with increasing block heights being mined, undercut depths are similarly increasing. Fig. 5 shows the range of undercut depths prior to 1950 as being 100–300 m, gradually increasing to current depths of 600 m or deeper. Similarly, the size of the undercut (i.e., in plan view) has also increased as operations move towards developing large panel caves instead of smaller blocks.

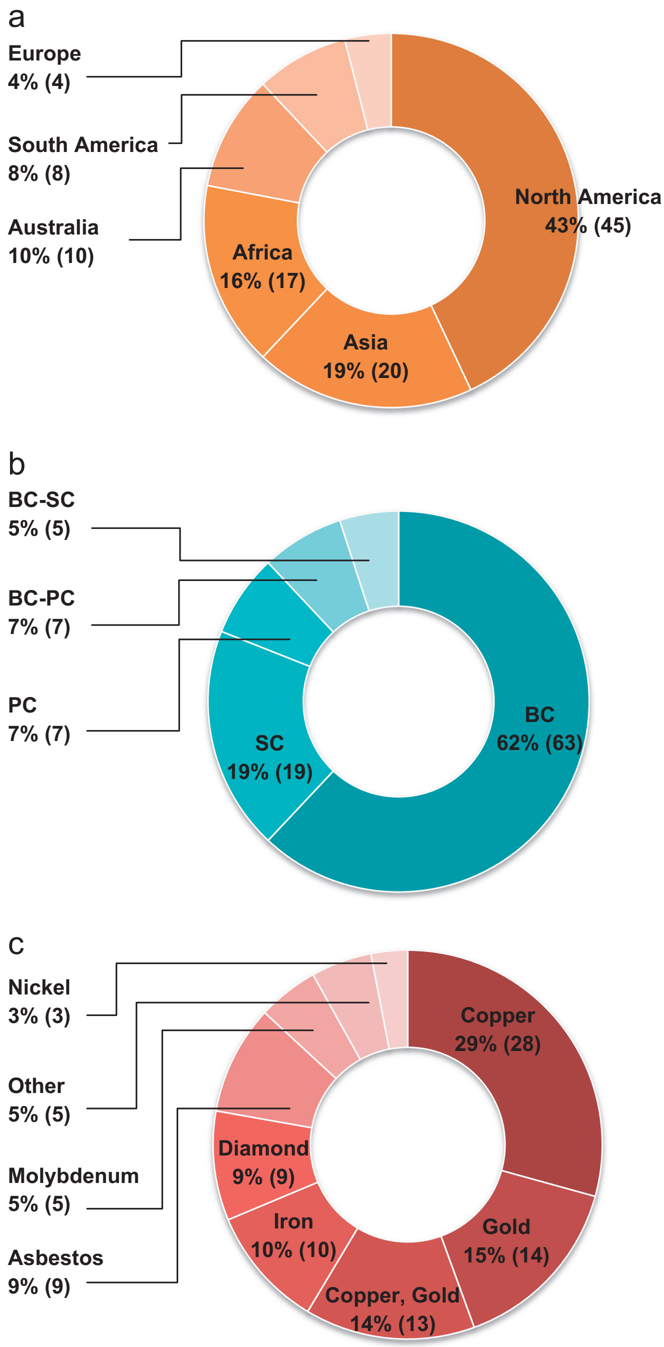

Fig. 3. General breakdown of cave mining data in database by: (a) regional distribution (b) mining method (BC=block cave, PC=panel cave, SC=sublevel cave), and (c) resource mined. Reported are the relative percentages followed by the total number of cases in parentheses. Symbols in each legend are ordered from highest percentage to lowest.

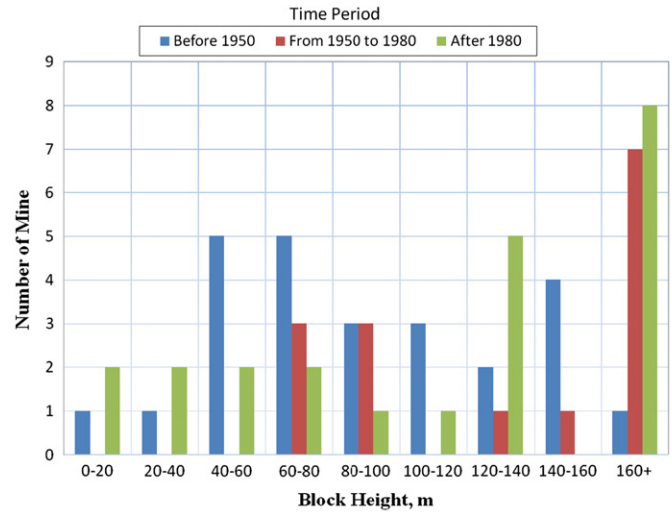

Fig. 4. Breakdown of block heights being mined for the block caving cases in the database, showing a trend towards the mining of larger blocks.

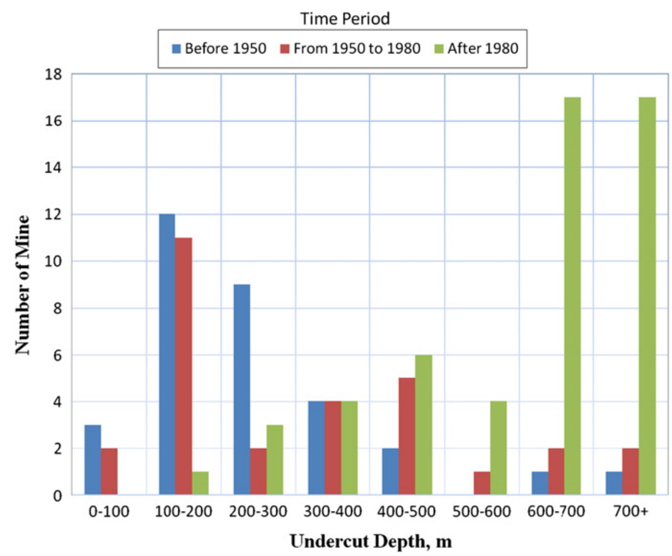

Fig. 5. Breakdown of undercut depths associated with the block caving cases in the database, showing a trend towards the development of deeper undercuts.

2.2. Caving-induced subsidence data

The use of block caving was first reported in 1895 in the Michigan iron and copper mines where large blocks of ore were undercut, allowing the ore to mine itself under gravity and crush through comminution to a size suitable for handling [3]. Soon after, the economic advantages gained by the method were being tempered by reports of its impact on surface and the need to better understand the factors controlling ground movements to help safeguard against property damage and loss of life [4]. Several detailed studies were carried out with these and other historic mines, but given the total number of mines populating the UBC database, those directly reporting subsidence measurements are actually few in number.

This is reflected in earlier databases on subsidence related to mass mining (Table 1). Flores and Karzulovic [5] carried out the first benchmark study as part of the international caving study stage II (ICS-II), citing 242 break angles measured at various depths from 11 block, panel and sub-level caving operations. Most of these involved operations that transitioned to underground from open pit mining. For scoping and prefeasibility use, they suggest typical caving angles of $>45^\circ$ and $>60^\circ$ for MRMR values <70 and >70, respectively. Van As et al. [2] systematically tabulated information for a number of mines including rock type, ore body dip, depth, caving angle, and angle of subsidence. Their treatment included 19 caving operations together with data from several stoping and room and pillar operations. A similar compilation was reported by Tetra Tech [6] providing caving angle and angle of draw (defined as 90° minus caving angle). They note that only 20% of the mines they reviewed experienced unexpected subsidence, with most anomalies arising from geologic structure such as faults.

Table 1
Comparison of previous databases reporting subsidence data for mass mining operations.

Mining method	Number of operations (total observations)			
	Flores and Karzulovic [5]	van As et al. [2]	Tetra Tech [6]	UBC Database
Block and panel caving	9 (229)	10 (15)	9 (9)	28 (47)
Sublevel caving/shrinkage stoping	1 (4)	7 (12)	10 (14)	16(49)
Open stope caving	–	1 (4)	2 (5)	–
Caving (unspecified)	–	1 (2)	3 (4)	–
Other stoping (sub-level, cut & fill)	–	4 (4)	4 (4)	–
Room and pillar	–	4 (5)	4 (4)	–
Unspecified	1 (9)	9 (16)	2 (2)	–
Total	11 (242)	36 (58)	34 (42)	44 (96)

Table 2
Comparison of caving angles reported in previous databases for block, panel, and sub-level caving operations. Caving angles greater than 90° indicates an overhanging condition where the extent of collapse on surface is smaller than the footprint of the undercut at depth.

Mining method	Caving angle range					
	Flores and Karzulovic [5]	van As et al. [2]		UBC Database		
	Break angle	Caving angle	Fracture initiation angle	Caving angle	Fracture initiation angle	Subsidence angle
Block caving	52–90	35–90	45–60	52–105	40–95	32–95
Panel caving	48–90	–	–	60–110	58–92	55
Sub-level caving	54–88	50–90	42	40–98	45–95	40–78

These existing databases were used as an initial starting point with each cited source (i.e., data observation) being consulted to independently review, confirm and extract additional data regarding caving angle asymmetry. One of the limiting factors of the previous databases is the consideration of only those sources that report subsidence data directly. This was seen to involve only 5% of the caving operations populating the UBC database. Closer inspection of the different published sources for each mine property revealed that in many cases, detailed cross-sections were provided that contained indirect information relating to the disturbance on surface caused by caving. In many cases, a caving angle could be measured from a scaled map or section and in some cases, a fracture initiation angle. The use of indirect data increased the number of mine properties accounted for to 44, with the number for block and panel caves (28) tripling those reported in previous databases. Furthermore, in several cases, multiple observations were provided for the same mine property, either for multiple blocks or different mine levels again almost doubling the number of data points considered (see totals in parentheses in Table 1).

Table 2 summarizes and compares the range of caving angles reported in the different studies as a function of mining method (block, panel and sub-level caving). The vast range in angles cited points to the significant variability present in the data owing to site specific differences between the individual cases making up each dataset. The influence of topography, geology and undercut depth are discussed in more detail in the following sections.

3. Database analysis: caving and fracture initiation angles

From the database, a subset of 47 direct and indirect subsidence observations were analyzed to determine the caving and fracture initiation angles for each. These are reported in Appendix A. References are provided for each data entry and a detailed background description for each is provided in Appendix B. Excluded from the analysis were those operations involving caving into a deep open pit. Where several angles are reported for different stages of cave development, only the greatest values (worst case) are reported. Emphasis was also placed on data provided in the form of cross-sections or plan view maps showing the extent of caving, surface cracks, or subsidence (see Appendix B for examples of data sources used). It was found that in many cases what was reported as a break angle or caving angle by the author(s) was actually the angle of draw (90° minus caving angle) estimated underground, as opposed to that considering the propagation of the cave to surface and the corresponding angle of its surface expression. Based on the definitions in Fig. 1, these were corrected where required.

Fig. 7 plots the caving and fracture initiation angles determined as a function of undercut depth for the entire dataset including sub-level operations. Fig. 6 shows a rather wide range of caving angles among the sub-level caving mines as the dip of the orebody causes a large variation between the caving angle seen on the opposing footwall and hangingwall sides. To discount the influence of orebody dip specific to sub-level caving operations, these were excluded from subsequent analyses. Figs. 8 and 9 show the relationships between caving and fracture initiation angles versus undercut depths in block and panel caving operations, respectively. Caving angles are generally seen to vary between 70 and 95°, where angles greater than 90° indicate overhanging angles (i.e., the extent of the zone in question fall within the footprint of the undercut). Angles for fracture initiation are broader and generally vary from 55 to 80°.

In each case, the extent of each line segment depicts the degree of asymmetry present when measuring the caving or fracture initiation angles from opposing sides of the undercut. Thus the range of angles reported in Table 2 not only reflect the site specific differences between the different cases but also incorporates the considerable degree of asymmetry present for almost every single case (ranging from 10° to 30°). Clearly a single caving angle as would be produced from an empirical analysis (e.g., see Fig. 1) would either over-or under-estimate the extent of caving for some portion of the zone of caving at surface.

3.1. Influence of topography

Fig. 10 shows the relationship between caving angle and surface topography. The surface topography considered is classified based on visual observation into two groups: generally flat (regular) topography

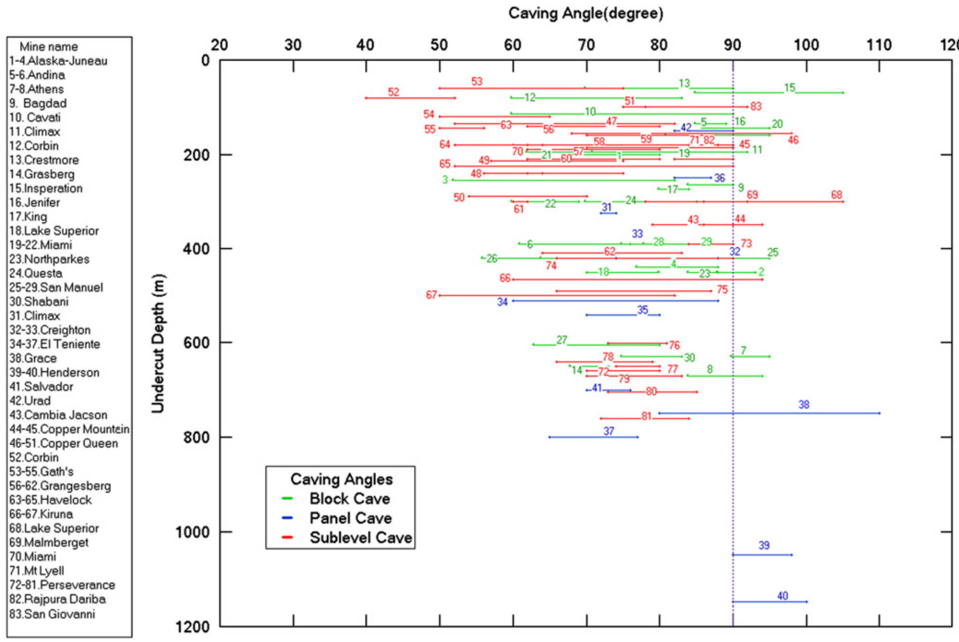

Fig. 6. Undercut depth versus caving angle for block, panel, and sub-level caving operations. Each line segment represents the range in caving angles measured from different sides of the undercut; the greater the range the higher the degree of asymmetry.

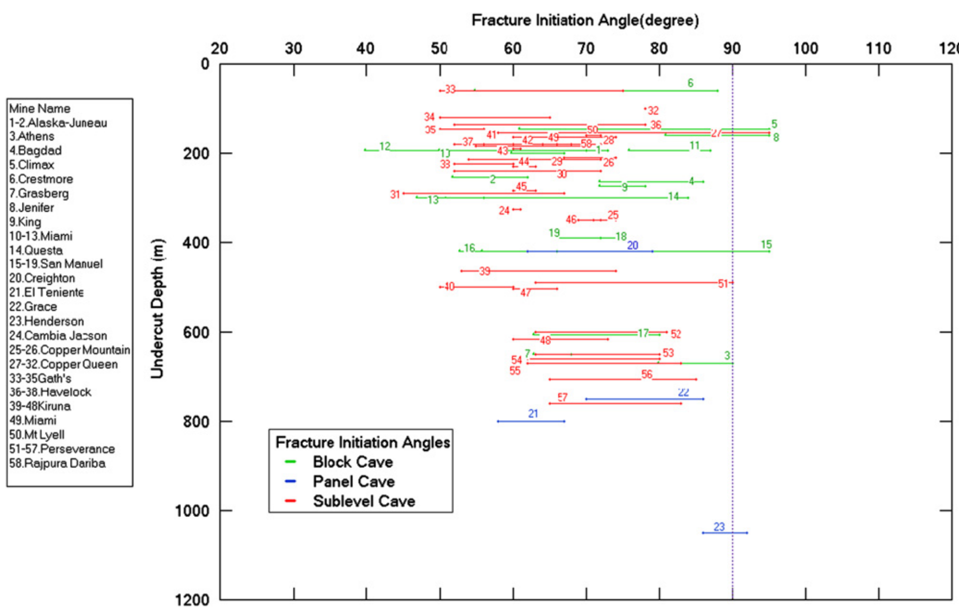

Fig. 7. Undercut depth versus fracture initiation angle for block, panel, and sub-level caving operations. Each line segment represents the range in fracture initiation angles measured from different sides of the undercut; the greater the range the higher the degree of asymmetry.

and irregular topography where the mine is situated beneath a mountain peak(s) or slope/flank. Although the trend is varied, in general, the influence of a more irregular topography is seen to result in lower caving angles as well as a larger range in measured angles (i.e., asymmetry). As previously noted, a larger range in angles signifies a greater degree of asymmetry in the subsidence profile. This is reflected in Google Earth satellite images collected for the different mine sites in the database. Those for caving operations under relatively flat topography, for example Northparkes (Fig. 11a), tend to show more symmetry in the shape of the caving zone on surface, whereas those under mountainous topography, for example Henderson (Fig. 11b), tend to be more irregularly shaped.

The influence of topography can also be clearly demonstrated using comparative numerical models. Typical surface profiles relative to the location of the undercut beneath were derived based on inspection of those in the caving database (Appendix B). These were then examined using the 2-D finite-element code Phase2 [7]. All input parameters were kept the same, including a conceptualized geology involving a joint network of varied persistence and spacing, two bounding faults to either side of the undercut, and several geological units assigned typical rock mass properties. An orthogonal joint pattern was adopted so as not to introduce asymmetry through dipping joints. The undercut depth was kept approximately the same in each model (1500 m), as was the block height caved (500 m). Simulation of caving was undertaken by incrementally changing the properties of the elements above the undercut from those of rock to those for caved rock. A horizontal to vertical stress ratio of 2 was assumed. Full details of

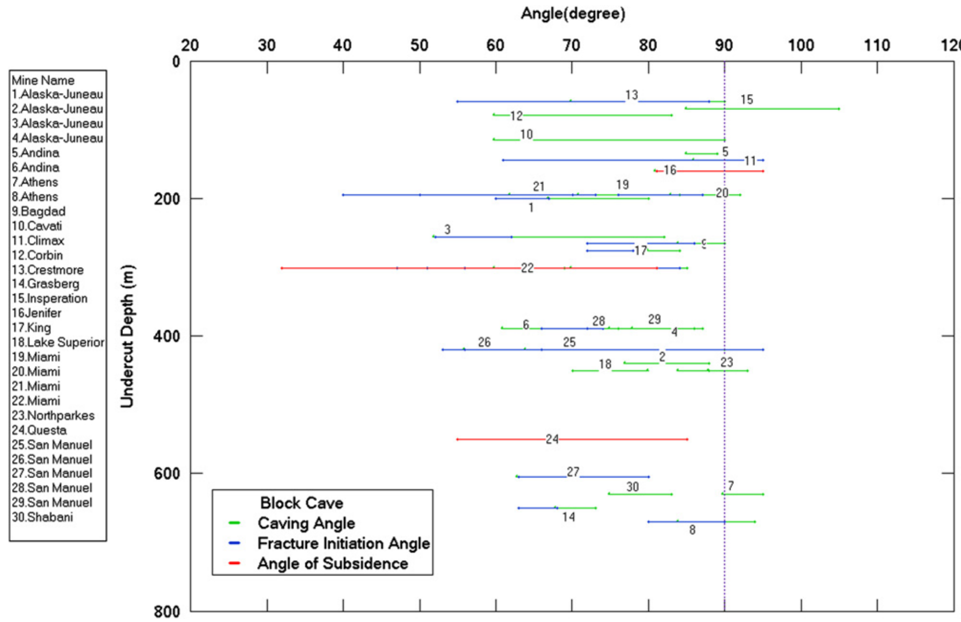

Fig. 8. Undercut depth versus caving, fracture initiation and subsidence angles for block caving operations. Each line segment represents the range in angles measured from different sides of the undercut; the greater the range the higher the degree of asymmetry.

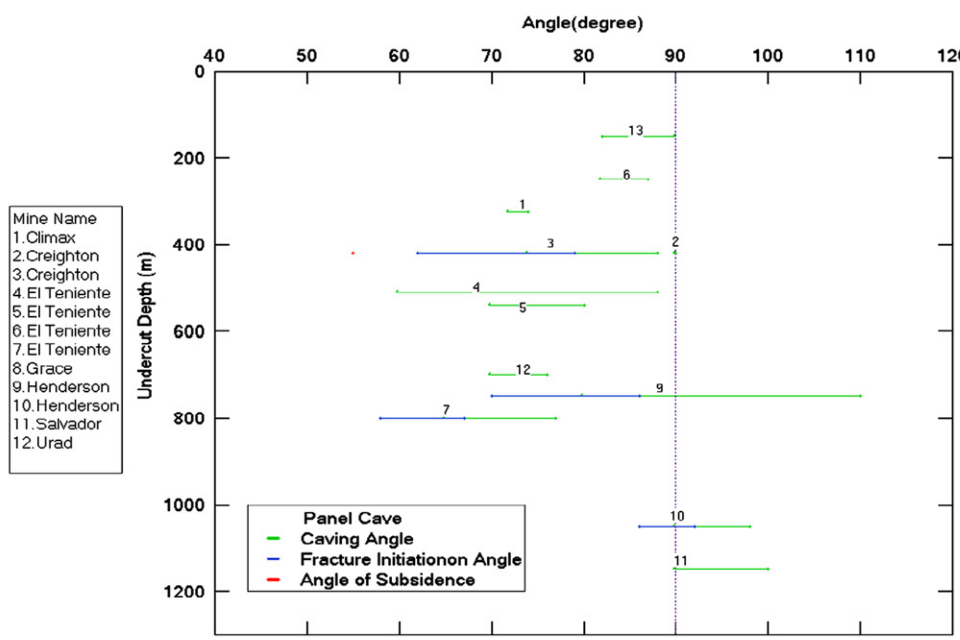

Fig. 9. Undercut depth versus caving, fracture initiation and subsidence angles for panel caving operations. Each line segment represents the range in angles measured from different from sides of the undercut; the greater the range the higher the degree of asymmetry.

the model setup are reported in Woo et al. [8], and are only presented here in a summarized form for illustrative purposes.

The modeling results show that when assuming a flat topography (Fig. 12a), both the caving and subsidence angles are similar on both sides of the undercut (i.e., symmetry). A similar result is obtained where the topography is irregular but approximately symmetrical relative to the position of the undercut (Fig. 12b). This case represents a caving operation directly beneath a mountain peak with sloping flanks at different angles. The presence of the slopes above either side of the undercut results in a broader caving zone compared to the flat topography case. Fig. 12c–e represents scenarios where the undercut is located beneath different slope configurations. The influence of a slope on the caving and subsidence angles to the left and right of the undercut is clearly visible for these different cases, with the up-slope side experiencing notably more subsidence. As the cave propagates towards surface, it undermines the slope on the uphill side promoting gravity driven down slope movements towards the cave. Thus, the empirical and numerical analyses show that symmetric surface conditions generally lead to symmetric subsidence patterns; whereas, asymmetric surface conditions in the form of a sloping surface above the undercut results in cave–surface interactions that draw cave propagation in the uphill direction resulting in asymmetric subsidence. A similar observation was made by Benko [9] who conducted a study

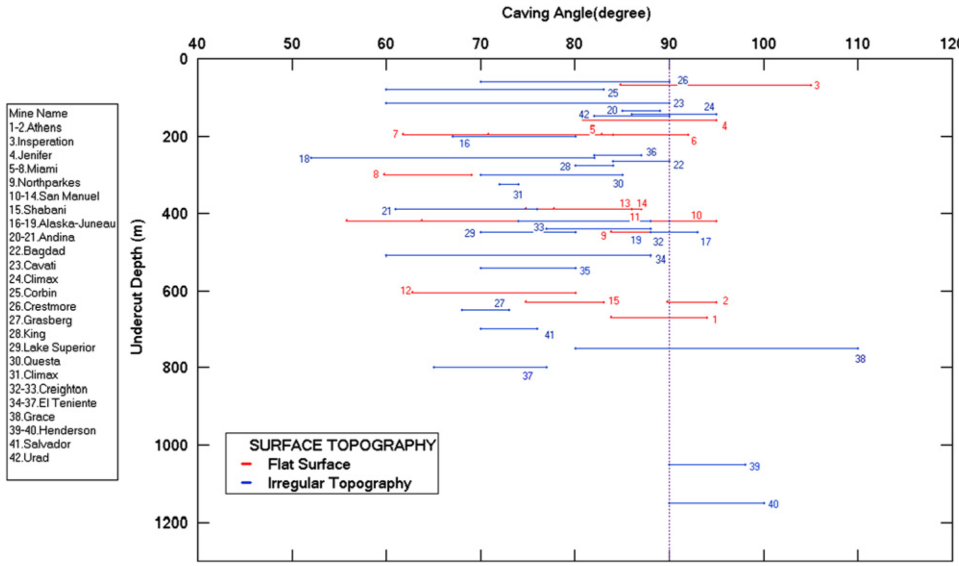

Fig. 10. Undercut depth versus caving angle for global block and panel caving operations, color coded according to the general characteristics of the surface topography. Each line segment represents the range in caving angles measured from different sides of the undercut; the greater the range the higher the degree of asymmetry. (For interpretation of the references to color in this figure caption, the reader is referred to the web version of this article.)

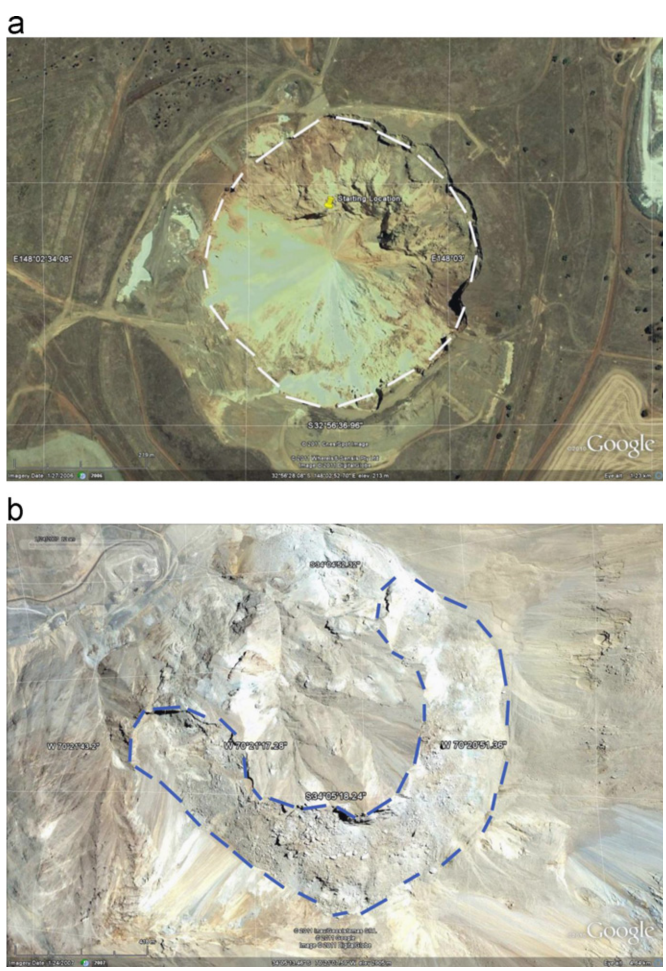

Fig. 11. Influence of topography observed visually in Google Earth satellite images: (a) flat topography (Northparkes mine, Australia), and (b) irregular topography (El Teniente mine, Chile). Surface subsidence area is marked by dashed line.

investigating the influence of a slope on surface subsidence above a longwall coal mine. According to Benko [9], surface subsidence above longwall operations where the topography is relatively flat tends to be symmetric while surface subsidence above mines where a slope is present shows a pattern of greater subsidence developing in the upper part of the slope.

As for the influence of faults, in cases where the surface topography above the caving area is symmetric (Fig. 12a and b), the area of subsidence exceeding 5 m (see contours color coded in blue) does not extend beyond the fault interfaces. The faults effectively constrain/limit the extent of subsidence. Where an irregular topography is present (Fig. 12c–e), however, the area of subsidence exceeding 5 m does extend beyond the boundary faults. This indicates a greater influence of topography on surface subsidence despite any limiting influence the faults may present. A similar observation was made by Vyazmensky et al. [10] who conducted an extensive investigation of the influence of faults on block caving induced surface subsidence.

3.2. Influence of orebody characteristics

Details of the site geology for the different cases populating the database were limited to that reported in the sources consulted. For a number of these, there was no geology data provided requiring alternative sources to be used to obtain basic geological information for the given mine property. The lack of detailed data prevented any extensive analysis into the influence of geological factors on caving angle, and instead, correlations were drawn using the only information that was consistently provided—that of the ore resource being mined. Further development of the database to populate it with more detailed geological data may make it possible to better clarify and separate relationships between undercut depth, caving angles and geological influences. However, for the purpose of the analysis carried out in this study, the ore body resource was used as a simple proxy for mine geology.

Fig. 13 plots the relationship between undercut depth versus caving angle for block and panel caving operations as a function of the mineral resource being mined. In general, diamond, iron, nickel and asbestos operations are seen to have steeper caving angles signifying a smaller impact footprint on surface. This is due in part to the typical shapes of these orebodies, which tend to be narrow and vertical, combined with strength contrasts between the weaker ore being caved and the stronger host rock. For

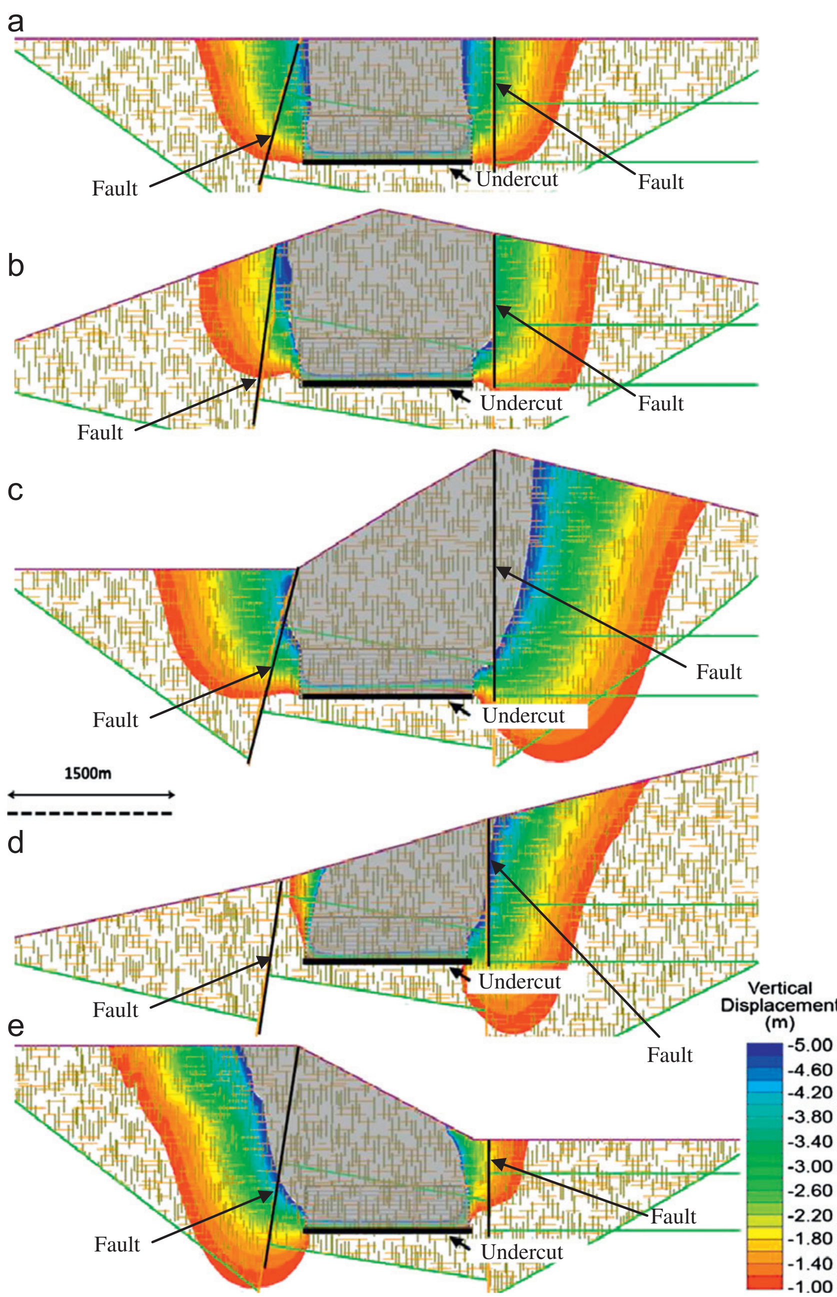

Fig. 12. Finite-element modeling of influence of topography on caving-induced subsidence assuming typical surface profiles visually identified in the UBC database. The same geological inputs used for the comparative models in Chapter 3 were applied. In order of increasing degree of asymmetry (cave–surface interactions) relative to the position of the undercut below, these are: (a) flat topography, (b) mountain peak, (c) rising slope ending in a mountain peak, (d) rising slope, and (e) slope with plateau. Note that gray shaded area approximates zone of caving. (For interpretation of the references to color in this figure caption, the reader is referred to the web version of this article.)

example, diamonds are predominantly mined from vertical kimberlite pipes. These are typically intruded into a stronger host rock, meaning that caving tends to follow the boundaries of the vertical orebody resulting in steep and symmetric caving angles. Symmetry in the caving angles is signified in Fig. 13 by the narrower range of caving angles, with those for diamond kimberlite and upturned bedded iron deposits rarely varying by more than 10°. In contrast, copper operations generally involve porphyry deposits that are more irregular in shape and have less contrast between the strength of the ore and host rock. As such, the caving angles can vary from 90° on one side of the undercut to 65° on the other side. Only a small number of cases involving sedimentary rocks (i.e., soft rock) populate the database, specifically #'s 41–44 in Fig. 13, making comparison of caving angles in hard versus soft rock tenuous. The soft rock cases are seen to involve shallow undercut depths and generally have lower minimum caving angles (60°) similar to those for the copper–molybdenum porphyry deposits. In both cases, the weaker rock types (with porphyry deposit rocks also being affected by hydrothermal alteration) results in both smaller caving angles and higher asymmetry.

Using orebody type and mineral resource as a proxy for geology, Fig. 13 shows that site geology has a significant influence in promoting asymmetry in caving-induced displacements. Similar to the influence of topography, the influence of geology is observable in the Google Earth satellite images in the UBC database (Fig. 14a and Figs. 15 and 14a) is the satellite image for the Kimberley diamond mine (kimberlite pipe). The caving

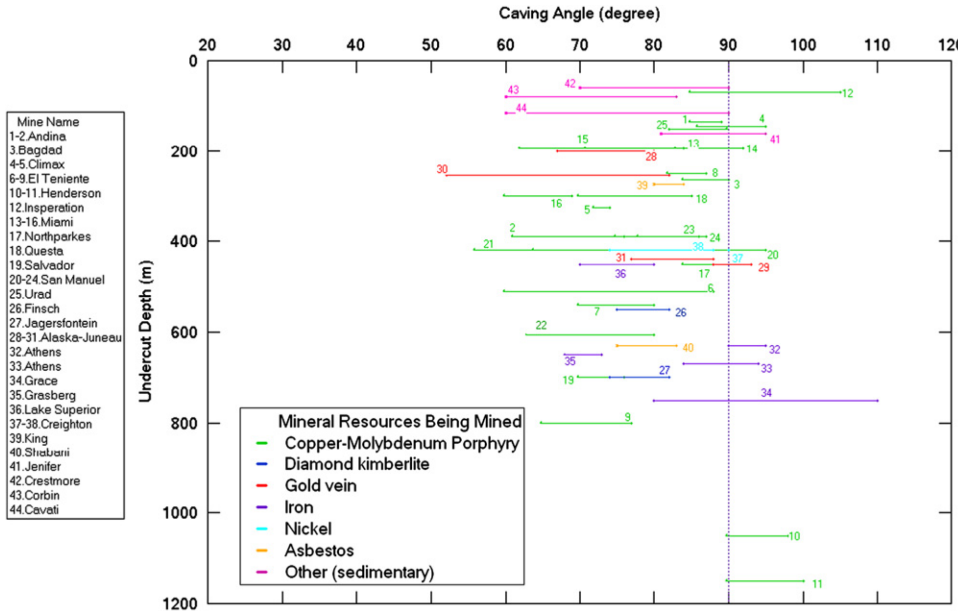

Fig. 13. Undercut depth versus caving angle for global block and panel caving operations, color coded according to the resource being mined. Each line segment represents the range in caving angles measured from different sides of the undercut; the greater the range the higher the degree of asymmetry. (For interpretation of the references to color in this figure caption, the reader is referred to the web version of this article.)

zone shown in the Google Earth image is approximately symmetric in shape centered by a collapse structure, which agrees with the symmetric geological distribution surrounding the kimberlite pipe illustrated in the geology cross-section in Fig. 14b [11]. This can be compared to Fig. 15a, which shows the outline of caving for the San Manuel copper mine. In this case the caving zone is highly irregular consistent with the asymmetric geological character of the mine geology presented in Fig. 15b [12]. These observations are consistent for similar cases in the database.

4. Discussion: influence of undercut depth

A thorough examination of the block and panel caving subsidence data compiled shows that the distribution of data is heavily weighted towards caving angles and macro deformations, Very little data is reported on the extent and magnitudes of smaller surface displacements (also known as micro deformation). This empirical bias towards macro-deformations is largely a function of the state of practice and measurement resolution available at the time of the investigation. The majority of the detailed investigations reporting on caving-induced ground deformations are more than 50 years old, and as such, rely heavily on visual mapping observations and low-resolution levelling surveys. Furthermore, the focus of the reported investigations was primarily placed on the area immediately above the undercut, thus characterizing the caving zone, and in some cases extending the survey outwards towards the edges of mine property to incorporate the fracture initiation zone.

To examine the potential impact of this sampling bias better, specifically with respect to the influence of undercut depth on the extent of surface subsidence, a series of conceptualized numerical models were developed. To be able to fully compare both discontinuous zones of macro-deformations (caving and fracture initiation angles) and continuous zone small strain micro-deformations (subsidence angles) a hybrid FEM-DEM approach incorporating brittle fracture capabilities was adopted using the commercial code ELFEN [13]. ELFEN allows for the representation of the pre-caving geological domain as a continuum populated by discrete fractures representing a brittle fracture network, that then may undergo subsequent fracturing in response to the stresses and strains induced through undercutting and cave propagation. The technique has been shown by Vyazmensky et al. [10] as being well-suited for capturing important block-caving mechanisms, including preferential rock fragmentation within the ore column and influence of geological structures on cave development and surface subsidence. Full details of the models shown here are provided in Woo et al. [8], but in summary models used for illustration of the effects of undercut depth, involve a joint network of varied persistence and spacing, two bounding faults to either side of the undercut, and several geological units assigned typical rock mass properties. The assumed presence of two bounding faults facilitates a preliminary examination of how faults influence small-strain subsidence in 2-D numerical analysis. In addition, Vyazmensky [14] previously analyzed the influence of shallow dipping faults on caving and fracture initiation angles, which were examined as a function of the distance between the caving area and the faults. Accordingly we chose to use steeply dipping faults and a vertical joint set to control the effect of faults and joints highlighting the role of undercut depth. As before, an orthogonal joint pattern was adopted so not introduce asymmetry through the presence of inclined dipping joints. A horizontal to vertical stress ratio of 2 was assumed, and caving was simulated for a block height of 200 m.

Fig. 16 shows the modeling results for different cases of increasing undercut depth with undercutting and caving progressing from right to left. In each case, the zone of caving is largely constrained by the presence of the bounding faults. For the 500 m deep undercut, where the 200 m high ore column represents a 40% extraction ratio, the impact on surface involves a caving zone extending from the edges of the undercut to the bounding faults (i.e., between 75 and 90°). For the 2000 m deep undercut, the caving angles are actually overhanging (>90°). This can be explained by the lower extraction ratio (10% extraction) when assuming the same height of the ore column being caved (200 m), and therefore a less extensive cave development and daylighting

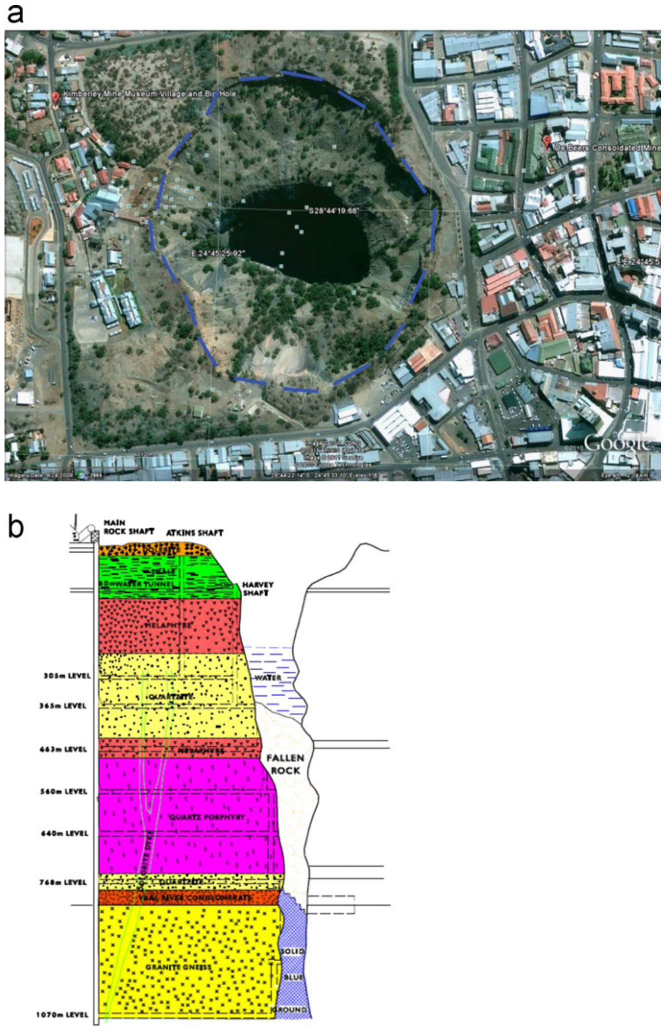

Fig. 14. Symmetric surface subsidence observed in association with a vertical kimberlite pipe–Kimberley diamond mine: (a) Google Earth satellite image, and (b) geological cross-section [11].

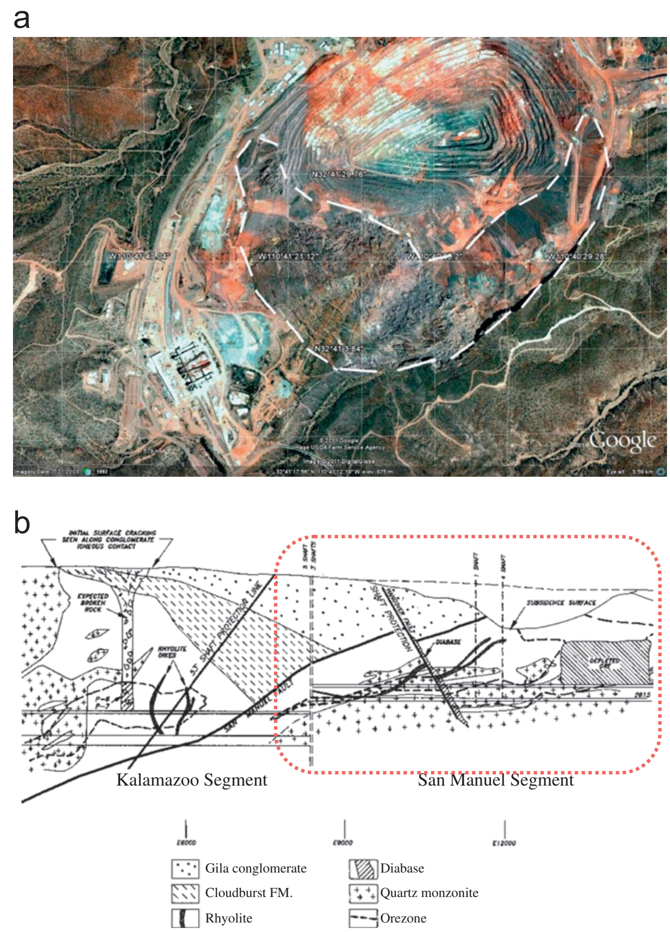

Fig. 15. Asymmetric surface subsidence observed in association with a copper porphyry ore deposit-San Manuel mine: (a) Google Earth satellite image, and (b) geological cross-section [12].

at surface. This agrees with the observations in the UBC block caving database (Fig. 13) where the caving angle is seen to increase with undercut depth and the two cases involving the deepest undercuts (>1000 m) involve overhanging caving angles.

Table 3 compares the caving angles measured from the ELFEN results to those that would have been derived using Laubscher's empirical chart in Fig. 1. While the caving angles are relatively similar, the empirical chart angles tend to be less sensitive to undercut depth (for a constant height of caved material) producing smaller angles than the ELFEN results. The ELFEN results, with respect to caving angle, are more directly influenced by the decreasing extraction ratio for the cases involving the deeper undercuts. Furthermore, the ELFEN results also show asymmetry in the caving angles resulting from the combined influence of the geological features represented in the model and the development of the cave from right to left in the modeled profile (see Fig. 16). Laubscher's empirical chart assumes homogeneous, isotropic conditions. Caution must therefore be exercised when deriving caving angles from existing empirical design charts and assuming these to be symmetric as this appears to be rarely the case.

Another key outcome from these results is the influence of undercut depth on the extent of smaller displacements. Here the opposite trend as observed for caving angle is seen with subsidence angles decreasing with increasing undercut depth. For the 500 m deep undercut, the subsidence angle only partly extends beyond the bounding faults and is not significantly different from the caving and fracture initiation angles. In contrast, the zone of subsidence for the 2000 m undercut extends well beyond the bounding faults and is much farther reaching.

This has important practical implications. If the location of critical infrastructure, or similarly a hazard assessment of the extent of caving-induced ground deformations, is based on empirical data then these will be biased towards observations of large-scale ground disturbance and collapse and would suggest that the impact of caving on surface is reduced for deeper undercuts. However, smaller subsidence may be of equal concern and its extent actually increases with undercut depth. These results therefore caution against relying solely on existing empirical design charts and databases for estimating the extent of caving-induced subsidence, especially where small strain subsidence is of concern, as the data being relied on does not correctly extrapolate beyond the macro deformations (i.e., caving angles) that make up the majority of the observations.

5. Conclusions

A detailed and comprehensive database of cave mining operations and caving-induced ground deformation observations has been developed to guide empirical relationships between caving depth and its impact on surface. The data shows that asymmetry in caving-

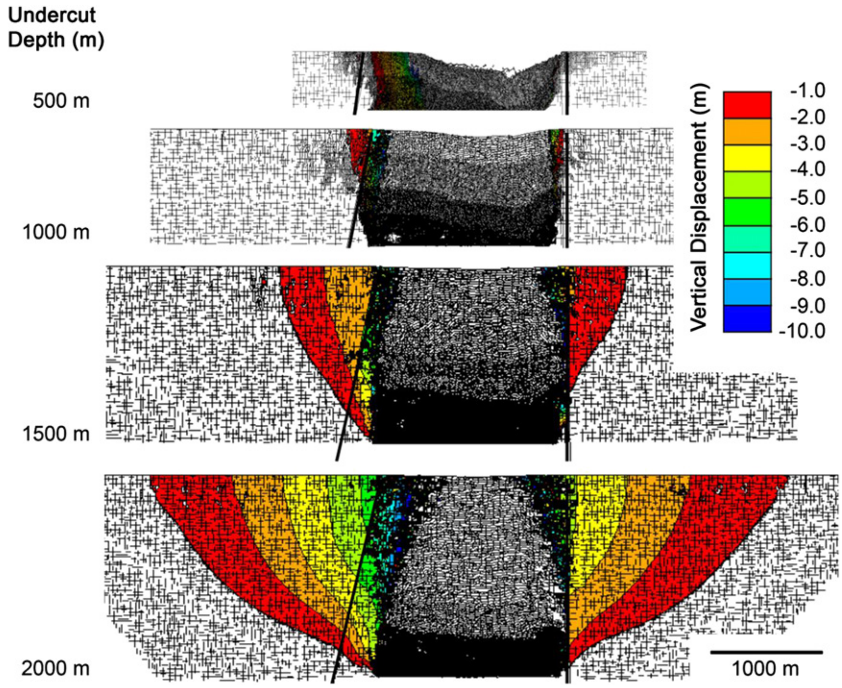

Fig. 16. ELFEN modeling results showing caving-induced brittle fracture and corresponding subsidence as a function of undercut depth. The continuous black lines to the left and right of the undercut are bounding faults.

Table 3
Comparison between caving angles measured from the ELFEN modeling results and those derived from Laubscher's empirical chart in Fig. 1.

Depth (m)	ELFEN-caving angle (deg)		Laubscher's caving angle (deg) Left/right
	Left	Right	
500	90	74	72
1000	90	84	80
1500	94	90	83
2000	104	98	85

induced subsidence is prevalent and largely controlled by topography and geology of the ore deposit and host rock. Where design calculations are carried out using methods that assume, directly or indirectly, symmetrical ground deformations relative to the projection of the undercut footprint at surface, caution must be taken to not under-predict their magnitudes and extent.

The availability and quality of subsidence data was also seen to be deficient as little attention has been paid to the measurement of subsidence angles compared to caving angles. The data on caving angles suggests that as undercut depth increases, the magnitude and extent of the caved zone on surface decreases. However, numerical modeling results indicate that the opposite is true with respect to smaller displacements and that subsidence angles increase and are farther reaching with increasing undercut depths. The results therefore caution against relying on existing empirical design charts and databases for estimating the extent of caving-induced subsidence where small strain subsidence is of concern, as the data being relied upon does not properly extrapolate beyond the macro deformations (i.e., caving angles) that make up the majority of the observations. Thus, with the new generation of deep block/panel caving projects being planned, and the higher geo-risk profiles being carried due to the capital investments and development times required, the need is clear for more detailed measurements to better understand cave–surface interactions as a function of undercut depth and potential asymmetry.

Acknowledgments

This work was funded through a Collaborative Research and Development grant from the Natural Science and Engineering Research Council of Canada (NSERC), in partnership with Rio Tinto, and a grant from the Centre for Excellence in Mining Innovation (CEMI). The authors would like to thank Dr. Andre van As (Rio Tinto Technical Services), and Dr. Peter Kaiser and Keith Bullock (CEMI), for their technical guidance and assistance.

Appendix A. Supplementary Information

Supplementary data associated with this article can be found in the online version at http://dx.doi.org/10.1016/j.ijrmms.2013.01.015.

References

[1] Laubscher D. Block caving manual. Report for the international caving study. JKMRC and Itasca Consulting Group. Brisbane; 2000.
[2] van As A, Davison J, Moss A. Subsidence definitions for block caving mines. Rio Tinto technical services; 2003.
[3] Bucky PB. Mining by block caving. Wilmington: Hercules Powder Company; 1945.
[4] Crane WR. Subsidence and ground movement in the copper and iron mines of the upper Peninsula Michigan. US Bureau Mines Bull 1929;295:66 p..
[5] Flores G, Karzulovic A. Geotechnical guidelines for a transition from open pit to underground mining; benchmarking report; 2002.
[6] Tetra Tech Inc., R Squared Inc. Final Geotechnical assessment, report sinkhole development at the troy mine and implications for the proposed rock creek mine, Lincoln and Sanders Counties, Montana. Technical Report, US Department of Agriculture, Forest Service Region 1; 2006. 116 p.
[7] Rocscience software. Phase2. Version 7.0; 2009; Rocscience Inc, Toronto, Canada.
[8] Woo KS, Eberhardt E, Elmo D, Stead D. Benchmark testing of numerical capabilities for modelling the influence of undercut depth on caving-induced subsidence. Rock Mech Rock Eng (in preparation).
[9] Benko B. Numerical modelling of complex slope deformations. PhD thesis, University of Saskatchewan, Saskatoon; 1997.
[10] Vyazmensky A, Elmo D, Stead D. Role of rock mass fabric and faulting in the development of block caving induced surface subsidence. Rock Mech Rock Eng 2010;43:533–56.

[11] Preece C, Wilson A, Guest AR. A summary of geotechnical information pertaining to the stability of the sidewalls of the Kimberley mine located in Kimberley, Northern Cape Province, Republic of South Africa and the relevance thereof to the adjacent Bultfontein Road. De Beers Consolidated Mines Limited; 2008. 28p.
[12] Sandibak L. Caving and subsidence at San Manuel mine, Arizona. In: The 5th Biennial Workshop was offered by the Interstate Technical Group on Abandoned Underground Mines (ITGAUM). Tucson; 2004.
[13] Rockfield Software. ELFEN Version 4.3.3; 2009: Swansea, UK.
[14] Vyazmensky A. Numerical modelling of surface subsidence associated with block cave mining using a finite element/discrete element approach. PhD thesis, Simon Fraser University; 2008.
[15] Bradley PR. Mining methods and costs: Alaska Juneau gold mining company, Juneau, Alaska. US Bur Mines Inform Circ 1929;6186:26.
[16] Petrillo JL, Hilbelink PA. Closing the historic Alaska-Juneau mine. Min Eng 1999;51(8):24–31.
[17] Torres R, Encina V, Segura C. Damp mineral and its effect on block caving with gravity transfer. In: Stewart DR, editor. Design and Operation of Caving and Sublevel Stoping Mines. New York: Society of Mining Engineers; 1981. p. 251–82.
[18] Flores G, Karzulovic A. Geotechnical guidelines for a transition from open pit to underground mining. Benchmarking Rep 2002:379.
[19] Allen CW. Subsidence resulting from Athens system of mining at Negaunee, Michigan. Trans Amer Inst Min Metall Eng 1934;109:195–202.
[20] Boyum BH. Subsidence case histories in Michigan mines. Min Indust Exp Stat Bull 1961;76:19–57.
[21] Hardwick WR. Block-caving mining methods and costs: Bagdad mine, Bagdad copper, Corp., Yavapai County, Ariz. US Bur Mines Inform Circ 1959;7890:29.
[22] Weisz HM. Evolution of block caving at Catavi. Eng Min J 1958;159(9):86–94.
[23] Vanderwilt JW. Ground movement adjacent to a caving block in the Climax molybdenum mine. Trans Amer Inst Min Metall Eng 1949;181:360–70.
[24] Warburton EL. Mining methods at Corbin B.C. Can Min Metall Bull 1936;29:39–48 285.
[25] Long AE, Obert L. Block caving in limestone at the Crestmore mine, Riverside Cement Co., Riverside. Calif US Bur Mines Inform Circ 1958;7838:21.
[26] Barber J, Dirdjosuwondo S, Casten T, Thomas L. Block caving the EESS deposit at PT Freeport Indonesia. In: Hustrulid WA, Bullock RL, editors. Underground Mining Methods: Engineering Fundamentals and International Case Studies. Denver: Society for Mining, Metallurgy & Exploration; 2001. p. 431–8.
[27] Hubert G, Dirdjosuwondo D, Plaisance R,Thomas L. Tele-operation at freeport to reduce wet muck hazards. In: MassMin 2000 Proceedings, Brisbane. The Australasian Institute of Mining and Metallurgy; 2000. p. 173–179.
[28] Hardwick WR. Mining methods and costs, inspiration consolidated copper, Co., open-pit mine, Gila County, Ariz. US Bur Mines Inform Circ 1963;8154:68.
[29] Obert L, Long AE. Underground borate mining, Kern County. Calif US Bur Mines Rep Invest 1962;6110:67.
[30] Brumleve CB. Rock reinforcement of a caving block in variable ground conditions, King mine, Zimbabwe. Trans Inst Min Metall (Sect A: Min Ind) 1988;97:A77–84.
[31] Duffield S, Design of the second block cave at Northparkes E26 mine. In: MassMin 2000 Proceedings, Brisbane. The Australasian Institute of Mining and Metallurgy; 2000. p. 335–346.
[32] Crane WR. Subsidence and ground movement in the copper and iron mines of the Upper Peninsula Michigan. US Bur Mines Bull 1929;295:66.
[33] MacLennan FW. Subsidence from block caving at Miami mine. Arizona Trans Amer Inst Min Metall Eng 1929;85:167–76.
[34] Fletcher JB. Ground movement and subsidence from block caving at Miami mine. Trans. Amer. Inst Min Metall Petrol Eng 1960;217:413–22.
[35] Gilbride LJ, Free KS, Kehrman R. Modeling block cave subsidence at the Molycorp, Inc., Questa mine – a case study. In: Alaska Rocks 2005, The 40th US symposium on rock mechanics: rock mechanics for energy, mineral and infrastructure development in the northern regions, Anchorage; 2005 ARMA/USRMS 05-881. p. 1–14.
[36] Buchanan JF, Buchella FH. History and development of the San Manuel mine. Trans Amer Inst Min Metall Petrol Eng 1960;217:394–404.
[37] Thomas LA. Subsidence and related caving phenomena at the San Manuel mine, Magma Copper Company, San Manuel Division. San Manuel, Arizona; 1971. 87 p.
[38] Wilson AD. The past focuses support for the future. In: MassMin 2000, Proceedings, Brisbane. The Australasian institute of mining and metallurgy; 2000. p. 385–394.
[39] Vera SG. Caving at climax. In: Stewart DR, editor. Design and operation of caving and sublevel stoping mines. New York: Society of Mining Engineers; 1981. p. 157–76.
[40] Brock AF, McCormick RJ, Taylor WJ. Panel caving at the Creighton mine of the international nickel company of Canada, Ltd. Trans Inst Min Metall 1956;65:37–53.
[41] Dickhout MH. Ground control at the Creighton mine of the international nickel company of Canada Limited. In: Proceedings of the 1st Canadian rock mechanics symposium, Montreal. Department of mines and technical surveys, Ottawa; 1963;. p. 121–144.
[42] Ovalle AW. Analysis and considerations for mining the El Teniente ore body. In: Stewart DR, editor. Design and operation of caving and sublevel stoping mines. New York: Society of Mining Engineers; 1981. p. 195–208.
[43] Kvapil R, Baeza L, Rosenthal J, Flores G. Block caving at El Teniente mine. Chile Trans Inst Min Metall (Section A: Min Ind) 1989;98:A43–56.
[44] Brown ET. Block caving geomechanics. Brisbane: Julius Kruttschnitt Mineral Research Centre; 2003 516 p.
[45] Rojas E, Molina R, Cavieres P. Pre-undercut caving in El Teniente mine, Chile. In: Hustrulid WA, Bullock RL, editors. Underground mining methods: engineering fundamentals and international case histories. Littleton: Society for Mining, Metallurgy and Exploration; 2003. p. 417–23.
[46] Sainsbury DP, Sainsbury BL, Lorig LJ. Investigation of caving induced subsidence at the abandoned Grace Mine. In: Proceedings of the 2nd International Symposium on Block and. Sublevel Caving, Perth. Y. Potvin, editor. Australian Centre for Geomechanics, Perth; 2010. p. 189–204.
[47] Brumleve CB, Maier MM. Applied investigations of rock mass response to panel caving: Henderson Mine, Colorado, USA. In: Stewart DR, editor. Design and operation of caving and sublevel stoping mines. New York: Society of Mining Engineers of AIME; 1981. p. 223–49.
[48] Stewart D, Rein R, Firewick D. Surface subsidence at the Henderson mine. In: Pariseau WG, editor. Geomechanics applications in underground hardrock mining. New York: Society of Mining Engineers; 1984. p. 203–12.
[49] Rech W, Keskimaki KW, Stewart DS. An update on cave development and draw control at the Henderson mine. In: MassMin 2000, Proceedings, Brisbane. The Australasian Institute of Mining and Metallurgy; 2000. p. 495–505.
[50] Escobar RN, Tapia MF. 'An underground air blast' – Codelco Chile – Division Salvador. In: MassMin 2000, Proceedings, Brisbane. The Australasian Institute of Mining and Metallurgy; 2000. p. 279–288.
[51] Kendrick R. Induction caving of the Urad mine. Min Cong J 1970;56(10): 39–44.
[52] Nelson WI, Fahrni KC. Caving and subsidence at the copper mountain mine. Can Min Metall Bull 1950;43(453):2–10.
[53] Kantner WH. Surface subsidence over the porphyry caving blocks, Phelps Dodge Corporation, Copper Queen Branch. Trans Amer Inst Min Metall Eng 1934;109:181–94.
[54] Brown ET, Ferguson GA. Prediction of progressive hanging-wall caving, Gath's mine, Rhodesia. Trans Inst Min Metall (Sect A: Min Ind) 1979;88:A92–105.
[55] Hoek E. Progressive caving induced by mining an inclined orebody. Trans. Inst Min Metall (Sect A: Min Ind) 1974;83:A133–9.
[56] Sisselman R. Sweden's Grangesberg switching over to continuous block caving. Min Eng 1974;26(1):36–8.
[57] Heslop TG. Failure by overturning in ground adjacent to cave mining at Havelock mine. In: Advances in rock mechanics: Proceedings of the third congress of the international society for rock mechanics, Denver. National Academy of Sciences: Washington; 1974 vol. 2 (Part B). p. 1085–1089.
[58] Henry E, Dahnér-Lindqvist C. Footwall stability at the LKAB's Kiruna sublevel caving operation, Sweden. In: MassMin 2000, Proceedings, Brisbane. The Australasian institute of mining and metallurgy. 2000; p. 527–533.
[59] Henry E, Mayer C, Rott H. Mapping mining-induced subsidence from space in a hard rock mine: example of SAR interferometry application at Kiruna mine. CIM Bull 2004;97(1083):1–5.
[60] Villegas TF. Numerical analyses of the hangingwall at the Kiirunavaara mine. Licentiate thesis, Luleå University of Technology, Luleå, Sweden; 2008. 109 p.
[61] Hannweg LA, Van Hout GJ. Draw control at Koffiefontein mine. In: Proceedings, 6th International Symposium on Mine Mechanization and automation, Johannesburg. The South African Institute of Mining and Metallurgy, Johannesburg; 2001. p. 97–102.
[62] North PG, Callaghan RP. Subsidence associated with mining at Mt. Lyell. In: New Zealand Conference, 1980, New Zealand. The Australasian Institute of Mining and Metallurgy: Parkville, Victoria.1980; vol. 9, p. 193–203.
[63] Jarosz A, Zahiri H, Warren M, Sowter A. Utilisation of InSAR for subsidence monitoring over the caved zone of underground metalliferous mine In: Fifth International workshop on ERS SAR interferometry (Fringe). Frascati, Italy: European Space Agency; 2007 p. 1–35.
[64] Tyler D, Campbell A, Haywood S. Development and measurement of the subsidence zone associated with SLC mining operations at Perseverance – WMC, Leinster Nickel Operations. In: MassMin 2004, Proceedings, Santiago. Karzulovic A, Alfaro MA, editors. Mineria Chilena: Santiago; 2004. p. 519–525.
[65] Singh UK, Stephansson OJ, Herdocia A. Simulation of progressive failure in hanging-wall and footwall for mining with sub-level caving. Trans Inst Min Metall (Sect A: Min Ind) 1993;102:A188–94.
[66] Balia R, Manca PP, Massacci G, Congiu M, Fioravanti E, Lai S, et al. Progressive hangingwall caving and subsidence prediction at the San Giovanni Mine, Italy. In: 9th international conference on ground control in mining, Proceedings, Morgantown, West Virgina. Peng SS, editor. West Virginia University: Morgantown, West Virgina; 1990. p. 303–311.
[67] Preece CA, Liebenberg B. Cave management at Finsch mine. In: Proceedings, 1st international symposium on block and sub-level caving, Cape Town. The Southern African Institute of Mining and Metallurgy, Johannesburg; 2007. p. 147–160.
[68] Stucke HJ. Dropping down to a new block cave level at Jagersfontein mine. J S Afr Inst Min Metall 1965;65:523–50.
[69] Pretorius D. The effect of dilution on the underground block cave ore reserves at Palabora Mining Company. In: Proceedings of 1st international symposium on block and sub-level caving, Cape Town. The Southern African Institute of Mining and Metallurgy, Johannesburg; 2007. p. 73–82.

Appendix A

Table 1: Subsidence data for <u>block cave</u> operations caving to surface exclusive of those caving into an open pit. Angles are reported as ranges where asymmetry occurs between the hangingwall and footwall sides of the ore body. Angles greater than 90° refer to overhanging angles.

Mine (location)	Orebody/Lift	Mining Period Reported	Undercut Depth (m)	Caving Angle	Fracture Initiation Angle	Angle of Subsidence	Data Confidence/Comments	Source
Alaska-Juneau (Alaska, USA)	South	1923-1929	200	67-80	60-67	-	Good (cross-section with scale bar). Lower fracture initiation angle in range corresponds with dip of large fault.	[15]
Alaska-Juneau (Alaska, USA)	North South Perseverance	1923-1944 1923-1944 1886-1921	450 255 440	88-93 52-82 77-88	- 52-62 -	- - -	Marginal (cross-section with scale bar). No information is given on mining operations.	[16]
Andina Rio Blanco (Chile)	Panel I (Block 1)	1970-1980	135	85-89	-	-	Marginal (cross-section without scale bar but with mine levels and depths; assumed to be drawn to scale). Early stage of cave development and production depicted.	[17]
Andina Rio Blanco (Chile)	Panels I & II	1978-1995	390	61-76	-	-	Poor (cross-section without scale bar but with mine levels; depths determined from other sources; assumed to be drawn to scale). Lower angle in range corresponds with uphill side of sloping surface.	[18]
Athens (Michigan, USA)	Blocks 1 & 2	1919-1932	630	90-95	-	-	Marginal (cross-section without scale bar but with mine levels and depths). Caving and subsidence on surface partly concealed by thick blanket of glacial till. Cave propagation and boundaries partly controlled by vertical dykes.	[19]
Athens (Michigan, USA)	Blocks 1-4 and 1 & 2, Lift 2	1919-1951	670	84-94	80-90	-	Good (cross-section with scale bar). Caving and subsidence on surface partly concealed by thick blanket of glacial till. Cave propagation and boundaries partly controlled by vertical dykes.	[20]

Bagdad (Arizona, USA)	West	1937-1947	265	84-90	72-86		Marginal (subsidence map with scale bar; depths determined from secondary information and used to calculate angles). Boundary level drifts used to control the lateral extent of caving.	[21]
Catavi (Bolivia)	Block 2	1948-1957	115	60-90	-		Marginal (cross-section with scale bar; full limits of caving zone not shown but reported in text). Undercut is located under steep topography.	[22]
Climax (Colorado, USA)	Phillipson Level	1940-1945	145	86-95	61-95	-	Good (cross-section with scale bar). Lower angles in ranges correspond with uphill side of sloping surface and retrogressive slumping towards cave.	[23]
Corbin (B.C, Canada)	No. 6 Mine - West	1917-1934	80	60-83	-	-	Poor (cross-section without scale bar but with mine levels; depths determined from other sources; assumed to be drawn to scale). Mining of thick interval of coal using multiple lifts. Neighbouring section mined by top slice method.	[24]
Crestmore (California, USA)	Stanley Bed – Block 1A	1930-1954	60	70-90	55-88	-	Good (cross-section with scale bar). Vertical cutoff stopes excavated on all four sides of block to control caving angles. Caving on footwall side of block extended beyond this to align with a dipping fault (lower angle in fracture initiation range).	[25]
Grasberg (Indonesia)	IOZ	1994-2000	650	68-73	63-68		Good (cross-section with scale bar). Undercut is located under a steep slope; lower caving angle in range corresponds to the uphill side.	[26,27]
Inspiration (Arizona, USA)	Transfer Block	1947-1963	70	85-105	-	-	Good (cross-section with scale bar). Caving of small transfer block following transition from block caving to open pit mining.	[28]
Jenifer (California, USA)	Jenifer	1952-1957	160	81-95	81-95	81-95	Good (subsidence map and cross-section with scale bars). Periphery of caving zone marked by single, continuous, steep-wall face with little to no change in subsidence outside this area.	[29]

King (Zimbabwe)	West Flank; W11-14 Blocks	? - 1988	275	80-84	72-78	-	Marginal (cross-section without scale bar but with mine levels and depths; assumed to be drawn to scale). Steeper angle in ranges coincides with caving parallel to footwall of dipping orebody; lower angles occur on uphill side of caving zone.	[30,31]
Lake Superior (Michigan, USA)	Marquette range (Case C; Types D-F)	?	450	80	70	-	Poor (schematic cross-section without scale bar; assumed to be roughly drawn to scale). No direct indication given of mining depth. Bedrock is covered by a thick blanket of glacial till that partly obscures the caving and subsidence zones at surface.	[32]
Miami (Arizona ,USA)	Low Grade Orebody	1926-1929	195	71-84	50-73	-	Good (cross-section with scale bar). Caving limits controlled by vertical boundary drifts. Caving on one side extends into the “Main Orebody” previously mined by sublevel caving. Lower angles are sub-parallel to foliation of schist.	[33]
	Stope 11	1928-1929	195	83-92	76-87	-	Good (cross-section with scale bar). Caving limits controlled by vertical boundary drifts.	
Miami (Arizona ,USA)	Main/Low Grade Orebodies	1910-1939	195	62-84	40-70	-	Marginal (subsidence map with scale; depths determined from secondary information and used to calculate angles). Caving limits controlled by vertical boundary drifts. Angles reported to have flattened considerably since 1929 measurements.	[34]
	720 -1000 Levels	1910-1958	300	60-69	47-56	-	Good (cross-section with scale bar). 1000 Level mined without vertical boundary cut-off drifts.	
Northparkes (Australia)	E26 Lift 1	1993-2000	450	84-88	-	-	Marginal (cross-section without scale bar but with mining level; scale estimated from other source; assumed to be roughly drawn to scale). Collapse of crown pillar related to change in geology resulted in near-vertical cave angles. Lift also caved into the bottom of small open pit.	[35]

Questa (New Mexico, USA)	Goathhill	1983-2000	300	70-85	51-84	32-81	Good (subsidence map with scale bar; depths determined from secondary information and used to calculate angles). Lower angle in ranges coincide with deformations related to shallow rockslide movements undercut by cave.	[35]
	D – Block 1	2000-2005	550	-	-	55-85	Marginal (subsidence map with scale bar; depths determined from secondary information and used to calculate angles). Subsidence not developed enough to allow measurement of caving or fracture initiation angles.	
San Manuel (Arizona, USA)	South Orebody, Lift 1	1956-1960	420	64-95	53-95	-	Good (cross-sections and subsidence map with scale bars).	[35, 36]
San Manuel (Arizona, USA)	South Orebody, Lift 1	1956-1962	420	56-90	56-66	-	Good (subsidence map with scale bar). Final reporting of subsidence for mining of South orebody, Lift 1.	[37]
	South Orebody, Lift 2	1962-1970	605	63-80	63-80	-	Good (cross-sections and subsidence map with scale bars). Active subsidence contained within established boundaries for Lift 1, with only minor activity outside this periphery.	
	North Orebody, West	1959-1970	390	78-86	66-74	-	Good (subsidence map with scale bar). West and East blocks separated from one another by a 200 m pillar.	
	North Orebody, East	1962-1970	390	75-87	66-72	-	Good (subsidence map with scale bar). West and East blocks separated from one another by a 200 m pillar.	
Shabani (Zimbabwe)	52 & 58	1987-1999	630	75-83	-	-	Good (cross-section with scale bar). Inclined undercut dipping at approximately 30° from horizontal.	[38]

Table 2: Subsidence data for <u>panel cave</u> operations caving to surface exclusive of those caving into an open pit. Angles are reported as ranges where asymmetry occurs between the hangingwall and footwall sides of the ore body. Angles greater than 90° refer to overhanging angles.

Mine (location)	Orebody/Lift	Mining Period Reported	Undercut Depth (m)	Caving Angle	Fracture Initiation Angle	Angle of Subsidence	Data Confidence/Comments	Source
Climax (Colorado, USA)	600 Level	1945-1980	325	72-74	-	-	Marginal (cross-section without scale bar but with mine levels and depths; assumed to be drawn to scale). Continuation following transition from block to panel caving.	[39]
Creighton (Ontario, Canada)	23 Level	1951-1955	420	90	-	-	Poor (cross-section without scale bar but with mine levels; depths determined from other sources; assumed to be drawn to scale). Blasting used to induce caving beyond limits of previously mined stopes.	[40]
Creighton (Ontario, Canada)	1900 Level	1951-1963	420	74-88	62-79	55	Good (subsidence map with measured angles together with cross-section without scale bar but with mine levels; depths determined from other sources; assumed to be drawn to scale).	[41]
El Teniente (Chile)	South 1 (Ten 1 Sur)	1940-1980	510	60-88	-	-	Marginal (cross-section without scale bar but with mine levels; depths determined from other sources; assumed to be drawn to scale). Undercut is positioned under a steep slope; lower caving angles occur on the uphill side.	[42]
	North 4 (Ten 4 Norte)	1960-1980	540	70-80	-	-		[42, 43]
El Teniente (Chile)	Regimiento 4	1982-1998	250	82-87	-	-	Poor (empirical chart of caving angle versus depth based on numerical modelling and field observations; no depth is reported for the undercut but can be estimated from other sources).	[44]

El Teniente (Chile)	Esmeralda	1997-2001	800	65-77	58-67	-	Marginal (cross-section without scale bar but with mine levels and depths, together with empirical chart of caving angle versus depth). Undercut is positioned under a steep slope; lower angles in range correspond to the uphill side of cave.	[45]
Grace (Pennsylvania, USA)		1958-2004	750	80-110	70-86	-	Marginal (subsidence map showing limits of surface cracking; angles estimated based on average depth of undercut). Inclined panel cave (20-30°). Cave breakthrough only occurred above half of the undercut, facilitated by a steeply dipping fault.	[46]
Henderson (Colorado, USA)	8100 Level Panel 1	1976-1983	1050	90-98	86-92	-	Good (cross-section with scale bar together with subsidence map). Vertically spaced boundary cutoff drifts together with steeply dipping faults contribute to vertical nature of cave.	[47,48]
Henderson (Colorado, USA)	7700 level	1976-2000	1150	90-100	-	-	Poor (cross-section without scale bar but with mine levels; depths determined from other sources; assumed to be drawn to scale)	[49]
Salvador (Chile)	Inca West	1994-2000	700	70-76	-	-	Marginal (cross-section without scale bar but with mine levels and depths; assumed to be drawn to scale). Caving zone depicted prior to and after air blast collapse of cave back.	[50]
Urad (Colorado, USA)	1100 Level	1967-1969	150	90	82	-	Poor (cross-section without scale bar but with mine levels; depths determined from other sources; assumed to be drawn to scale). Undercut beneath steep hill. Caving limits controlled by vertical boundary cut-off stopes (shrinkage stopes). Considerable blasting required to aid caving.	[51]

Table 3: Subsidence data for sublevel caving/shrinkage stoping/top slicing operations caving to surface exclusive of those caving into an open pit. Angles are reported as ranges where asymmetry occurs between the hangingwall and footwall sides of the ore body. Angles greater than 90° refer to overhanging angles.

Mine (location)	Orebody/Lift	Period Reported	Undercut Depth (m)	Caving Angle	Fracture Initiation Angle	Angle of Subsidence	Data Confidence/Comments	Source
Cambria Jackson (Michigan, USA)	260 Sublevel	1942-1945	350	86-94	71-72	-	Good (cross-section with scale bar). Cave propagation through competent diorite sill capping weak hematite iron formation.	[20]
Copper Mountain (B.C., Canada)	Contact Block	1937-1949	350	79-90	69-74	65	Good (cross-section with scale bar).	[52]
	122-East Block	1941-1949	210	82-90	67-74	-	Good (cross-section with scale bar). Lower angle in range aligns with dipping fault.	
Copper Queen – East Orebody (Arizona, USA)	600 & 650 Lift	1925-1927	155	68-98	58-95	-	Good (multiple cross-sections without scale bars but with mine levels and depths; assumed to be drawn to scale). Lower angles correspond with weak hangingwall rock, relative to higher angles in stronger footwall rock.	[53]
	725 Lift	1927-1928	180	64-88	56-72	-		
	850 Lift	1928-1930	215	57-75	54-72	-		
	950 Lift	1930-1931	240	56-75	52-72	-		
	1100 Lift	1931-1933	290	54-70	45-67	-		
Copper Queen – Queen Hill (Arizona, USA	Queen Hill Block	1913-1933	100	78	78	78	Marginal (cross-section without scale bar but with mine levels and depths; assumed to be drawn to scale). Caved block is bound on all sides by faults, along which the block drops and across which subsidence is limited.	[9]
Corbin (B.C, Canada)	No. 6 Mine - East	1917-1934	80	40-52	-	-	Marginal (cross-section without scale bar; scale estimated from other data provided; assumed to be roughly drawn to scale). Undercut inclined at 38°, extending from surface to same level at depth of neighbouring section mined by block caving.	[24]
Gath's	99 Level	1971-1976	60	50-75	50-75	-	Good (cross-section with caving angles	[54]

(Rhodesia/ Zimbabwe)	158 Level		120	50-65	50-65	-	reported). Lower angles correspond with dip of orebody; steeper angles correspond to caving in dipping hangingwall.	
	183 Level		145	50-56	50-56	-		
Grangesberg (Sweden)	140 Level	?-1921	140	62-80	-	-	Marginal (cross-section without scale bar but with caving angles and sublevel depths). Caving angle on footwall side coincides with dip of inclined orebody at 62°.	[55]
	180 Level	1921-1933	180	62-88	-	-		
	190 Level	1933-1936	190	62-80	-	-		
	210 Level	1936-1939	210	62-80	-	-		
	240 Level	1939-1943	240	62-64	-	-		
	300 Level	1943-1961	300	60-62	-	-		
Grangesberg (Sweden)	410 Level	1960-1974	410	64-83	-	-	Marginal (cross-section without scale bar but with sublevel depths; assumed to be roughly drawn to scale). Caving angle on footwall side coincides with dip of inclined orebody at 64°.	[56]
Havelock (Swaziland)	Level 1	1952-1972	135	52-82	52-78	-	Good (cross-section with scale bar). Lower angles in range controlled by dip of bedding in footwall. Deformation in hangingwall develops through flexural toppling and shearing along bedding.	[57]
	Level 2	1963-1972	180	52-90	52-64	-		
	Level 3	1966-1972	225	52-90	52-60	-		
Kiirunavaara/ Kiruna (Sweden)	700 Level	1965-1995	465	60-94	53-74	40-60	Marginal (subsidence map but without indication of the sublevel depth; sublevel depth estimated from other sources). Caving angle on footwall side coincides with dip of orebody. Higher caving angle points to overhanging nature of dipping hangingwall.	[58, 59]
Kiirunavaara/ Kiruna (Sweden)	785 Level	1965-2000	500	50-82	50-60	40-50	Marginal (subsidence map; angles calculated based on projection of lowest sublevel undercut and depth at time of data reporting). Angles on the footwall side are shown to coincide with one another at 50°.	[59]
Kiirunavaara/ Kiruna (Sweden)	400 Level	1965-1971	165	-	60-74	-	Good (cross-section without scale bar but with sublevel depths; assumed to be drawn to scale). Only fracture initiation angle on hangingwall side provided; no indication of caving angles for the same periods. Fracture initiation angle on footwall side reported as coinciding with dip of orebody (60°).	60]
	415 Level	1971-1974	180	-	60-66	-		
	425 Level	1974-1977	190	-	60-61	-		
	465 Level	1977-1981	230	-	60-63	-		
	530 Level	1981-1985	285	-	60-63	-		
	570 Level	1985-1989	325	-	60-61	-		
	750 Level	1989-1995	505	-	60-66	-		
	865 Level	1995-2005	615	-	60-73	-		

Lake Superior (Michigan, USA)	Gogebic range (Case B; Type C)	?	300	86-105	-	-	Poor (cross-section without scale bar or mining depth, but with caving angles; assumed to be drawn to scale). Caving occurs primarily along steeply dipping footwall slates.	[32]
Malmberget (Sweden)	Pillar Recovery 300 Level	1970-1974	300	78-92	-	-	Good (cross-section with scale bar). Lower angle coincides with footwall, whereas higher angle points to overhanging hangingwall.	[61]
Miami (Arizona ,USA)	Main Orebody	1910-1925	180	60-84	60-68	-	Good (cross-section with scale bar). Mostly mined by top slicing and sublevel caving. Caving limits controlled by vertical boundary drifts. Lower angles are sub-parallel to foliation of schist.	[33]
Mt. Lyell (Tasmania)	Cape Horn (#5 Stope)	1972-1980	160	70-86	70-72	-	Marginal (cross-section without scale bar but with sublevel depths; assumed to be drawn to scale). Lower angles coincide with dip of footwall (70°).	[62]
Perseverance (Australia)	9920 Level	1989-1997	640	66-79	-	-	Good (cross-section with scale bar). Sublevel caving beneath large open pit. Lower caving angle extends beyond pit limits on hangingwall side of orebody.	[63]
Perseverance (Australia)	10130 Level	1989-1995	390	84-90	-	-	Marginal (subsidence map without scale bar; depths determined from secondary information and used to calculate angles; assumed to be drawn to scale). Sublevel caving beneath large open pit. Lower caving and fracture initiation angles extend beyond pit limits on hangingwall side of orebody.	[64]
	10100 Level	1995-1996	420	66-90	-	-		
	10030 Level	1996-1997	490	66-87	63-90	-		
	9920 Level	1997-1998	600	73-81	63-81	-		
	9870 Level	1998-1999	650	74-80	63-80	-		
	9860 Level	1999-2000	660	70-80	62-80	-		
	9850 Level	2000-2001	670	70-83	62-83	-		
	9815 Level	2001-2002	705	73-85	65-85	-		
	9760 Level	2002-2003	760	72-84	66-83	-		
Rajpura Dariba (India)	South 465 Level	?	185	70-90	55-70	-	Poor (no data provided; angles cited in text). 70° angle coincides with dip of footwall.	[65]
San Giovanni (Italy)	Contatto Ovest	1985-1990	100	75-92	-	-	Marginal (subsidence map and cross-section without scale bar but with mining levels and depths; assumed to be drawn to scale).	[66]

Table 4: Subsidence data for block cave operations caving to surface into an open pit.

Mine (location)	Orebody/Lift	Mining Period Reported	Undercut Depth (m)	Caving Angle	Fracture Initiation Angle	Angle of Subsidence	Data Confidence/Comments	Source
Finsch (South Africa)	Block 4	2004-2006	700	74-82	-	-	Good (cross-section with scale bar). Block caving into existing workings mined by open stoping, and earlier by large open pit. Caving angles coincide with walls of already existing crater.	[67]
Jagersfontein (South Africa)	1870 level	1947-1962	550	75-82	-	-	Good (cross-section with scale bar). Block caving into existing underground workings and open pit. Caving angles incorporate open pit and sloughing of wall rock.	[68]
Koffiefontein (South Africa)	49 Level	1987-2001	480	90	-	-	Poor (cross-section without scale bar but with mine levels; depths determined from other sources; assumed to be drawn to scale).	[61]
Palabora (South Africa)	Lift 1	2001-2007	1200	84-86	60-84	-	Poor (cross-section without scale bar but with mining level; depths determined from other sources). Lower fracture initiation angle coincides with back scarp of large rockslide that developed in deep open pit.	[69]

APPENDIX B

Alaska-Juneau (Alaska, USA) – 1929

Source: Bradley (1929)

Caving Period Reported: 1916-1929

Summary: Block cave mining methods applied to the Alaska-Juneau gold mine are reported. In describing the system of caving, a schematic cross-section is included that depicts the caving zone and surface fractures that develop over a single block undercut from the 4 Level at 200 m depth. It is assumed that the section is based on visual indicators; no indication is given that subsidence measurements were made. The sections are to scale and show the depth of the undercut workings and original surface. Blasting was used to aid the caving process, and the presence of a dipping fault plays a controlling role in the extent of caving and subsidence on the footwall side of the orebody.

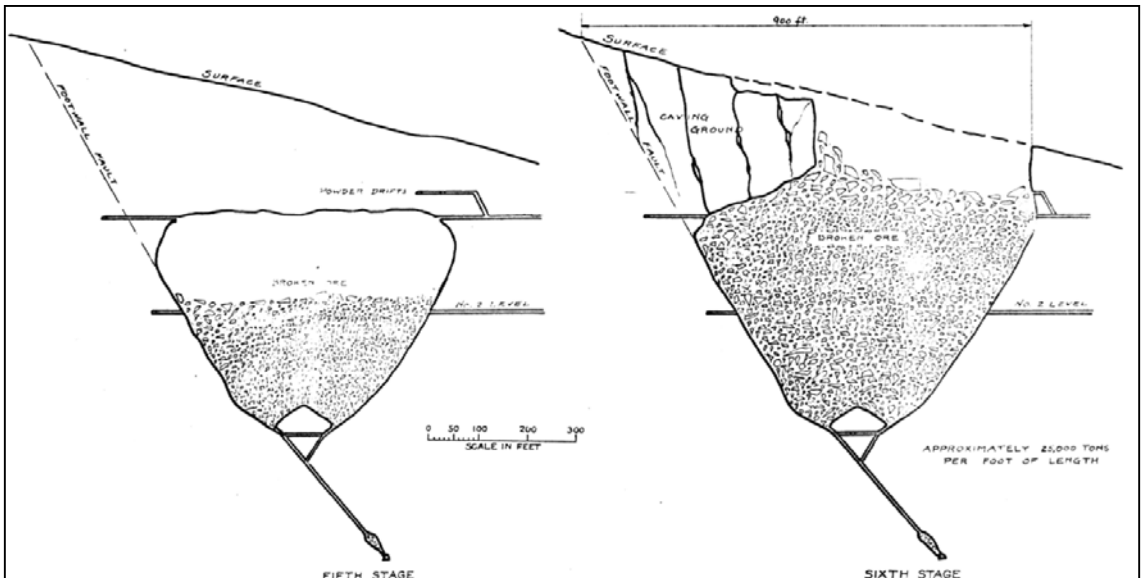

Figure 2c, Development of stopes at the Alaska Juneau (continued)

Alaska-Juneau (Alaska, USA) – 1944

Source: Petrillo & Hilbelink (1999)

Caving Period Reported: 1923-1944

Summary: The history of the Alaska-Juneau gold mine is reported, encompassing the North, South and Perseverance orebodies, which were mined using a combination of block caving and shrinkage stoping. Minimal data is provided regarding the mining operations and no specific data regarding subsidence measurements are reported. However, a scaled cross-section is provided, which shows the caving zone and undercuts from which the caving angles can be estimated.

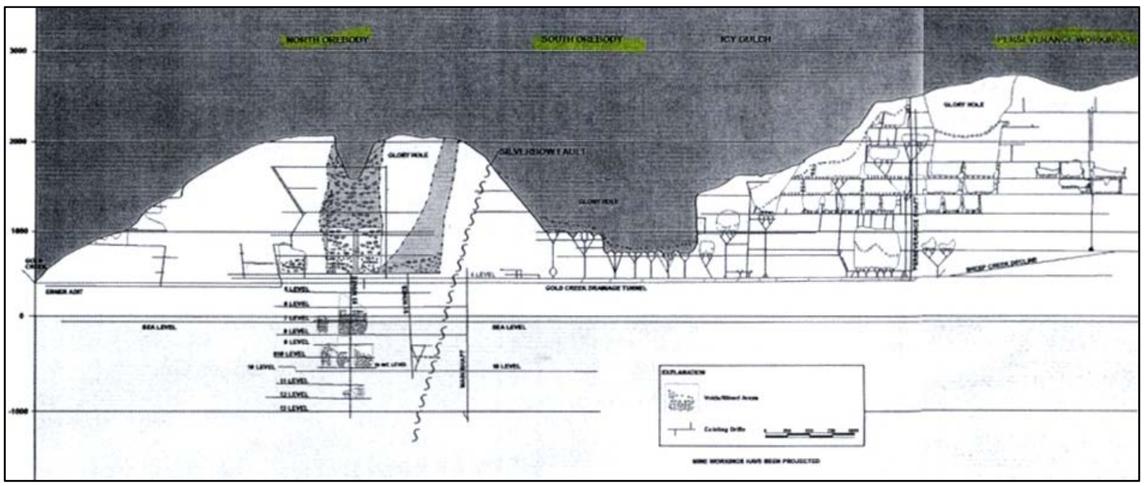

Andina-Rio Blanco (Chile) – Panel I

Source: Torres et al. (1981)

Caving Period Reported: 1970-1980

Summary: The block caving operations for Panel I at Andina's Rio Blanco mine are described. This includes a cross-section showing the surface profile, undercut level, mining of the first block in Panel I, and the corresponding caved area at surface. No direct data in the form of subsidence measurements is given, but it is assumed that the altered surface profile is based on visual observations. It is also assumed the cross-section is to scale; no scale bar is provided, but the different mine levels are shown with their respective elevations from which the depth of mining can be approximated. The undercut is located under the steep slope of a mountain. However, the early stage of cave development and production depicted is not yet shown to be influenced by topography.

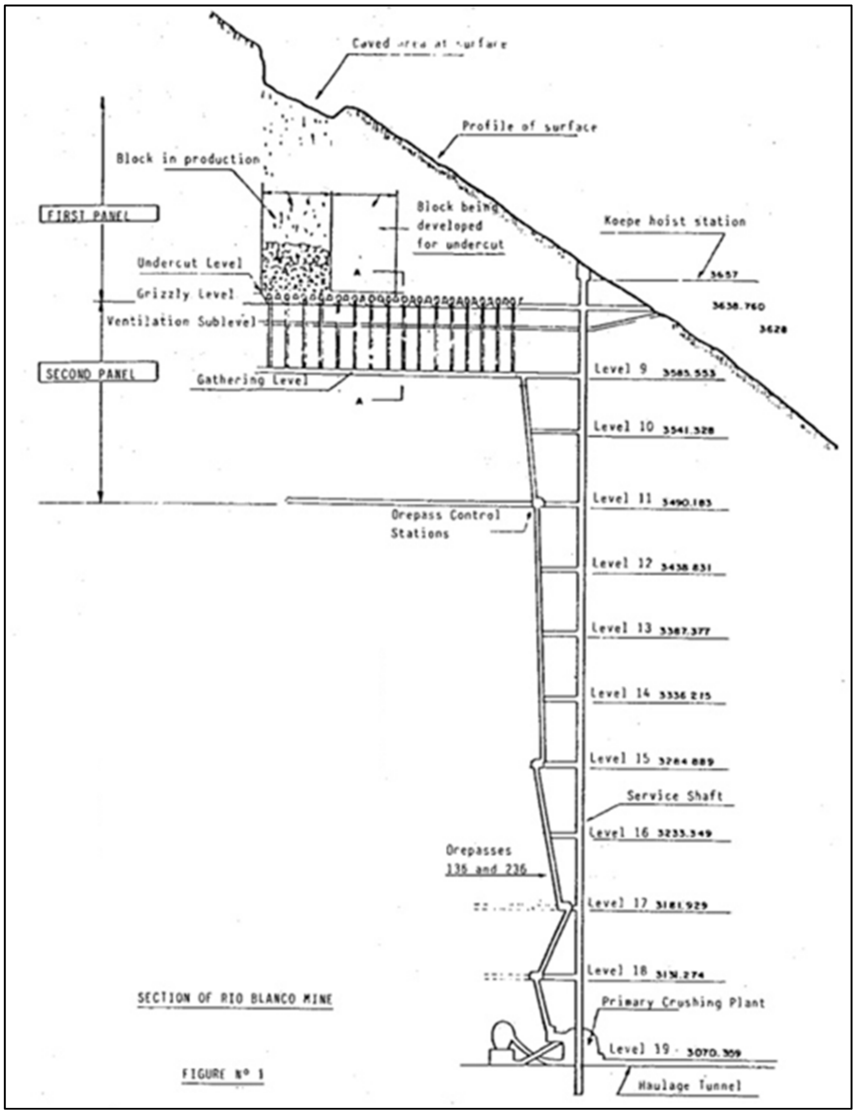

SECTION OF RIO BLANCO MINE

FIGURE N° 1

Andina-Rio Blanco (Chile) – Panel I & II

Source: Flores & Karzulovic (2002)

Caving Period Reported:

Summary: Data is reported from the ICS II benchmarking study for the Andina mine (formerly the Rio Blanco mine). Focus is placed on the planned third lift (Panel III), which will be mined by panel caving. However, a schematic cross-section is provided showing the state of caving above Panels I and II, mined by block caving. It is assumed the cross-section is to scale; no scale bar is provided, but the undercut levels are indicated from which the depth can be approximated based on the reported elevations of the Panel II and III undercuts. The caving zone is located under the steep slope of a mountain, for which the lower angle of caving corresponds with the uphill side of sloping surface. The report also provides a range of break angles, defined as the mean inclination of the caving crater walls at various depths for different ranges of MRMR values. However, because the angles do not appear to be measured with respect to the undercut level, they are not reported in the above Tables. The ranges cited are 52-90° for MRMR 41 to 50, 58-90° for MRMR 51 to 60, and 70-90° for MRMR 61 to 70.

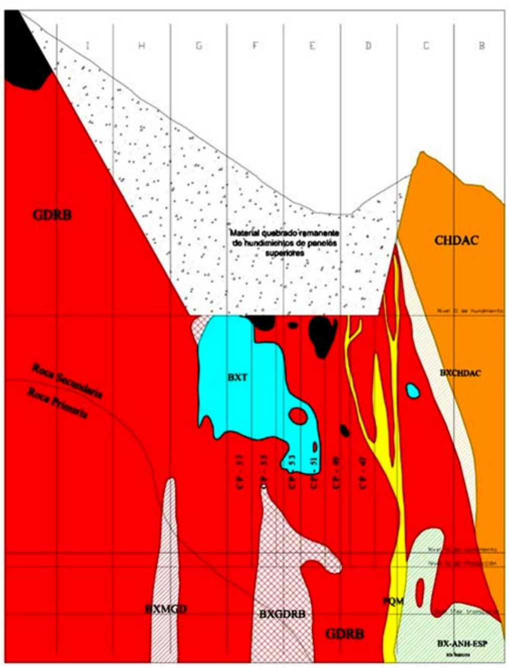

Photograph 9.9: Typical subsidence crater of a block caving mine, II Panel, Andina Mine, Chile.

Athens (Michigan, USA) – 1932

Source: Allen (1934)

Caving Period Reported: 1918-1932

Summary: Data is reported for the Athens mine in the Marquette iron range. This is one of the unnamed regions reported by Crane [12]; see Lake Superior District below. The caving period reported is from the start of mining to the completion of Blocks 1 and 2 at 630 m depth. Mining was carried out using a combined block caving and top slicing approach progressing upward in successive blocks to the east. A scaled cross-section is provided based on surface observations of caving features, which shows the extent of caving on surface, depth of mining and caving angles. The cross-section also shows that a thick blanket of glacial till covers the bedrock, partly obscuring the subsidence zones at surface. Upward propagation of the cave is shown to be bounded and controlled in part by two vertical diorite dykes.

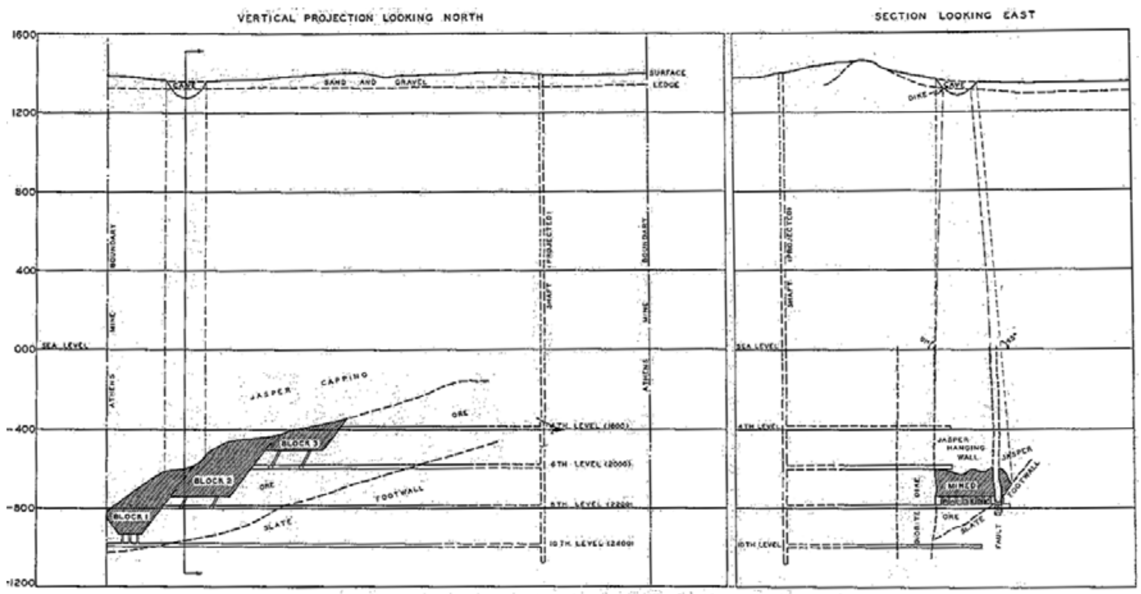

Fig. 1.—Mining system and resulting subsidence, Athens mine.

Athens (Michigan, USA) – 1950

Source: Boyum (1961)

Caving Period Reported: 1918-1950

Summary: This report updates the subsidence observations of Allen [1], providing data on the extension of the subsidence zone for the mining carried out up to the suspension of the operations in 1951. Repeated are the data for the mining of Blocks 1 and 2, supplemented with data for the mining of the neighbouring blocks (3 and 4) and extension of Blocks 1 and 2 to 670 m depth (from 630 m). As before, mining was carried out using a combined block caving and top slicing approach. A scaled cross-section is provided showing the extent of caving at surface relative to the underground workings. Also included are surface fractures observed despite the thick blanket of glacial till that covers the bedrock. The section is based on surveys of subsidence pins laid out on a grid over the area. Present are vertical diorite dykes that partly bound and control the upward propagation of the cave.

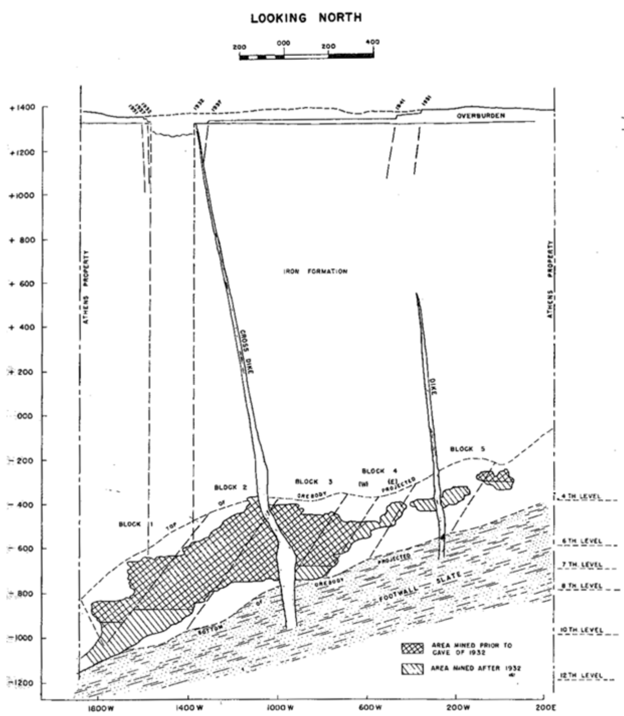

Fig. 29. Athens Mine, east-west longitudinal section.

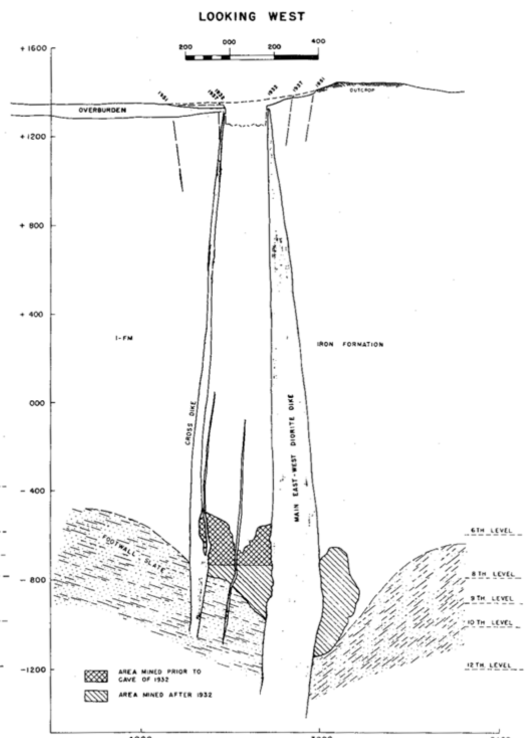

Fig. 30. Athens Mine, north-south cross section.

Bagdad (Arizona, USA)

Source: Hardwick(1959)

Caving Period Reported: 1937-1944

Summary: Mining methods applied at the Bagdad mine are reported, including the block caving of the West orebody. A scaled surface subsidence map is provided showing the boundary of the subsidence area, several collapse features, and the outline of the undercut (note that only the northwest half of the undercut was caved). Based on the reported depth of the undercut (2990 Level, 265 m below surface), it is possible to estimate the caving and fracture initiation angles. No indication is given as to how the subsidence area was measured, although it is assumed that it is not at a resolution that depicts the limits of continuous subsidence but more likely fracture initiation. The source notes that the subsidence area coincides with an area where the top of the ore block is close to surface. Subsequent to this, block caving for the remaining West orebody was gradually phased out. Boundary level drifts were used to control the lateral extent of caving.

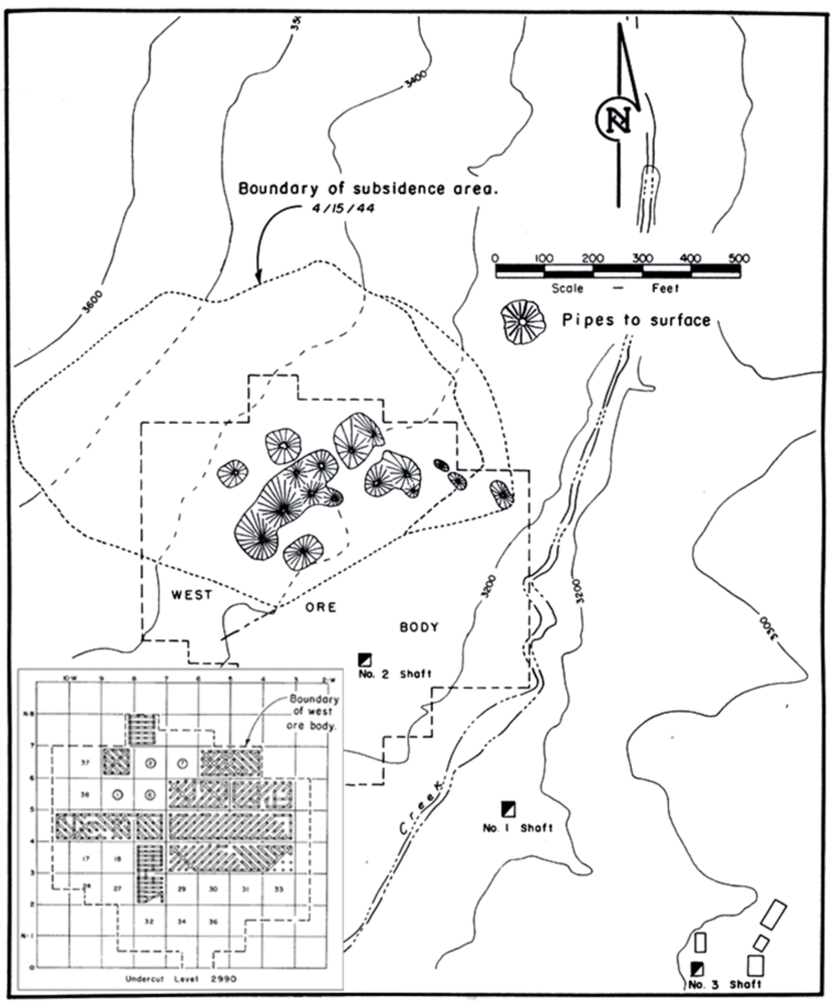

FIGURE 16. - Surface Subsidence.

Cambria Jackson (Michigan, USA)

Source: Boyum (1961), Crane (1929)

Caving Period Reported: 1941-1945

Summary: Data is reported for a sublevel caving operation in hematite iron ore in the Marquette Iron Range of the Negaunee district. This is one of the unnamed regions reported by Crane [12]; see Lake Superior District below. The lowermost level at the time of reporting was at 350 m depth (260 level), with 50 m of mined ore above. The mining method was initially top slicing and then chanced to sublevel caving. A scaled cross-section is provided showing the original topography and the zones of caving and fracture initiation. No direct indication is given as to how the subsidence was measured, but it can assumed that surface surveys were carried out. Cave propagation occurs primarily through a thick, weak hematite iron formation but also through a competent diorite sill near surface.

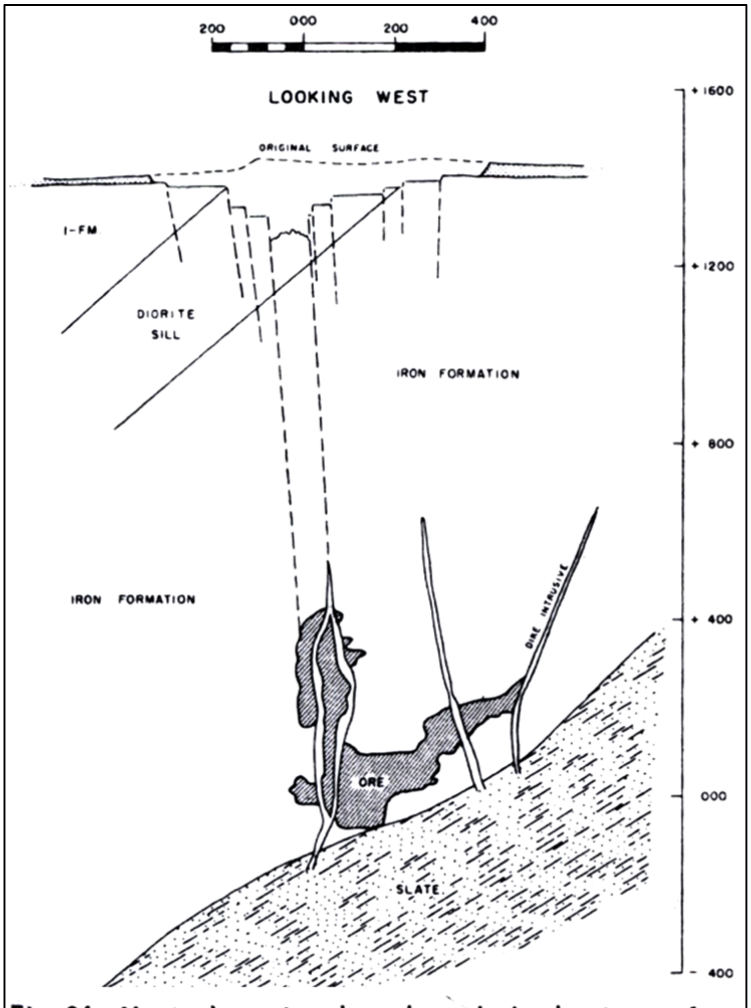

Fig. 26. Vertical section through ore body showing surface cave and terraces.

Catavi (Bolivia)

Source: Weisz (1958)

Caving Period Reported: 1948-1957

Summary: The block caving operations for the Catavi tin mine are described. This includes a cross-section showing the original surface profile, undercut levels, and mining of Block 2 with the corresponding caved area at surface. No direct data in the form of subsidence measurements is given, but the cross section is drawn to scale. Caving is depicted as extending from the 160 level (115 m depth). The extended limits of the subsidence boundary are not included, but the source text reports that surface subsidence of approximately 60° occurred above the undercut level in the first year of block caving.

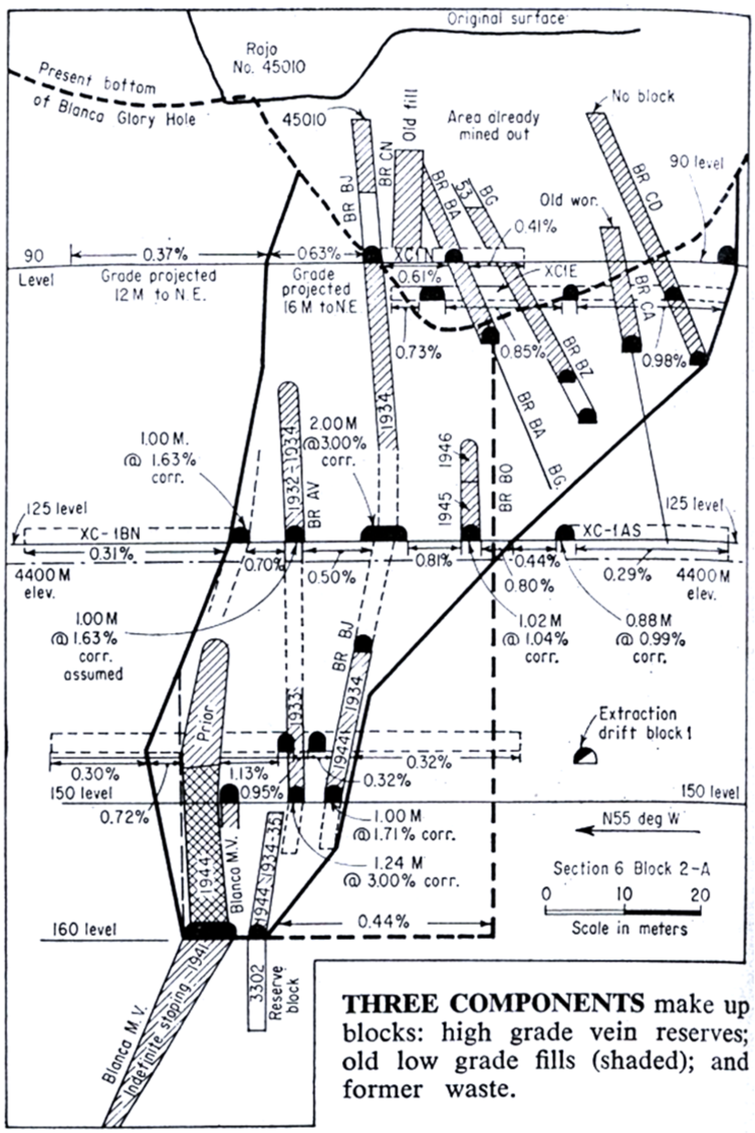

THREE COMPONENTS make up blocks: high grade vein reserves; old low grade fills (shaded); and former waste.

Climax – 1945 (Colorado, USA)

Source: Vanderwilt (1949)

Caving Period Reported: 1940-1945

Summary: Ground movements are reported for the Climax molybdenum mine for block caving above the Phillipson Level. The average undercut depth for this level is 145 m, with caving extending to surface. A representative cross-section is provided that reports initial (1943) and updated caving angles (1945). The cross-section is based on surface observations and mapping and shows the original topography together with a clear zone of caving/collapse from which an angle of fracture initiation can be inferred. Notably, the angle of fracture initiation appears to be affected by the sloping surface topography with subsidence extending up slope through retrogressive slumping of the upper rock scarp.

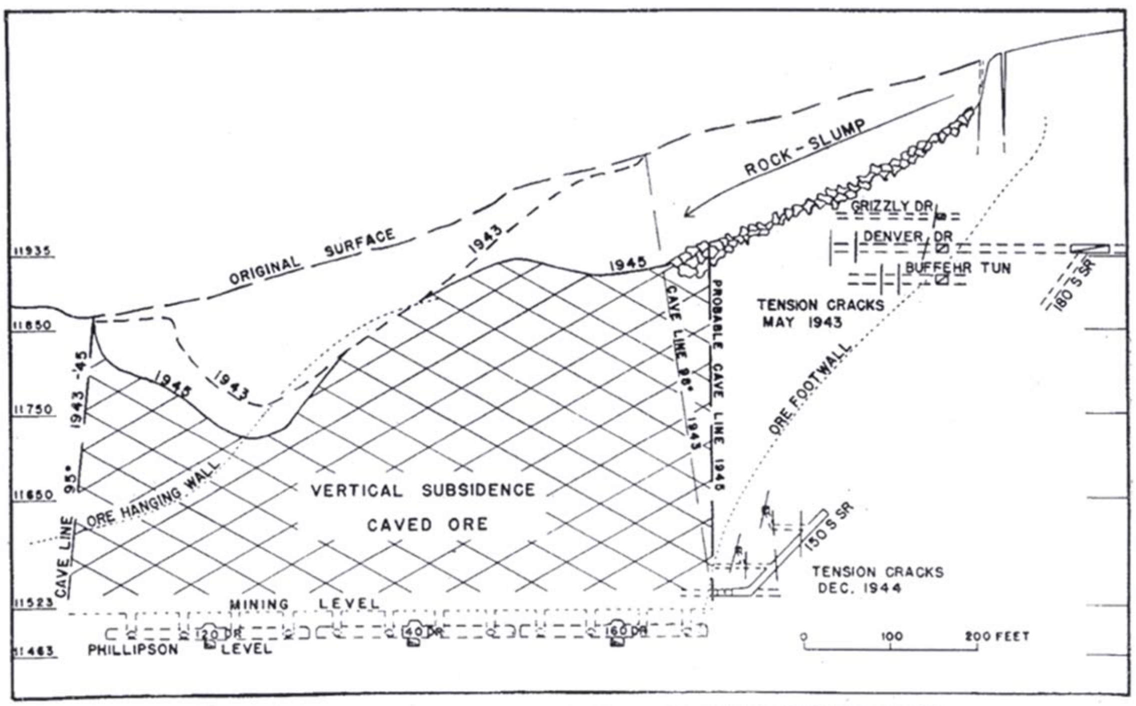

FIG. 3.—SUBSIDENCE, TENSION CRACKS AND ROCK-SLUMP IN THE CLIMAX MOLYBDENUM MINE.

Climax – 1980 (Colorado, USA)

Source: Vera (1981)

Caving Period Reported: 1945-1980

Summary: Caving operations at Climax are described, reporting the changeover to continuous retreat panel caving from block caving of the Phillipson level [56] as the mine moves to deeper levels. No direct data is provided in the form of subsidence measurements, but a schematic cross-section is included which shows the increase in the caving zone with the progression of mining across three levels. No scale bar is provided, but the elevations of the levels are provided from which the scale can be inferred. The panel caves are located under a sloping surface resulting in variable depths to the lowermost undercut (600 Level). With 90 m spacings between levels, the 600 Level is 180 m below the Phillipson and has an average depth of 325 m. The caving angle information provided in the cross section is significantly less detailed than the earlier data provided by the Vanderwilt [56], as the paper is more focussed on the general operations.

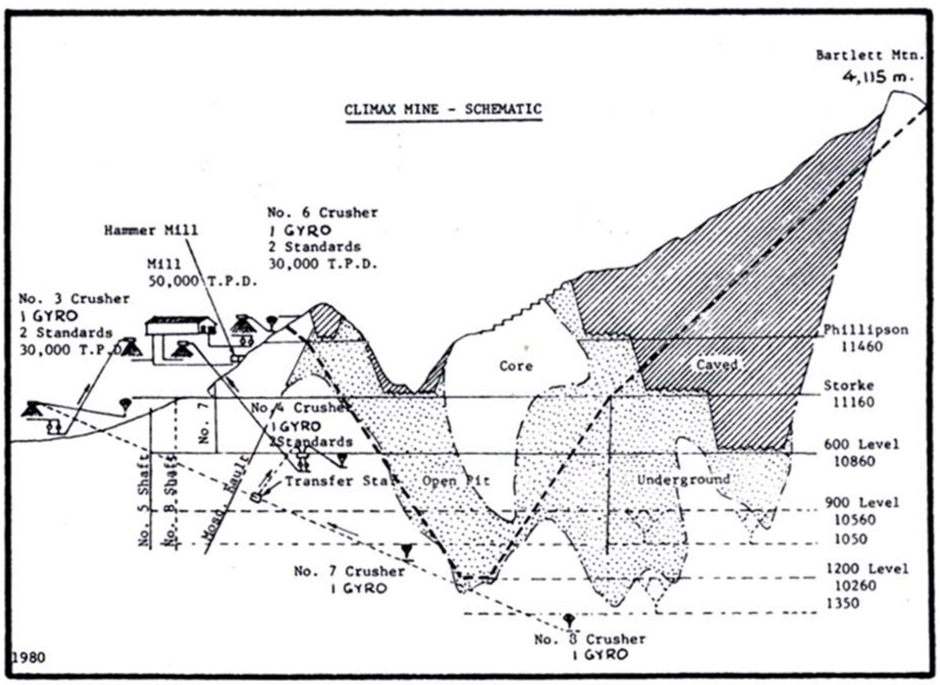

Figure 32. General Mine Layout-Schematic

Copper Mountain (B.C., Canada)

Source: Nelson & Fahrni (1950)

Caving Period Reported: 1937-1949

Summary: Subsidence data is reported for a combination of shrinkage stoping and sublevel caving of two copper porphyry ore bodies, named Contact Block and 122-East Block. In both cases, the caved ground extends to surface. The maximum undercut depths are 350 m (Contact Block) and 210 m (122-East Block) with sub-levels above. Scaled cross-sections are provided for both blocks showing the original topography, extent of subsidence, surface scarps and zone of caving/collapse. From these, the angle of subsidence is reported and angles of fracture initiation and caving can be inferred. For the 122-East Block, the angle of subsidence measured from the cross-section varies with the lower angle reported being parallel to a dipping fault. The subsidence features reported in these cross-sections were based on surface surveys, mapping and aerial photographs. These were subsequently used to calculate ratios of total subsidence to ore extraction for the two blocks.

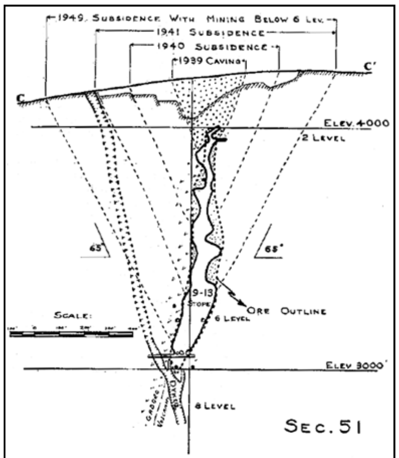

Figure 1.— Section across contact orebody.

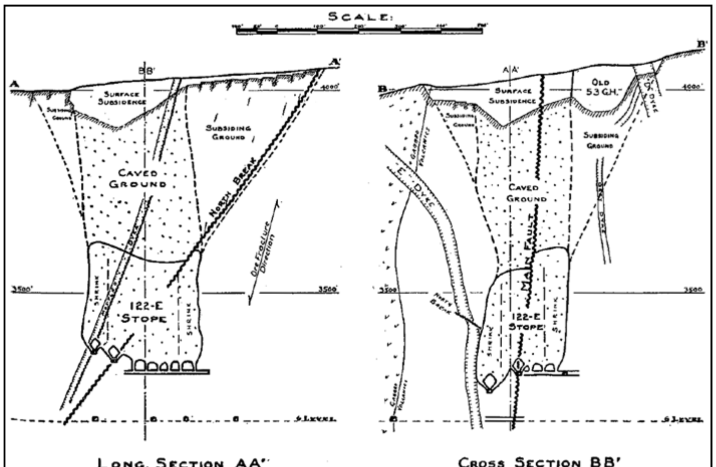

Figure 2.—Sections through 122E orebody.

Copper Queen Branch – East Orebody (Arizona, USA)

Source: Kantner (1934)

Caving Period Reported: 1925-1933

Summary: Data is reported for block caving of several lifts of a copper porphyry deposit (East Orebody), which due to their short heights (9-36 m) and inclined nature, is more representative of a sublevel caving operation (and is classified as such in the above Tables). The initial and final undercut levels in the source paper are 140 and 285 m below the surface, respectively. Caving at surface appears in the form of measured subsidence (elevation surveys), tension cracks and several small glory holes, the latter likely reflecting the sublevel nature of the caving. A scaled cross-section is provided reporting the angle of break and angle of subsidence for each lift. However, the terms used by the author differ from the terminology used here by Van As et al. (2003). In the Discussion that follows the paper, reference is made to subsidence being the steeper angle of “marked” subsidence, with the break angle being the limit of visible cracking in the same section. These are interpreted here as referring to the caving and fracture initiation angles, respectively. Rock mass conditions influence the resulting angles, with lower angles developing in the weaker hangingwall relative to those that develop in the stronger footwall. The presence of a major fault to the north and northwest may also play a controlling role as no cracking beyond this fault was observed for a period of time.

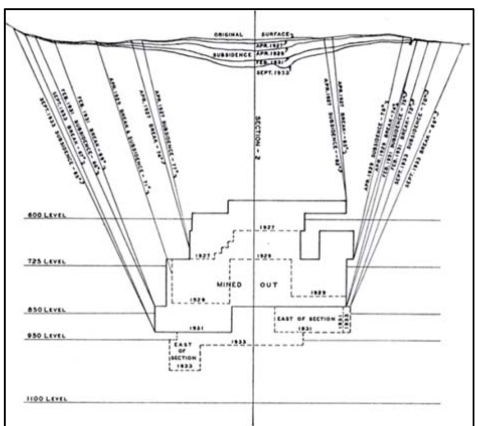

FIG. 3.—SECTION 1. LOOKING WEST. SHOWING BREAK, SUBSIDENCE AND MINING AS OF APRIL, 1927 AND 1929, FEBRUARY, 1931 AND SEPTEMBER, 1933.

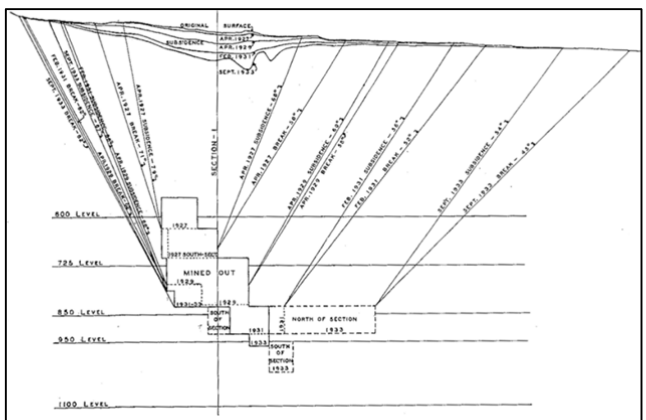

FIG. 4.—SECTION 2. LOOKING NORTH. SHOWING BREAK, SUBSIDENCE AND MINING AS OF APRIL, 1927 AND 1929, FEBRUARY, 1931 AND SEPTEMBER, 1933.

Copper Queen Branch – Queen Hill Block (Arizona, USA)

Source: Trischka (1934)

Caving Period Reported: 1913-1933

Summary: Data is provided for the Queen Hill Block of the Copper Queen mining area, near but separate from the East Orebody block described above. The top slicing mining method was utilized with two main levels being caved (200 and 300 Levels) along a sub-horizontal, tabular orebody. The mining levels cross under a steep hill with depths ranging from 30 to 210 m. A cross-section is provided showing the pre-mining and "present" topography (note that no indication is given as to when mining was completed; top slicing was initiated in 1913 replacing a square set method). Reported is the fracture initiation angle, although this also corresponds to the caving angle and subsidence angle as the caved block is described as being bounded on all four sides by faults, along which the block drops and across which the subsidence disturbance is limited.

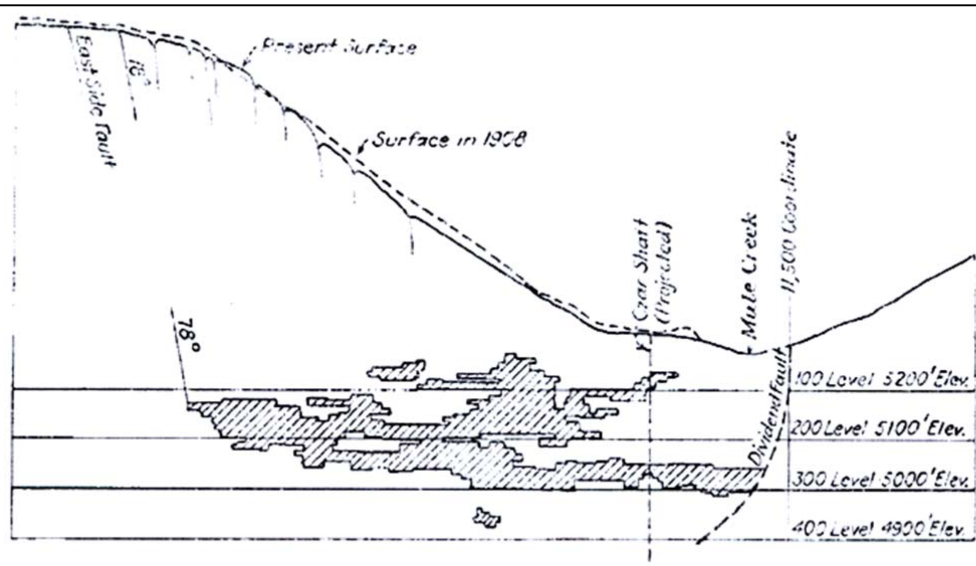

FIG. 2.—SECTION A-A OF FIG. 1. LOOKING NORTHWEST THROUGH OREBODIES PROJECTED 100 FT. EACH SIDE OF SECTION.

Corbin

Source: Warburton (1936)

Caving Period Reported: 1917-1934

Summary: Data is provided for the mining of a thick coal seam (No. 6 mine) split into two sections, West and East, separated by a rock instruction (i.e. wedge of waste rock). The West block was mined by block caving using a number of lifts at 20 m intervals, the lowest of which being at 80 m at the time of reporting. The neighbouring East block was mined by top slicing, the undercut for which is inclined, dipping at 38° and extending from surface to 2 Level at 95 m depth. A schematic cross-section is provided from which the caving angles and undercut depths can be estimated. No scale is provided, but associated information is provided that allows the scale to be approximated. The lower caving angle for the East block aligns with the dip of the undercut.

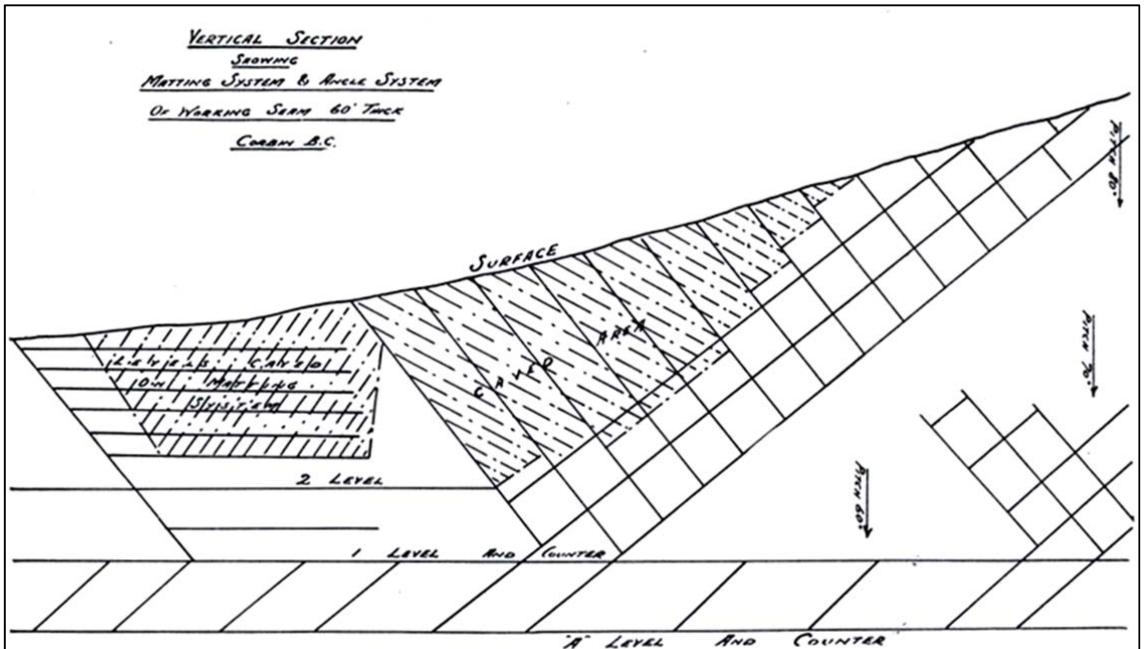

Figure 2.

Creighton (Ontario, Canada) – 1955

Source: Brock et al. (1956)

Caving Period Reported: 1951-1955

Summary: Data is reported for panel caving at the Creighton mine, subsequent to earlier mining by shrinkage stoping. Blasting was used to induce caving beyond limits of previously mined stopes. A schematic cross-section is provided that shows the caved stopes mined by shrinkage stoping beneath a 60 m deep open pit, and the neighbouring cave mined by panel caving along the strike of the orebody. From this cross-section, a caving angle can be estimated at the time of break through at surface, but little additional information is provided. Draw in the panel cave is limited by a cut-off grade given the dilution arising from the cap rock above hangingwall.

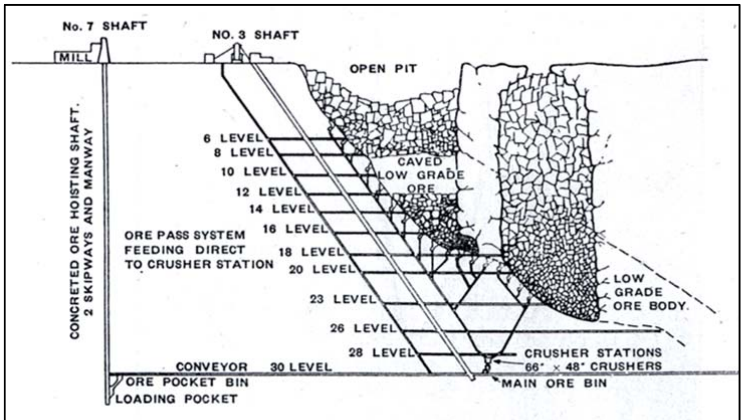

Fig. 7.—Diagrammatic section, first stage of panel caving.

Creighton (Ontario, Canada) – 1963

Source: Dickhout (1963)

Caving Period Reported: 1951-1963

Summary: Mining operations and ground control issues for the Creighton mine are reported. The increased time interval from that reported by Brock et al. [6] represents a more fully developed cave, which although not specified, appears to include the pillar between the earlier shrinkage stoping operation and subsequent panel caving. No direct subsidence measurements are reported, however a general cross-section is provided that shows the development of caving relative to the different levels, from which the depth of mining can be estimated (420 m). Furthermore, in the Discussion that follows the paper, it is explained that the outline of the surface cave closely follows the outline of the completed undercut, with the exception of the hangingwall where the cave extends beyond the footprint of the undercut. A plan view map showing the outline of the limit of fracturing is provided and the angles of caving and fracture initiation relative to the undercut are specified. Strain gauge measurements are also reported with respect to specifying the angle of subsidence.

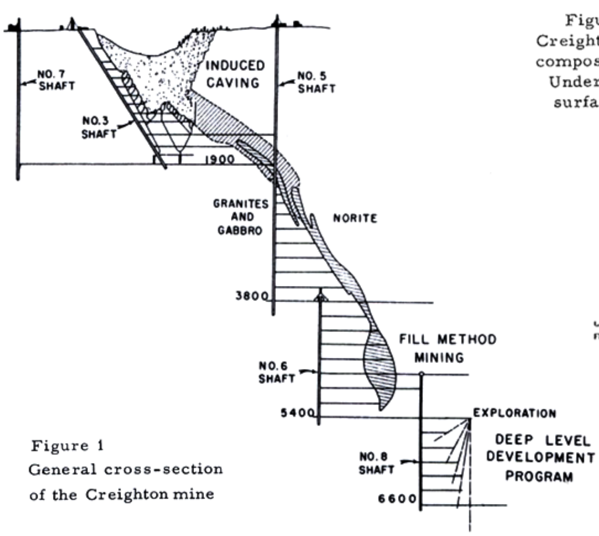

Figure 1
General cross-section of the Creighton mine

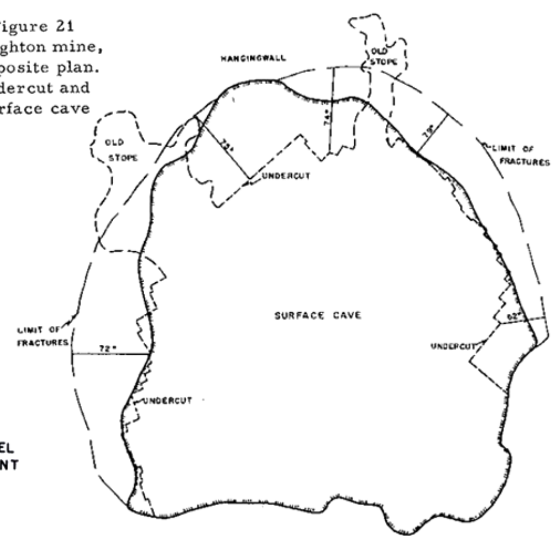

Figure 21
Creighton mine, composite plan. Undercut and surface cave

Crestmore (California, USA)

Source: Long and Obert (1958)

Caving Period Reported: 1930-1954

Summary: Mining operations are reported for the block caving of a dipping limestone bed. No direct data is provided in the form of subsidence measurements, but a schematic cross-section is included illustrating the mining of Block 1A. Included are the caved ground at surface and a rough outline of the fracture initiation from which an estimate of its angle is possible. The depth of the undercut is 60 meters. Vertical cutoff stopes were excavated on all four sides of the block to limit the caving angle. However, the fracture initiation angle on the footwall side of block extended beyond the cutoff stope to align with a shallower dipping fault.

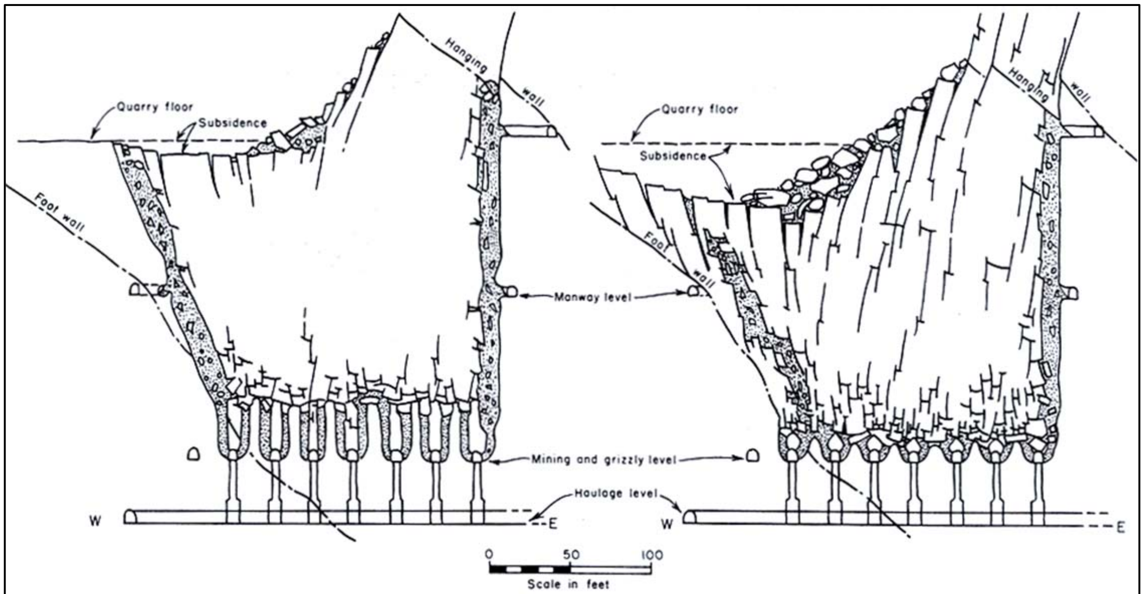

FIGURE 10. - Section A-A' Through Block 1A After Vertical Pillars Z and W Had Been Broken by Blasting.

FIGURE 11. - Section A-A' Through Block 1A, Showing the Initiation of Caving Action After Remnants of the Undercut Pillars Had Been Removed by Blasting.

El Teniente (Chile) – South 1 & North 4

Source: Ovalle (1981), Kvapil et al. (1989)

Caving Period Reported: 1940-1980

Summary: Mining operations at the El Teniente mine are reported for the panel caving of the South and North blocks from the Teniente 1 and 4 levels, respectively. No direct data is provided with respect to subsidence measurements, however two schematic cross-sections are included illustrating the mining of the North and South blocks. Shown are those caves already exhausted and those currently in production, together with the original and caved surface profiles. A similar cross-section for the North block is produced by Kvapil et al. [32] but is less detailed. No scale bar is provided, but the different mine levels are shown from which the undercut depths can be estimated. Because the mine is positioned below a steep slope, with the South block being downslope of the North block, the depths to the respective undercut levels, Teniente 1 and 4, are approximately the same (510 and 540 m, respectively). The lower caving angles occur on the uphill side.

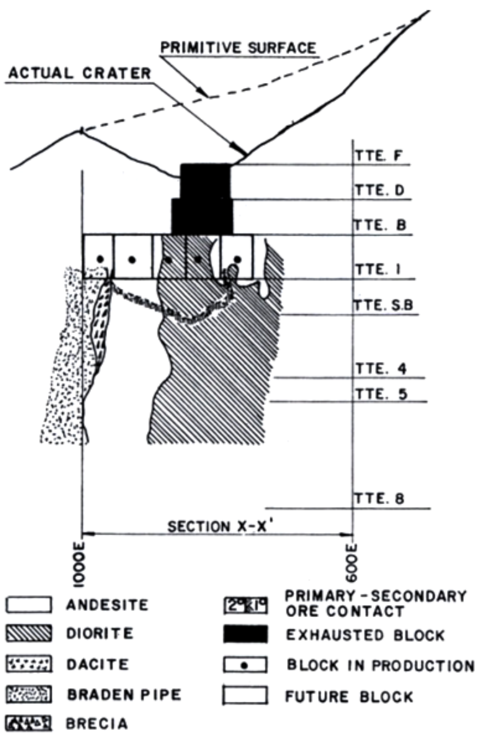

FIGURE 4. Geology and Blocks. South Mine Cross Section

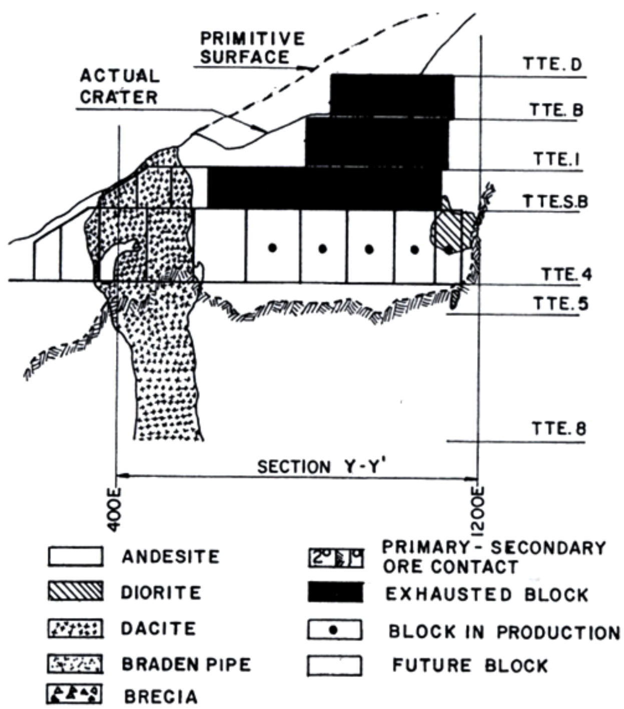

FIGURE 5. Geology and Blocks. North Mine Cross Section

El Teniente (Chile) – Regimiento 4

Source: Brown (2003)

Caving Period Reported: 1982-1998

Summary: A review of break angles is reported for the caved zone above El Teniente's 4 Level, Regimiento Sector. Curves are provided for estimating break angles measured as a function of depth along the crater walls. These show that angles near the undercut are sub-vertical, gradually flattening towards surface. Minimal details are given with respect to the data the curves are based on. Similar curves for other sectors at El Teniente are reported to be based on observations of fracturing in galleries at different levels [44]. In this case, reference is made to the use of numerical models calibrated against observations. No depth is given, but based on other sources can be estimated to be approximately 250 m deep (averaging for steep topography). From this, the caving angle at surface can be estimated from the respective curves.

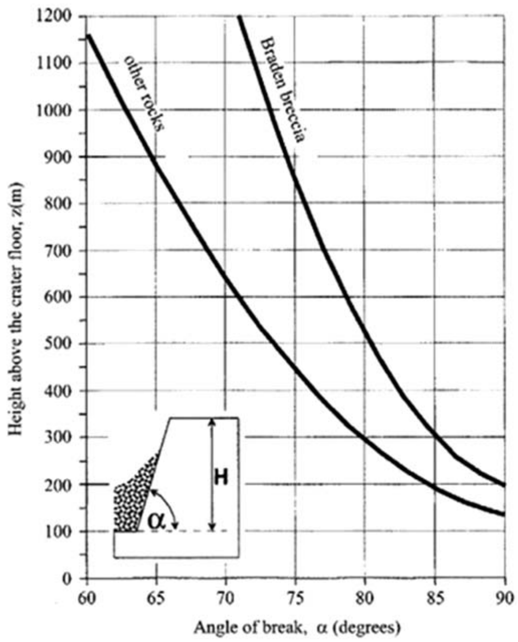

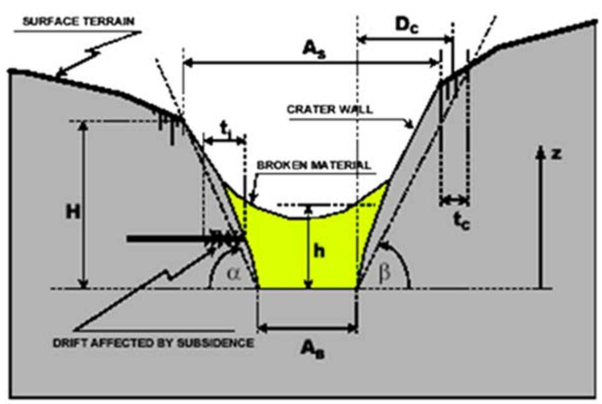

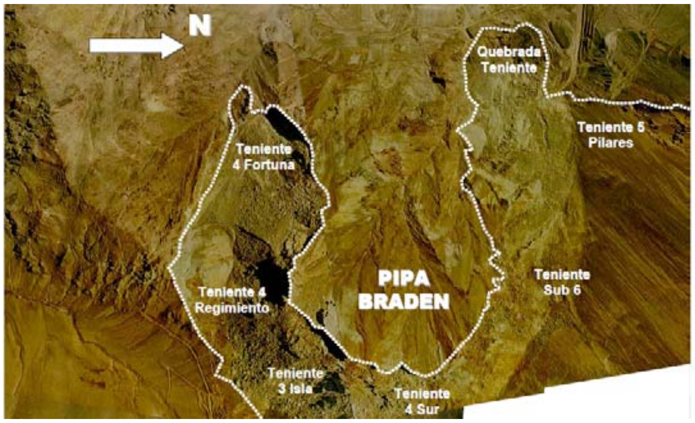

El Teniente (Chile) – Esmeralda

Source: Rojas et al. (2001)

Caving Period Reported: 1997-2001

Summary: Panel caving operations for the Esmeralda sector are reviewed. Included is a design chart of break angles as a function of height above the undercut, based on numerical models calibrated against crater geometry data and observations of fracturing in galleries at different elevations. Separate curves are provided for the uphill and downhill sides of the cave. A cross-section is also provided that depicts the caving angle and angle of fracture initiation referred to as the “influence level”. The undercut is located under steep slope at an average depth of approximately 800 m.

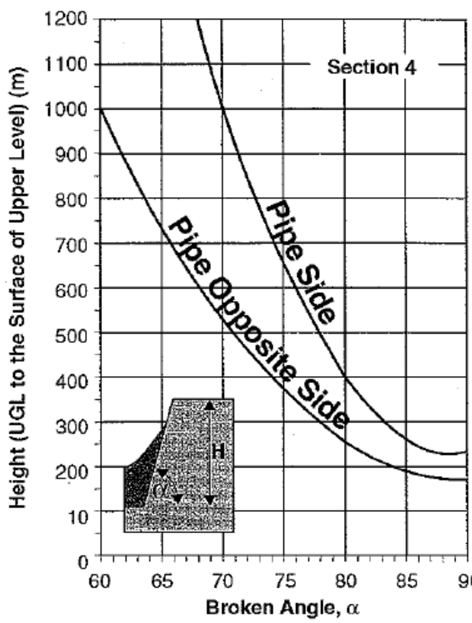

FIGURE 51.17 Variation of breakage angle with height over undercut level for section 4 (El Teniente Sur and Esmeralda sector)

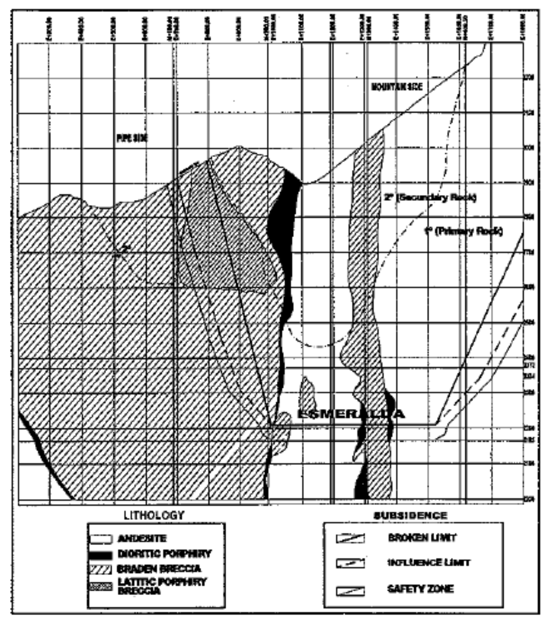

FIGURE 51.18 Southwest-northeast section through Esmeralda sector showing expected subsidence limits (defined by breakage angle and zone of influence)

Finsch (South Africa)

Source: Preece & Liebenberg (2007)

Caving Period Reported: 2004-2006

Summary: Cave management operations are reported for the block caving of Block 4 at the Finsch diamond mine. Caving of the kimberlite pipe above the undercut at 700 m depth occurs over a block height of 150 m that then opens up into the bottom of a 550 m deep open pit that had been subsequently deepened by the mining of previous blocks using open stoping techniques. A cross-section is provided, which shows the limits of the caving zone, which coincides with the angles of the already existing crater.

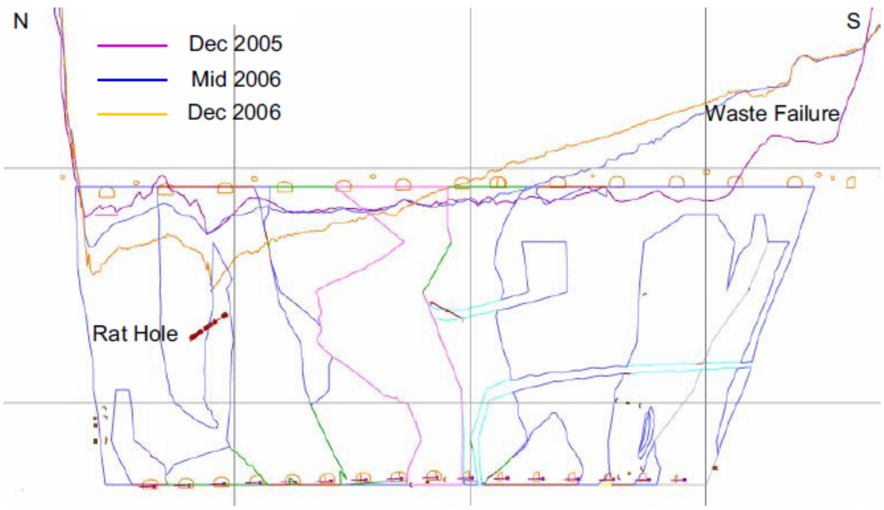

Fig.11. GEMCOM generated section showing ALS profiles with outline geology and drift positions on 53 and 63 Levels showing

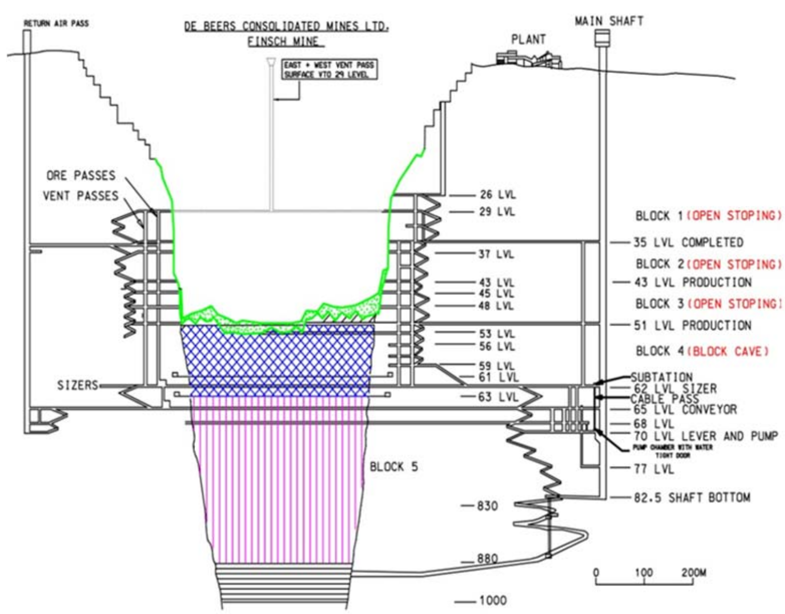

Fig. 2 Section through Finsch Mine showing mining blocks

Gath's (Zimbabwe)

Source: Brown and Ferguson (1979)

Caving Period Reported: 1971-1976

Summary: Data is provided for a sub-level shrinkage stoping operation for three different sublevels (99, 158 and 183 Levels; block caving is planned for subsequent deeper levels). Caving occurs in the hangingwall and extends to surface above the 40-50° dipping orebody. The depth of each level is variable as the topography above is steep across what appears to be a 100 m deep open pit slope. A cross-section is provided, which shows the different angles of break and surface tension cracks for each sub-level. Caving angles on the footwall side of the orebody coincide with the dip of the orebody and footwall parallel jointing.

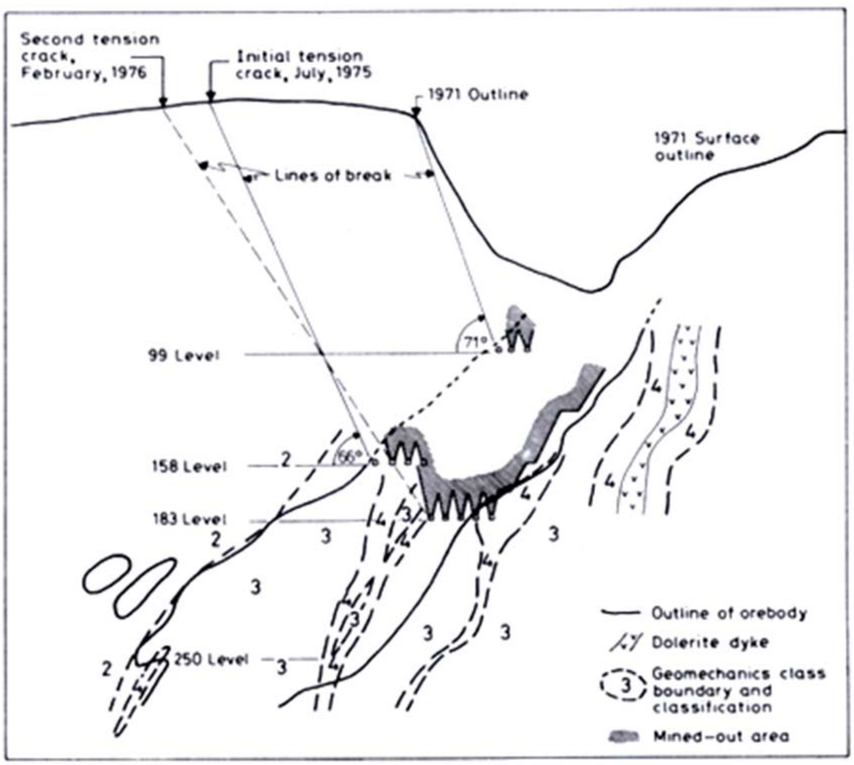

Fig. 2 Section through orebody, 620 section

Grace (Pennsylvania, USA)

Source: Sainsbury (2010)

Caving Period Reported: 1958-1977

Summary: Subsidence observed after the closure of the Grace iron mine is reported following panel caving of the deposit from 1958 to 1977. Reported are surface observations together with survey data based on levelling measurements of subsidence pins. A subsidence map is provided showing the limits of surface cracking and the outlines of a lake that formed in the caving zone and the relative position of the undercut. Based on the approximate depth of the undercut, caving and fracture initiation angles can be estimated. It should be noted that cave breakthrough only occurred above one half of the undercut, facilitated by a steeply dipping fault.

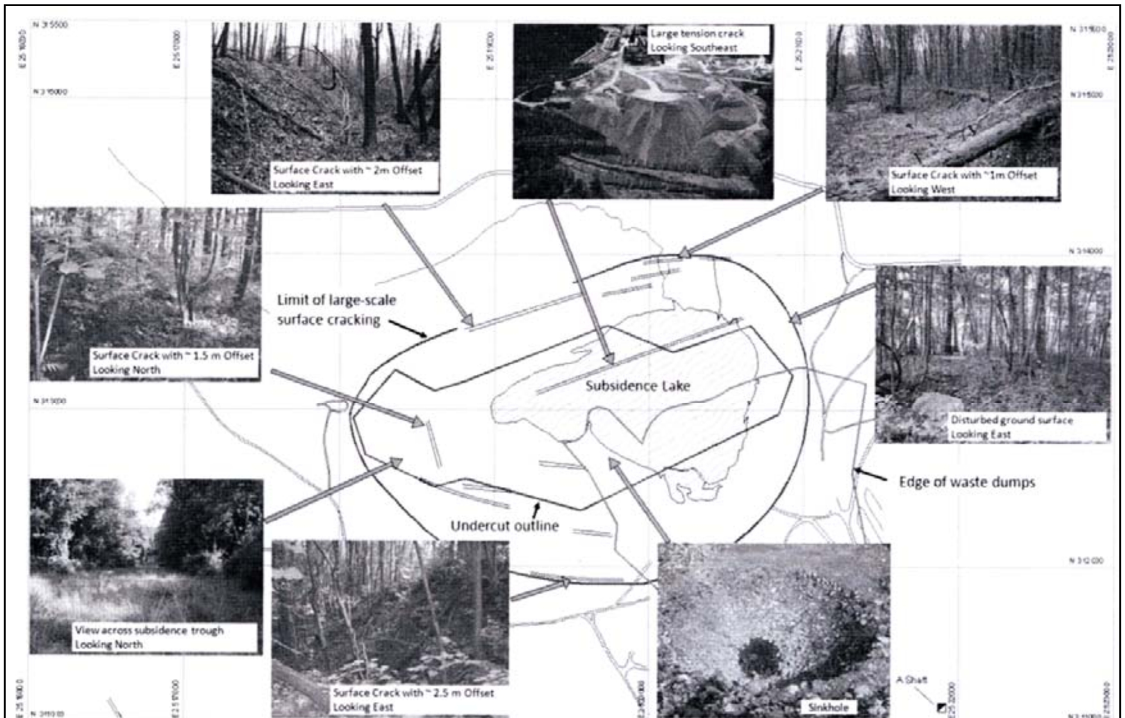

Figure 7 Limit of large-scale surface cracking

Grangesberg (Sweden) - 1961

Source: Hoek (1974)

Caving Period Reported: 1921-1961

Summary: Hangingwall failures induced by sub-level caving are reported for six different sublevels (from 140 to 300 m depth) during the mining of an iron ore deposit. The orebody is approximately 54 m thick dipping at 64°. Data is provided in the form of a simplified cross-section showing the caving angle for each sublevel. Few additional details are provided, with references pointing to a Swedish report as the original source. It was observed that the deeper the caving, the lower the caving angle on the hangingwall side. The angle of caving on the footwall side is shown to be constant (with depth), coincident with the contact between the orebody and host rock.

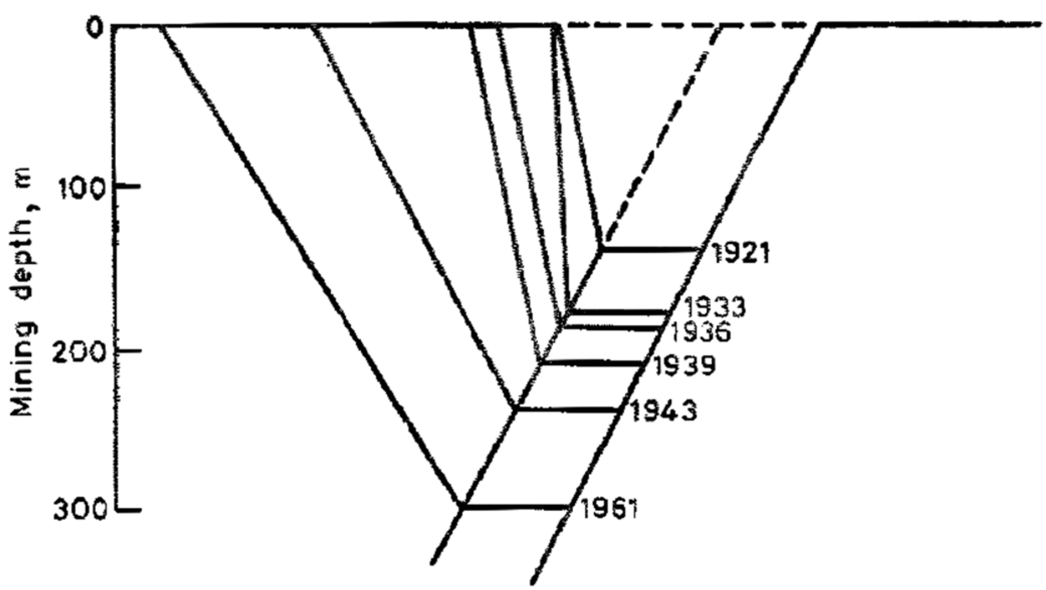

Fig. 8 Hanging-wall failure induced by caving at Grangesborg

Grangesberg (Sweden) - 1974

Source: Sisselman (1974)

Caving Period Reported: 1960-1975

Summary: Mining operations at the Grangesberg iron ore mine are described, reporting the use of both sublevel and block caving methods depending on the ore thickness. Approximately 70% of the mining is by block caving. A cross-section is provided showing the extent of the caving zone relative to the undercut level at 410 m depth. The orebody is approximately 54 m thick dipping at 64°. No details are provided with respect to the measurement of surface subsidence. The angle of caving on the footwall side is shown to be coincident with the contact between the orebody and host rock.

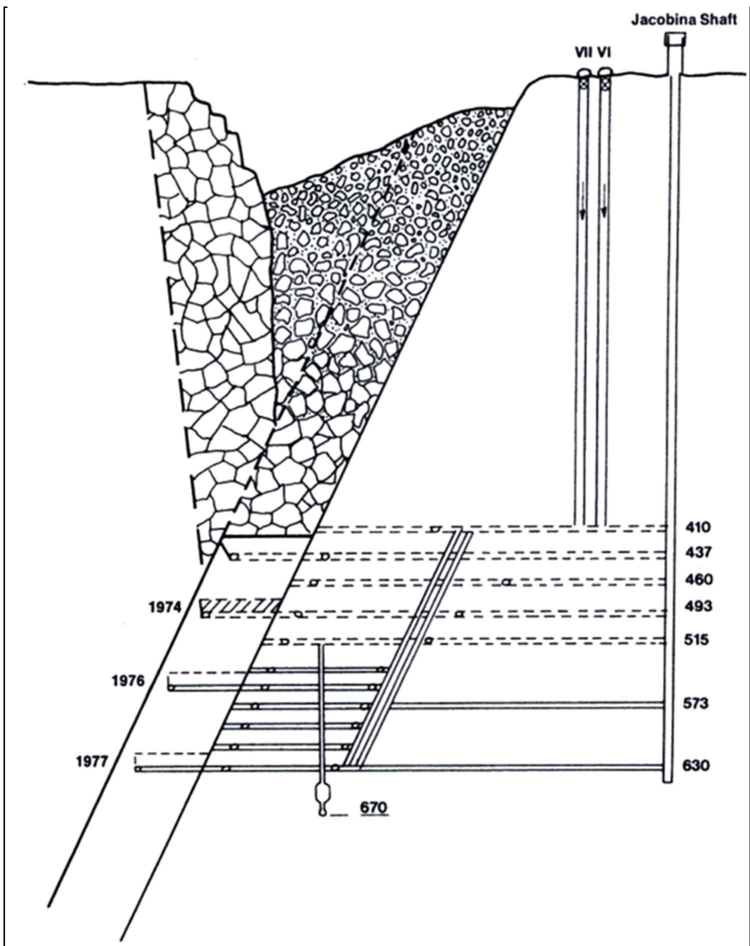

(Left) Cross-section of continuous block caving. New method will greatly reduce risk of accident when ore is loaded, transported and when handling rock hang-ups.

Grasberg (Indonesia) – IOZ

Source: Hubert et al. (2000), Barber et al. (2001)

Caving Period Reported: 1980-2000

Summary: Block caving of P.T. Freeport's Ertsberg East Skarn System is reported, including the operations for the Gunung Bijih Timur (GBT), Intermediate Ore Zone (IOZ) and Deep Ore Zone (DOZ) caving sectors. Focus is given to the IOZ. No direct data is provided in the form of subsidence measurements in either source, but scaled cross-sections are included showing the development of caving above the IOZ. Included are the boundaries of the caving zone relative to the undercut level at 650 m depth. The cross-section in Hubert et al. [27] also includes the limits of fracture initiation referred to as the "subsidence zone". The IOZ undercut is located under a steep slope, for which the lower caving angle corresponds with the uphill side.

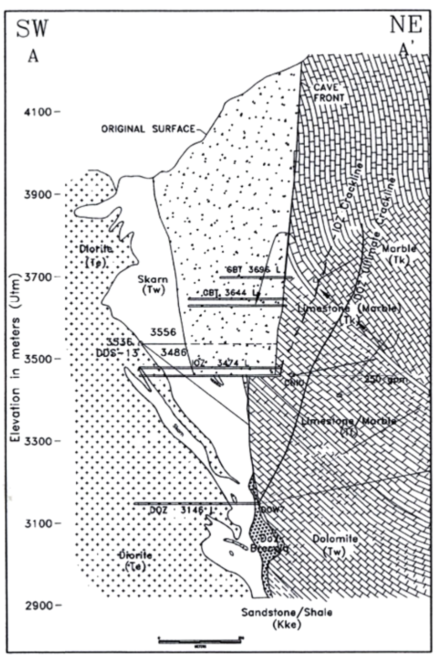

FIGURE 53.4 Geological section of EESS

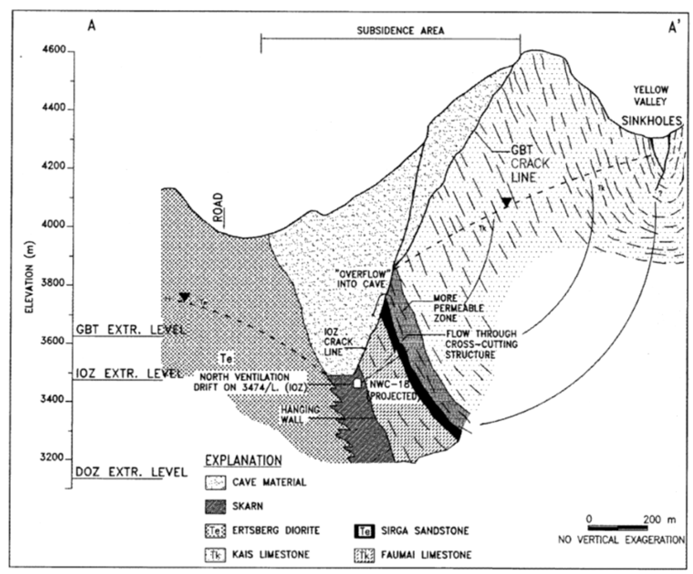

FIG 2 - Schematic long section of GBT, IOZ and DOZ.

Havelock (Swaziland)

Source: Heslop (1974)

Caving Period Reported: 1952-1966

Summary: Data is reported for three levels of a shrinkage stoping and sublevel caving asbestos operation. The lowermost undercut is at approximately 225 m depth (no direct information for depth is given; estimates can be made based on a scaled cross-section). A cross-section is provided, which shows the different angles of caving and extent of flexural toppling and surface fracturing above the hangingwall for different periods of time corresponding to the development of the different levels. Caving angles on the hangingwall side are seen to remain constant, while the zone of fracture initiation increases. Caving angles on the footwall footwall side are likewise shown as being constant and aligned parallel to the dip of the foliation and bedding.

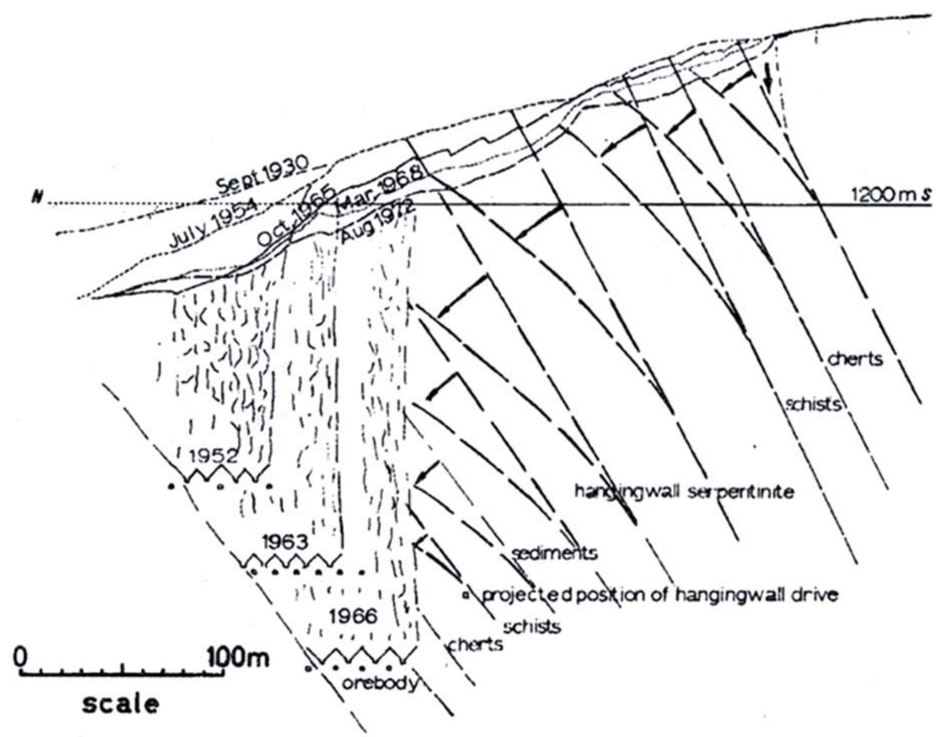

FIG 2 SECTION THROUGH THE HAVELOCK SUBSIDENCE ZONE
Illustrating the development of the subsidence zone by tilting towards the mining.

Henderson (Colorado, USA) – 8100

Source: Brumleve & Maier (1981), Stewart (1984)

Caving Period Reported: 1976-1983

Summary: Subsidence at Henderson is reported by Stewart [48] for panel caving of the 8100 Level along Panel 1. The cave zone is reported to have appeared on surface four years after caving was initiated, with cave growth and subsidence being measured using aerial photography, surface surveys and TDR. Data is provided in the form of a block diagram and subsidence maps showing the outline of the caving zone on surface relative to the undercut at 1050 m depth. A cross-section showing the caving angles extended from the undercut is provided by Brumleve & Maier [10] in their description of the rock mass response to panel caving. These were used to estimate the angles of caving. Vertically spaced boundary cutoff drifts together with steeply dipping faults contributed to the vertical nature of the cave that developed. The caving zone was observed to not change in its direction despite the advance of the caveline, likely due to the controlling influence of topography and faulting.

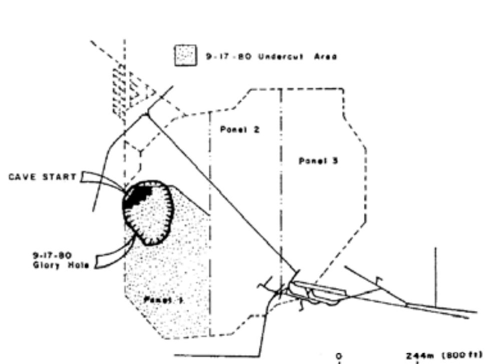

Figure 5. Position of initial surface disturbance relative to undercut area

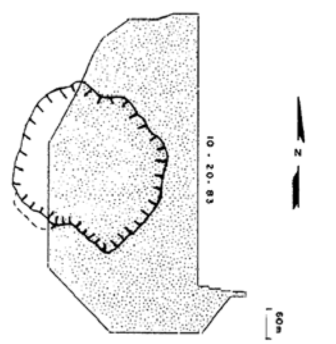

Figure 10. Glory-hole growth between September 1980 and October, 1983

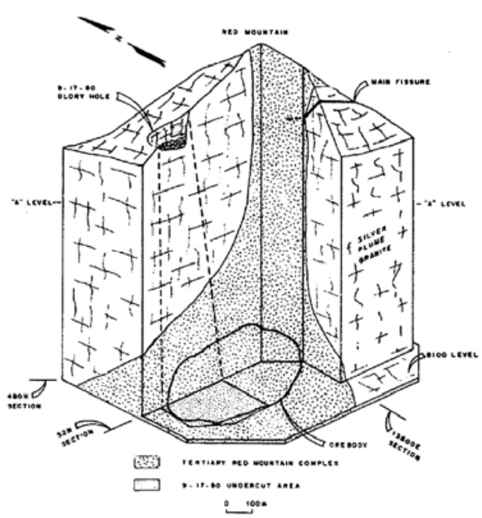

Figure 8. Position of initial surface disturbance relative to the Red Mountain igneous complex

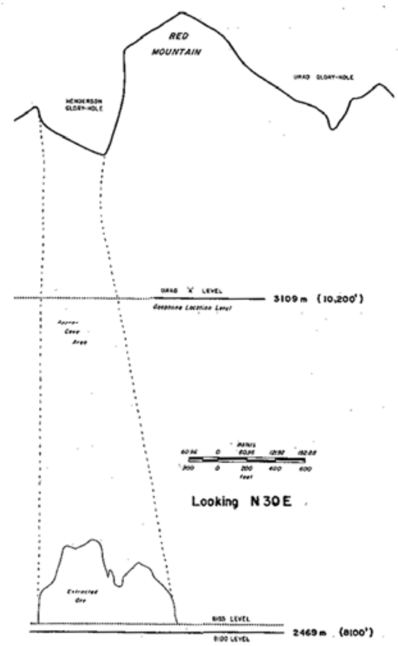

Figure 20. Cross section of Urad and Henderson mines.

Henderson (Colorado, USA) – 7700 Level

Source: Rech et al. (2000)

Caving Period Reported: 1976-2000

Summary: An update on the panel caving operations at Henerson is reported, describing the mining of the 7700 Level following the depletion of the 8100 Level. The 7700 Level is 100 m below the 8100 Level at approximately 1150 m depth. No direct data is provided in the form of subsidence measurements, but a schematic cross-section is included showing the boundaries of the caving zone above the 7700 Level undercut. No scale bar is provided, but the different levels are shown from which the scale can be calculated. It is assumed the section is roughly drawn to scale. Vertically spaced boundary cutoff drifts together with steeply dipping faults contribute to the vertical nature of the cave that developed.

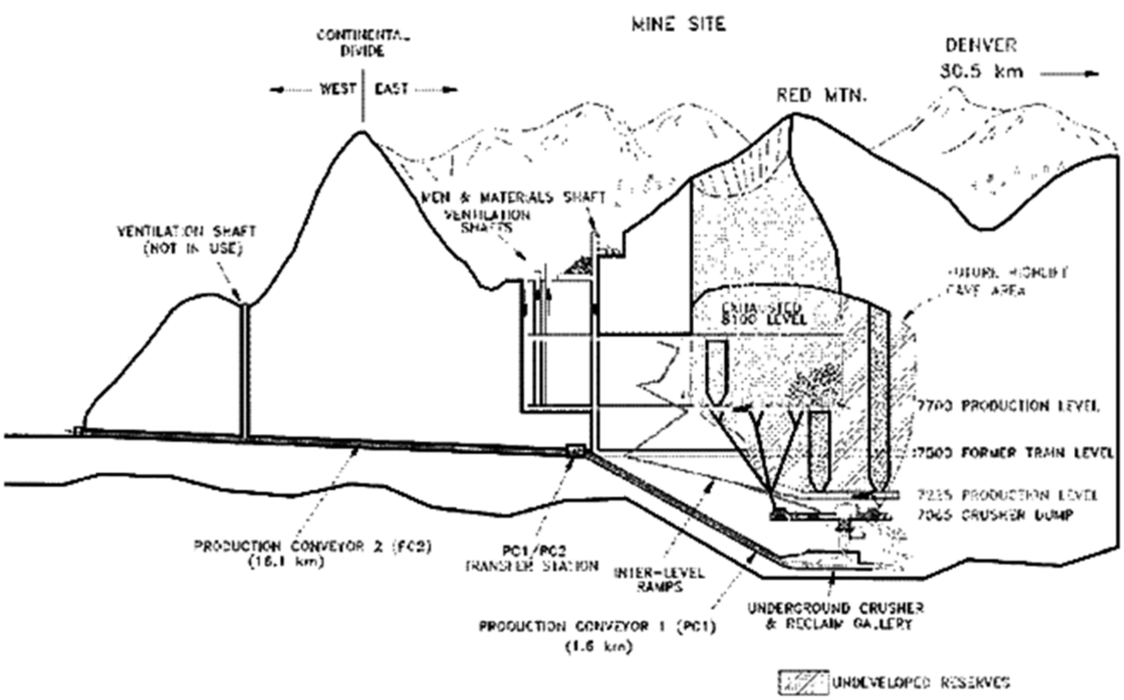

FIG 1 - General cross-section of the Henderson Mine and Mill.

Inspiration (Arizona, USA)

Source: Hardwick(1963)

Caving Period Reported: 1954

Summary: The history of mining operations at Inspiration is reviewed; the Inspiration mine is adjacent to the Miami block cave mine. The report includes details on the transition from block caving to open pit mining in 1954. Specifically, the block caving of a transfer block is reported from an undercut 70 m below the pit bottom. Data is provided in the form of a scaled cross-section showing the outlines of the caving zone over time, from which the caving angles can be calculated.

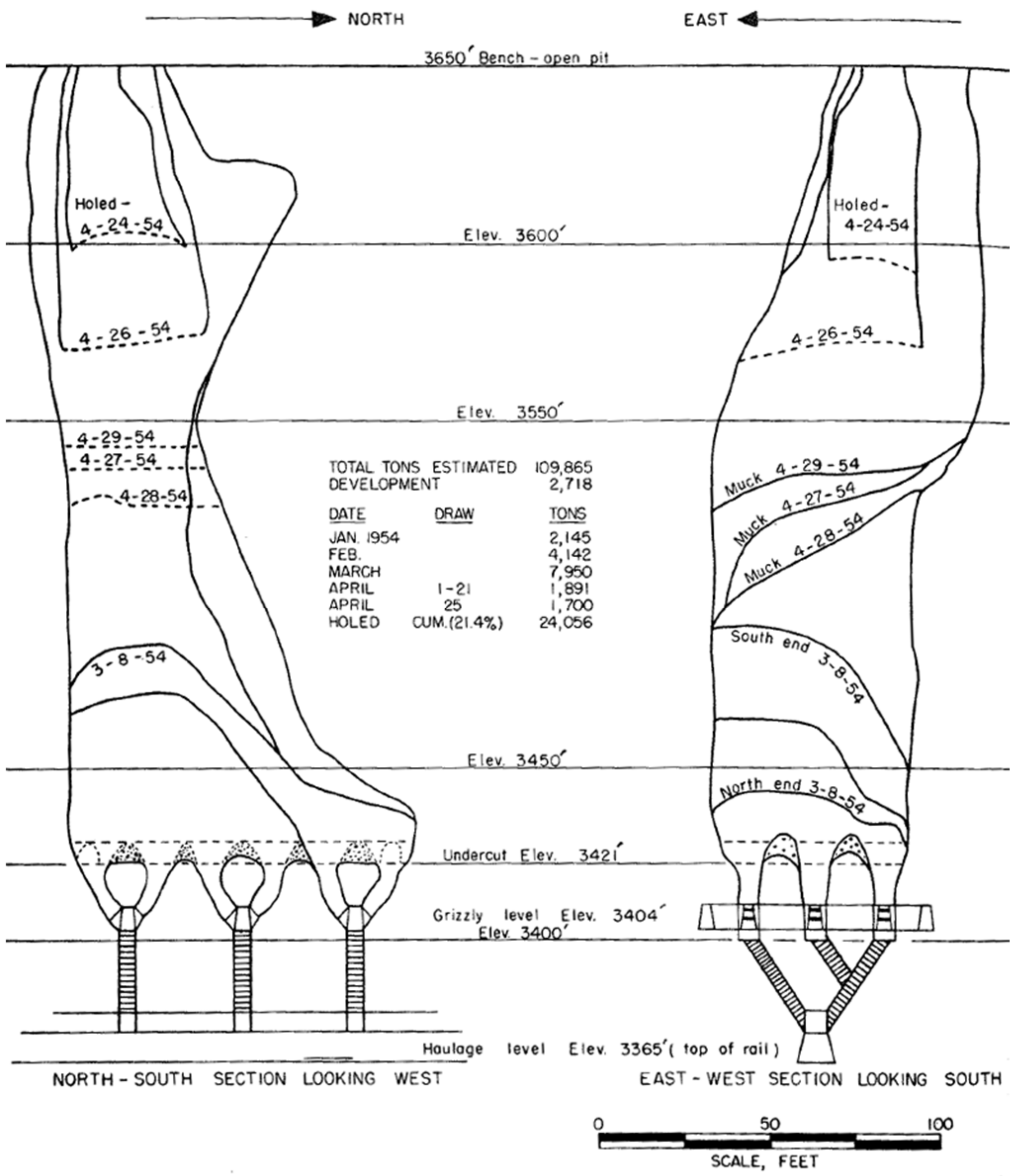

FIGURE 8. - Section Through Transfer Block.

Jagersfontein (South Africa)

Source: Stucke (1965)

Caving Period Reported: 1947-1962

Summary: Plans to block cave a new lift at the Jagersfontein diamond mine are reported. The description includes a schematic cross-section showing the current block caving undercut level at 550 m depth and earlier workings, including an older open pit operation. The cross section shows that the limits of the caving zone roughly coincide with the boundaries of the kimberlite pipe and already existing crater. It is reported that approximately one million tonnes of waste rock from the crater walls slough into the crater each year.

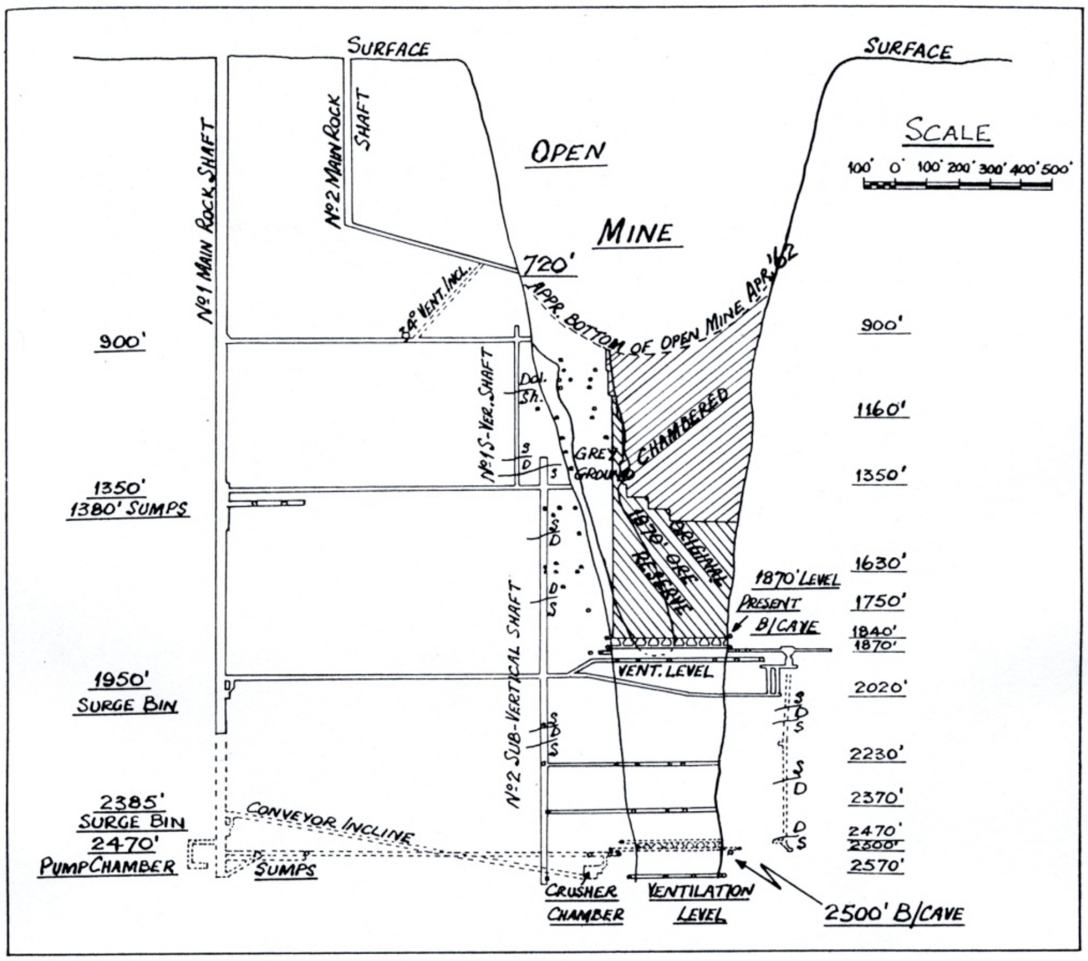

Fig. 1—Jagersfontein Mine. Diagrammatic section through Y + 31660 looking west

Jenifer (California, USA)

Source: Obert & Long (1962)

Caving Period Reported: 1952-1957

Summary: Data is reported for a single block cave experiment in a thick, sub-horizontal borate deposit, where previous mining was by room and pillar. The undercut level is at a depth of 160 m with a block height of 70 m. Caving of the orebody and overlying cap rocks extended to surface, although longhole blasting at intermediate depths was required to aid caving of the ore. A scaled cross-section is provided showing a clear zone of caving/collapse, and a plan view map is provided showing subsidence contours (with 10' contour intervals). Both show that the caved ground propagated slightly to the southeast of the undercut area. One of the unique features of the caving zone was that its periphery was marked by a single, continuous, steep-wall face. Little to no change in the peripheral outline of the subsided area occurred over the 4.5 year period following the initial subsidence.

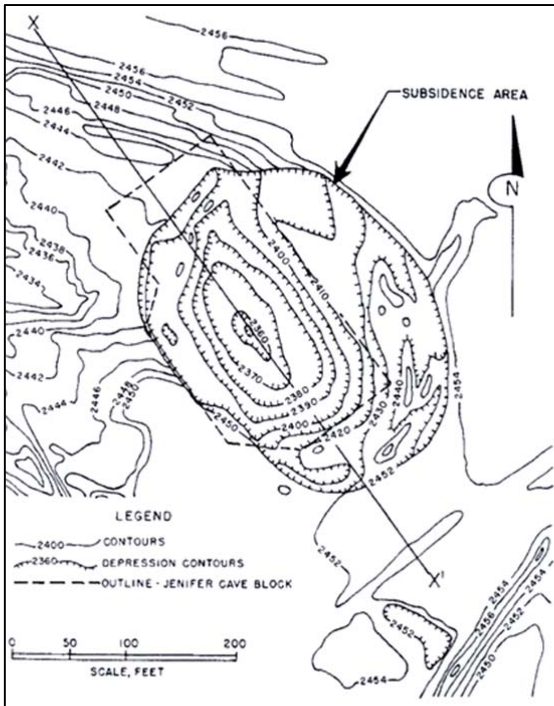

FIGURE 32. - Contour Map Showing Areal Extent and Configuration of the Subsidence Pit at the Surface Over the Jenifer Mine Cave Block.

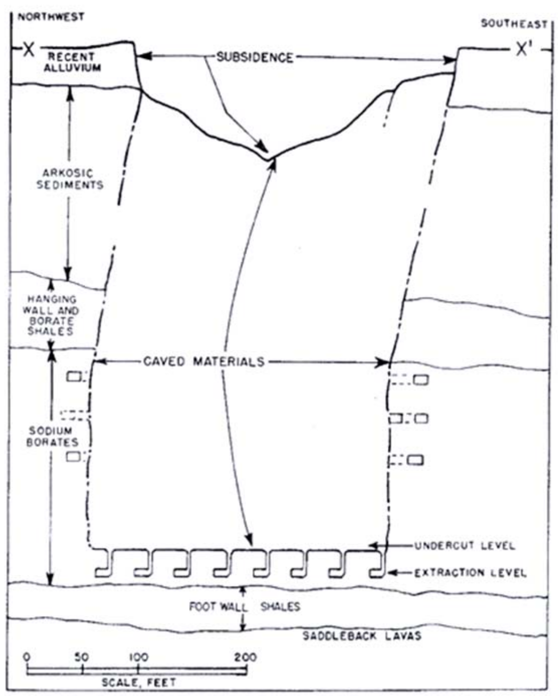

FIGURE 33. - Idealized Cross Section, Line X-X', Figure 32, Through the Jenifer Caved and Subsided Area.

King (Zimbabwe)

Source: Brumleve (1988), Wilson 2000

Caving Period Reported: None given (<1983 – 1988)

Summary: Block caving of the West Flank (W11-14 blocks) of the King asbestos mine is described. Caving of the steeply dipping orebody was initiated below the foot of a steep hill and extended towards its 250 m high peak; the corresponding average depth of the undercut is 275 m. Schematic cross-sections are provided in both sources showing the extent of caving on surface relative to the undercut on the 276 Level. Wilson's [14] section shows more detail, including lines connecting the undercut to surface fractures (fracture initiation angle) but for an earlier stage of cave development. Neither cross-section includes a scale bar. Caving angles on the footwall side of the orebody are shown to coincide with the dip of the orebody.

FIG 4 - Schematic cross-section; King.

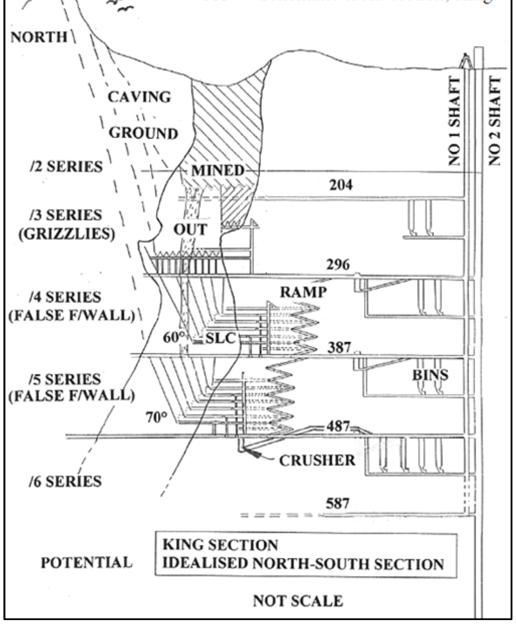

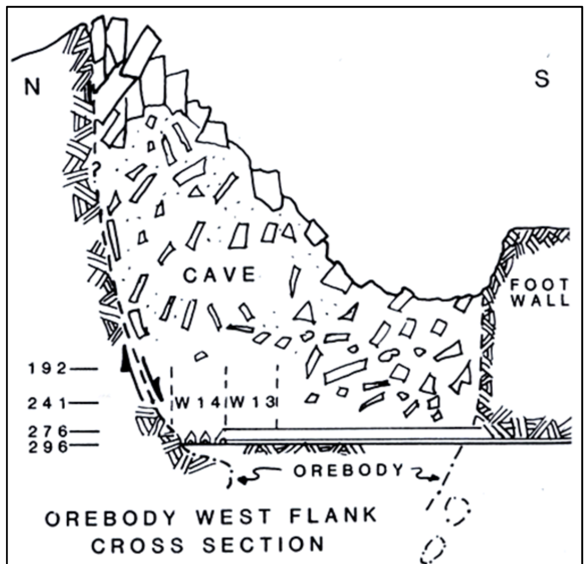

Fig. 3 North–south section through west flank showing cave, production levels 192, 241 and 276 and haulage level 296. (Line of section shown in Fig. 1)

Kiirunavaara/Kiruna (Sweden) - 1995

Source: Lupo (1997), Henry & Dahnér-Lindqvist (2000)

Caving Period Reported: 1965-1995

Summary: Analysis of the progressive failure of the hangingwall and footwall at the Kiirunavaara iron ore sublevel cave mine is reported. The source papers briefly describe the history of hangingwall failures above the sublevel caving, and the more recent failure of the footwall (previous caving angles had coincided with the footwall contact of the orebody dipping at 60°). Lupo [34] provides an air photo outlining the zones of caving, surface cracking and subsidence. The exact depth of the sublevel undercut for these zones is not reported but can be estimated as approximately 560 m depth. Henry & Dahnér-Lindqvist [23] provide a scaled cross section for the same footwall failure event from which the undercut level and caving angle can be estimated. The caving angle on the footwall side coincides with the dip of the orebody, whereas the higher caving angle results from the overhanging nature of the dipping hangingwall. Values for the caving, fracture initiation and subsidence angles from these sources is also reviewed by [24].

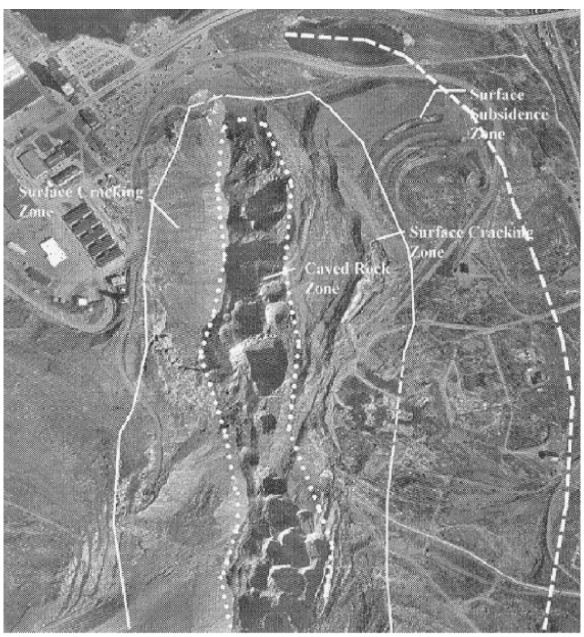

Photograph 1. North End of Kiirunavaara Mine

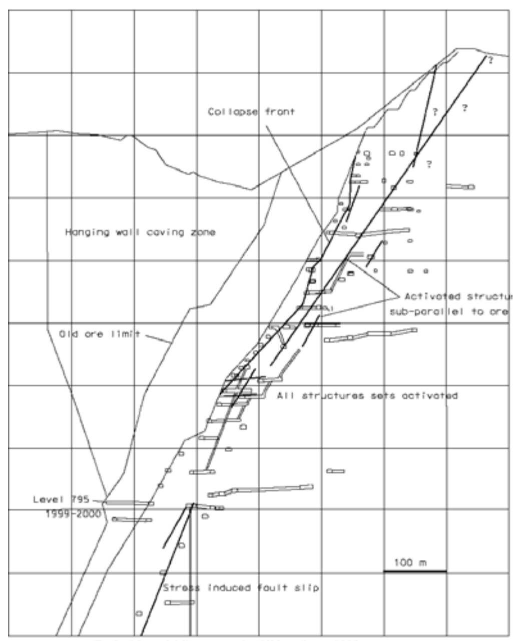

FIG 3 - Mapped failure on section Y23 until year 2000.

Kiirunavaara/Kiruna (Sweden) - 2000

Source: Henry et al. (2004)

Caving Period Reported: 1965-2000

Summary: The application of InSAR monitoring of mining-induced deformations is reported for the Kiirunavaara iron ore sublevel cave mine. The source largely focuses on InSAR principles, but includes a subsidence map of the caving, fracture initiation and subsidence zones. These are based on surface geodetic and benchmark surveys. The outline of the lowermost sublevel undercut for the measurement period (500 m depth) is not provided on the map, but can be approximated, from which the respective angles can be calculated. Caving, fracture initiation and subsidence angles on the footwall side are shown to coincide with one another at approximately 50°.

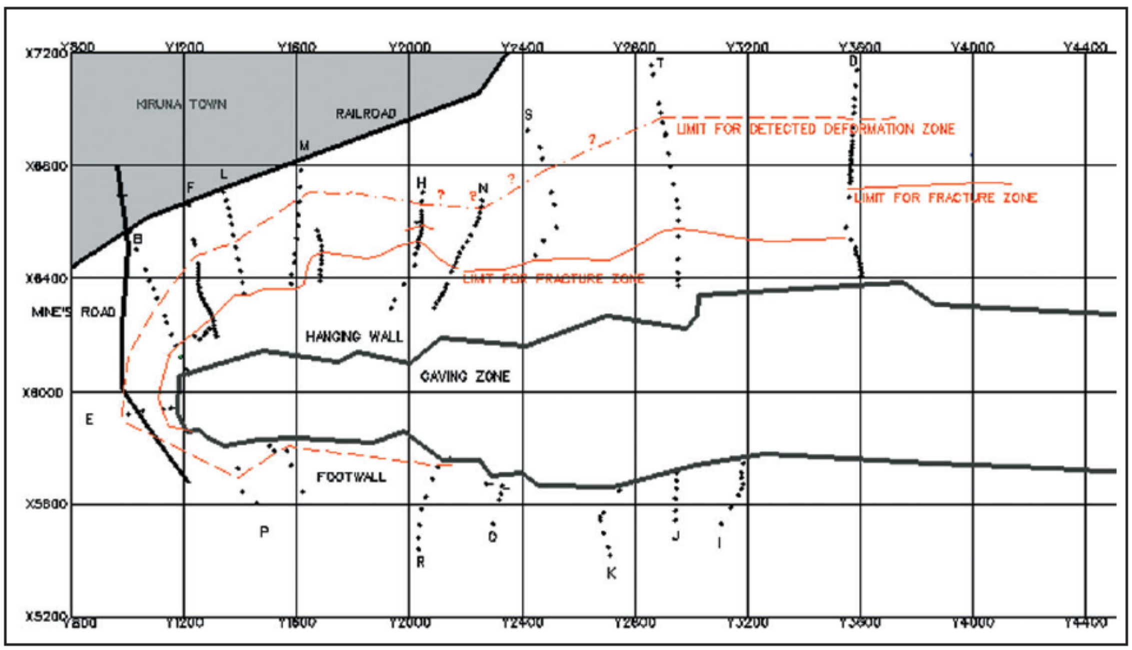

Fig. 1. Location of the caving, fracture, and deformation zones in 2000 and benchmark line networks (black points) at Kiruna mine.

Kiirunavaara/Kiruna (Sweden) - 2005

Source: Villegas (2008)

Caving Period Reported: 1965-2005

Summary: A thesis study is reported involving the numerical analysis of the hangingwall at the Kiirunavaara iron ore sublevel cave mine. A detailed description of the modelling input is provided (rock mass characteristics, properties and in situ stresses), together with the modelling results. A simplified cross-section is also provided as a form of model constraint showing the extent of the farthest surface crack observed on the hangingwall side of the orebody for several different time periods. These are interpreted as representing the limits of the fracture initiation zone. Although exact undercut depths for each sublevel are not provided, they can be approximated from the cross-section. No indication is given as to the caving angles for the same period, or the caving and fracture initiation angles on the footwall side.

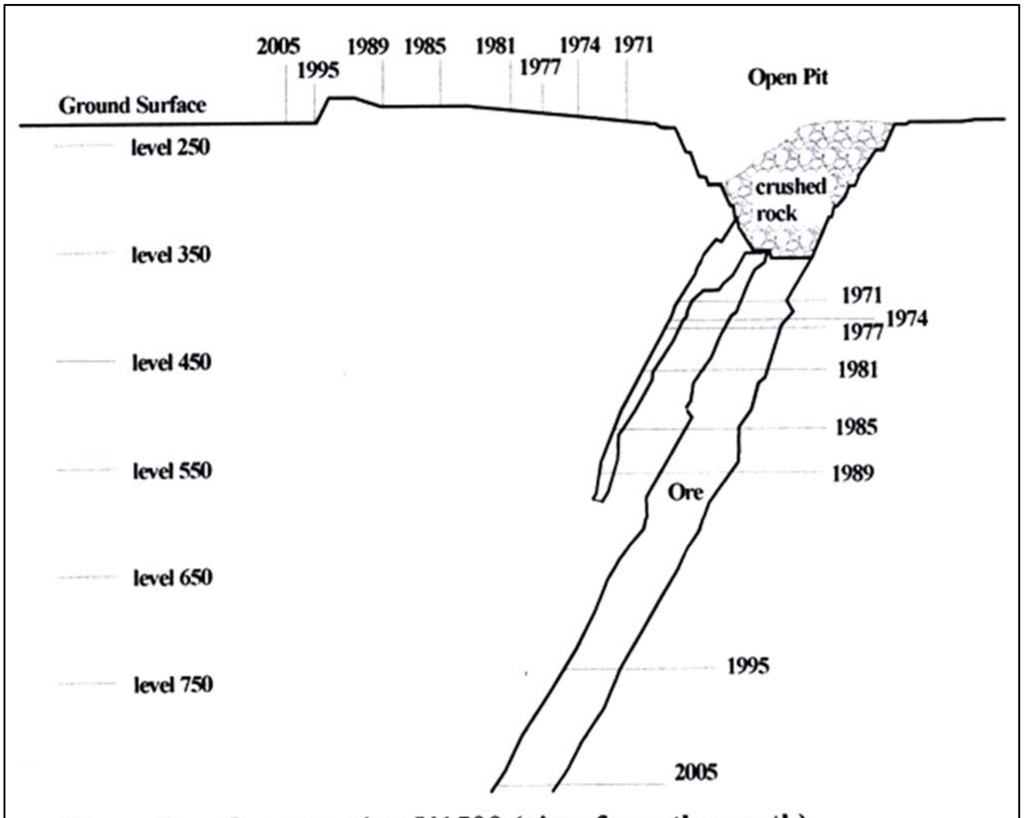

Figure 2 Cross section Y1500 (view from the north)

Koffiefontein (South Africa)

Source: Hannweg (2001)

Caving Period Reported: 1987-2001

Summary: Caving operations at the Koffiefontein diamond mine are reported, describing the use of a front caving method that combines aspects of block and sub-level caving. The undercut occurs at 480 m depth and caves into previous underground workings and the bottom of a deep open pit. This is shown in a schematic cross-section, from which the caving angles can be estimated. These are shown as being sub-vertical and confined within the limits of the pit bottom.

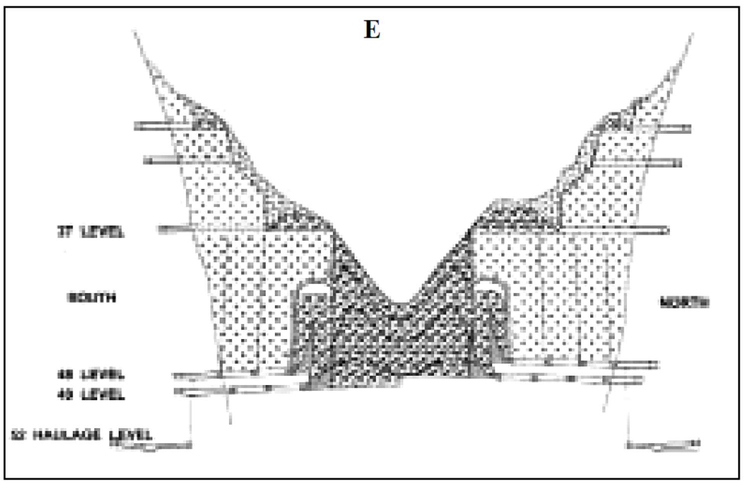

Lake Superior District (Michigan, USA)

Source: Crane (1929)

Caving Period Reported: none

Summary: Data is presented for several cases involving copper and iron mines, but without specific reference to the mine location, mining period or mining method. Based on the "type cases" reported, most appear to involve open stoping where failure (caving) of the hangingwall has occurred, although indication is given that a small number of sublevel caving cases are also included. Angles of break are reported, but these are defined as the angles observed underground with reference to the backs of hangingwall failures and not necessarily the angles representing the extension of caving to surface. Cross-sections are provided for two cases, showing examples of caving and subsidence at surface, which appear to be sublevel or block caving mines. Both are without scale bars. The first is described as Case B (also Type C), involving an iron-bearing formation lying on highly inclined slate. The angle of caving on the footwall side aligns with the dip of the slates. No depth is given for the mining depth. Reference is made to 300-400 m as a minimum, although references are also made to multiple depths and sub-levels. The second case (Case C, Types D,E,F), appears to refer to the block caving of lenticular iron ore deposits. A cross section is provided showing the caving angle extending from the undercut, but again, no scale is provided. Other information provided suggests a depth of 450 m, including a thick blanket of glacial till that partly obscures the caving and subsidence zones at surface.

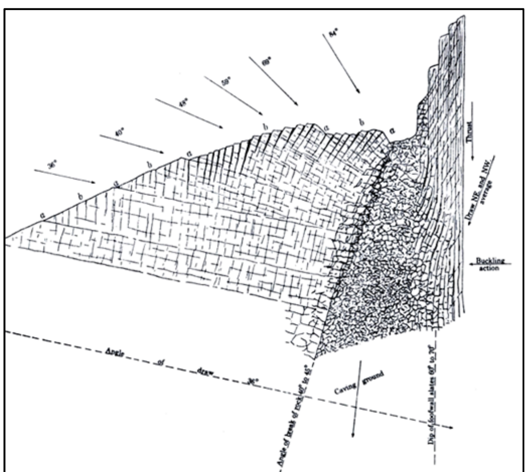

Sketch giving cross section of footwall slates and ore formation and showing effects of ground movement due to draw and thrust resulting from weight of rock masses. Surface points a show draw and points b cracks due to overturn

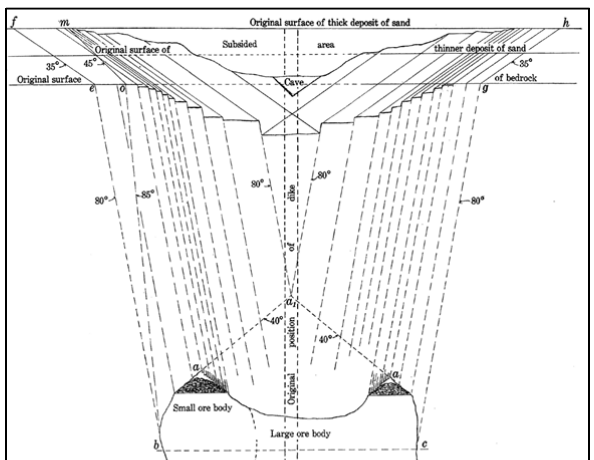

43.—Sketch showing method of failure of formations overlying ore bodies as the initial break at a and a, and the ultimate failure at bef and cgh or bow. The effect of dike as the initial cause of failure is also shown. Two angles of break in the top formation are indicated. With the 80° angle in the rock use the 35° angle in surface materials and with the 85° angle use 45° in the surface material. When the ore body is worked full width as bc the cave will extend to a_1, while in narrower portions the height will be less as a

Malmberget (Sweden)

Source: Haglund & Heberg (1975)

Caving Period Reported: 1970-1974

Summary: Recovery of a 160 m high pillar is described using a modified block caving method referred to as 'slotblocking'. However, the dipping nature of the orebody and multiple use of sublevels, more closely resembles a sublevel caving approach and is classifies as such in the Tables above. Previous and subsequent mining of the iron ore deposits involved a combination of shrinkage and sublevel stoping and sublevel and block caving. No direct data is provided in the form of subsidence measurements, but a scaled cross-section is included showing the boundaries of the caving zone on surface relative to several undercut levels below. The most relevant is the block caving of the 300 Level (300 m depth), with lower levels acting more like a sublevel caving operation. The cross-section shows that the caving zone on the footwall side aligns with the orebody contact, whereas the overhanging hangingwall collapses into the cave.

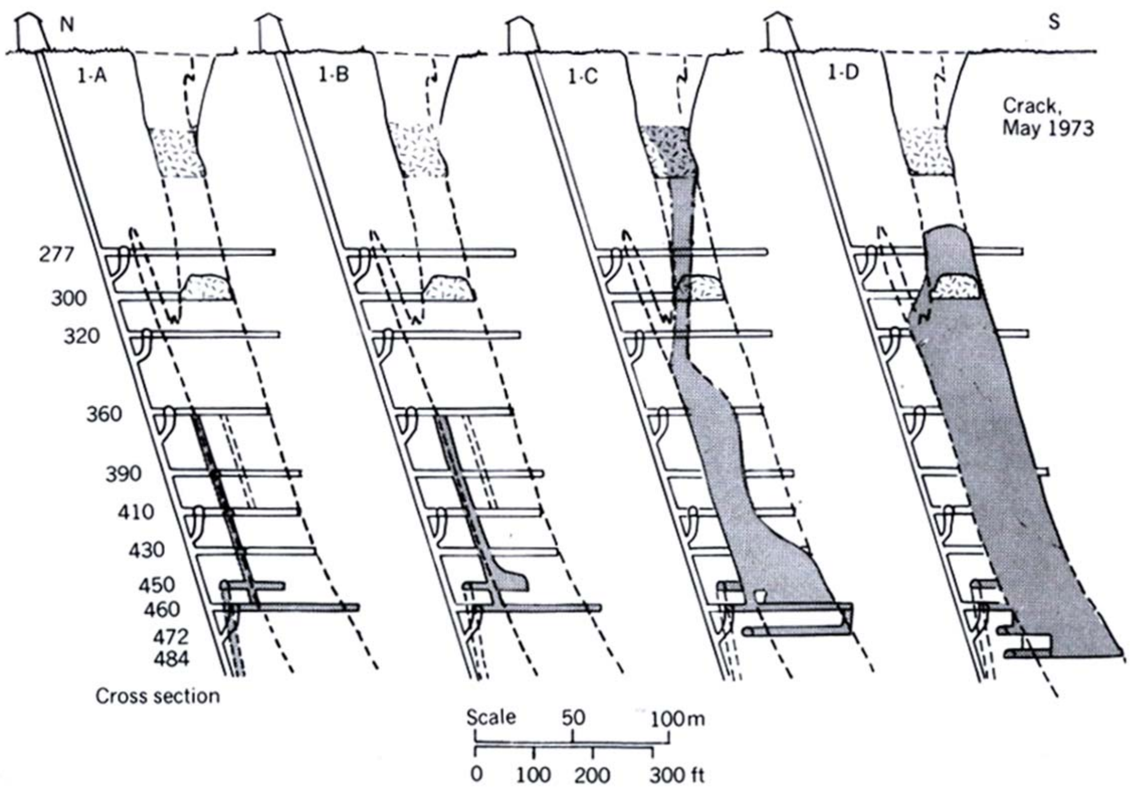

Miami – 1928 (Arizona, USA)

Source: Maclennan (1929)

Caving Period Reported: 1926-1928

Summary: The source reports data from the block caving of two ore bodies, referred to as Main and Low Grade, together with a smaller block named Stope 11. Earlier mining was by shrinkage stoping and top slicing. At the time of reporting, mining of the Low Grade orebody was still in progress. The depths of the three undercuts vary from 180-195 m for ore blocks 65 to 120 m high. Boundary caving drifts were driven at suitable vertical intervals to limit the amount of caving beyond them. The south boundary of the Low Grade block caves into the already caved Main block. A plan view subsidence map and several cross-sections are provided showing the extent of measured subsidence on surface relative to the undercut level, including limiting scarps from which the angle of fracture initiation can be estimated. Caving angles and angles for fracture initiation are reported in the paper, but are measured from the top of the mined block (i.e. ore column); angles reported here, in the Tables above, have been corrected to be measured from the extraction level. Lower caving/fracture initiation angles for the Main and Low Grade blocks were observed to be sub-parallel to foliation of schist.

.

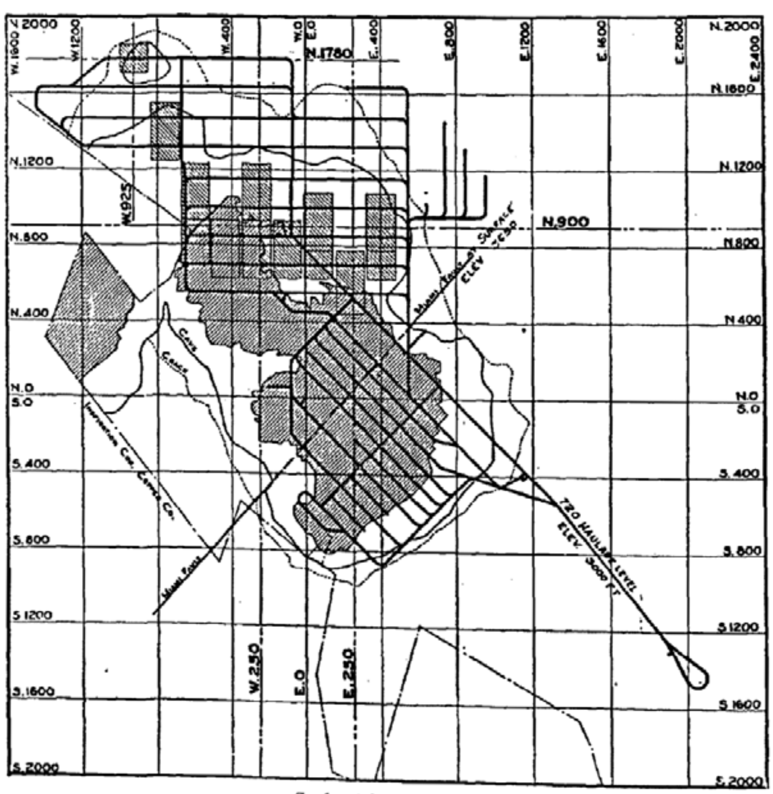

Scale: 1 in. = 540 ft.

Fig. 1.—Plan of 720-ft. haulage level, showing caved areas and resulting surface subsidence.

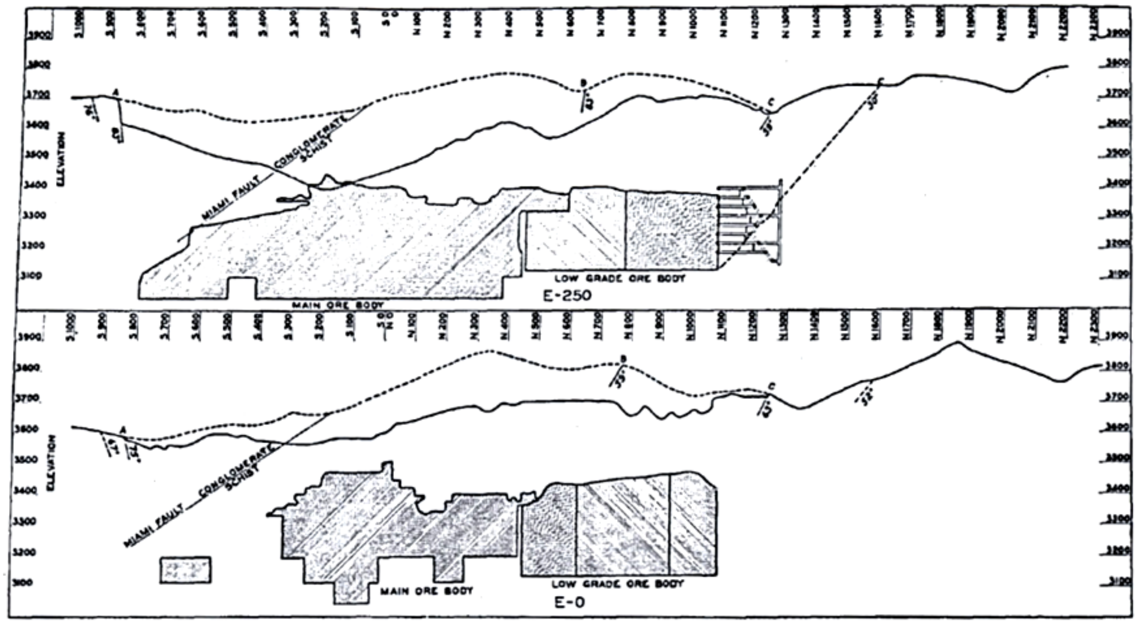

Scale: 1 in. = 118 ft.

FIG. 2.—SECTIONS THROUGH OREBODY SHOWING STOPED AREAS AND RESULTING SURFACE SUBSIDENCE.

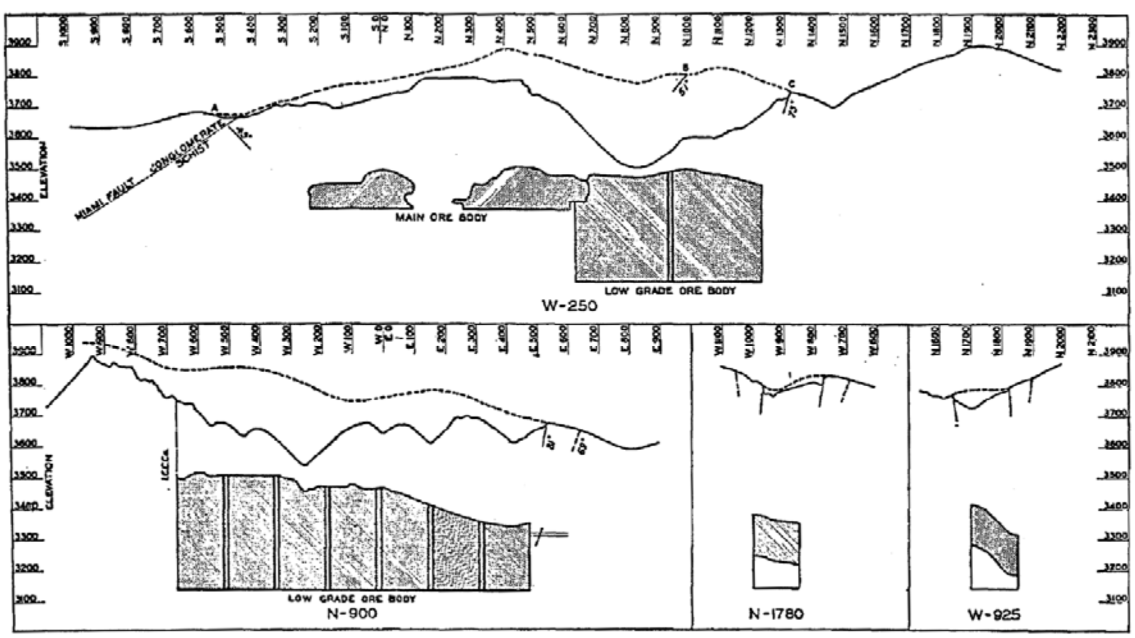

Scale: 1 in. = 118 ft.

FIG. 3.—SECTIONS THROUGH OREBODY SHOWING STOPED AREAS AND RESULTING SURFACE SUBSIDENCE.

Miami – 1958 (Arizona, USA)

Source: Fletcher (1960)

Caving Period Reported: 1910-1958

Summary: This report updates the subsidence observations of MacLennan (1929) with an intermediate set of observations from 1939 and current measurements as of 1958. The data for 1939 involves a plan view map showing the limits of caving and fracture initiation relative to the caved ore bodies. This period continues the mining of the low grade orebody, as reported in 1929, from the same mining depth (approximately 195 m). As before, boundary caving drifts were driven at different vertical intervals to limit the amount of caving beyond them. Fletcher (1960) reports that the caving angles have flattened considerably since the 1929 set of measurements. The data reported for the mining period up to 1959 incorporates an extension of the High Grade orebody to greater depths through lifts at the 700 and 1000 (foot) Levels, with a bottom undercut at 300 m depth. Unlike previous blocks, those undercut at the 1000 Level were done so without the vertical boundary cutoff drifts. Scaled cross-sections are provided for the deeper lifts, showing the original topography, extent of subsidence, and surface scarps. It should be noted that although a large fault (the Miami fault) cuts across the deposit, separating the schist-hosted orebody from the conglomerate cap, it is not seen to have any influence on the caving or fracture initiation limits.

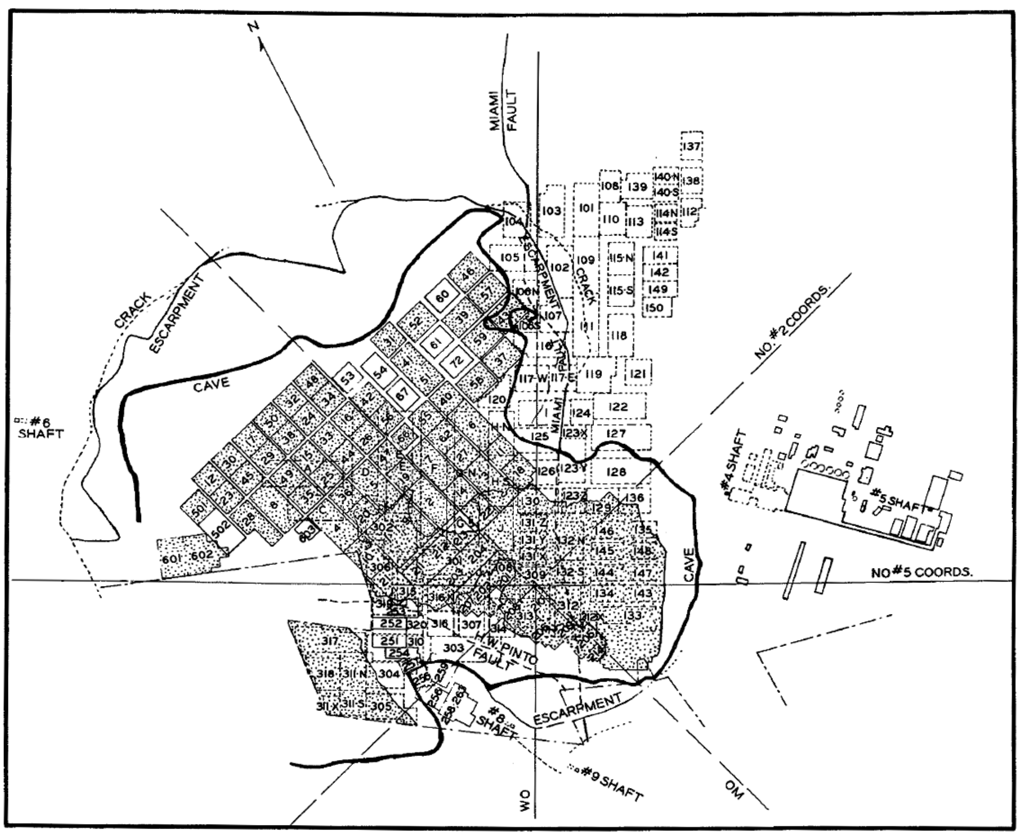

FIG. 4 Plan showing caved areas and resulting surface subsidence, July 31, 1939.

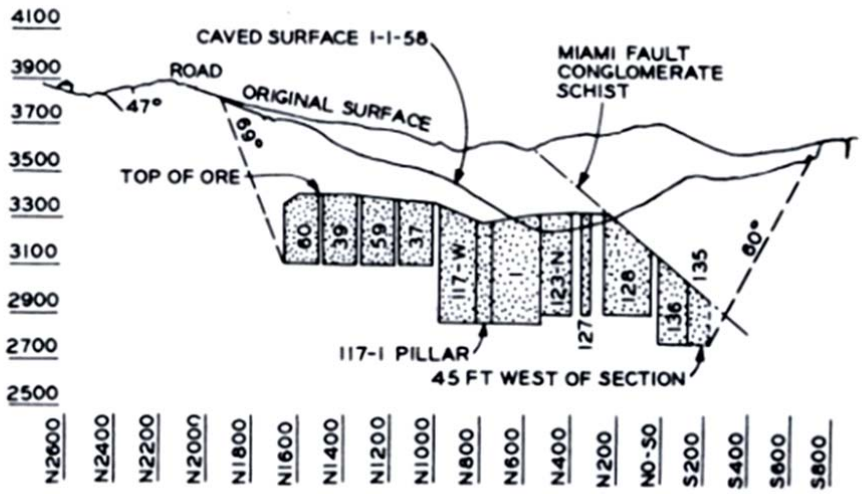

FIG. 8 E 800 section, No. 2 coordinates, showing stoped areas and subsidence, Feb. 14, 1958.

Mt. Lyell – Cave Horn (Tasmania, Australia)

Source: North & Callaghan (1980)

Caving Period Reported: 1972-1980

Summary: Subsidence related to the mining of several different orebodies is reported at Mt. Lyell, including the Cape Horn orebody mined by a combination of sublevel caving and stoping. A schematic cross-section is provided that shows the extent of caving above the #5 undercut at 160 m depth, together with the angle of fracture initiation above the hangingwall. The latter is described as a concentric pattern of surface cracking. Caving on the footwall side is shown to coincide with the dip of the orebody (70°).

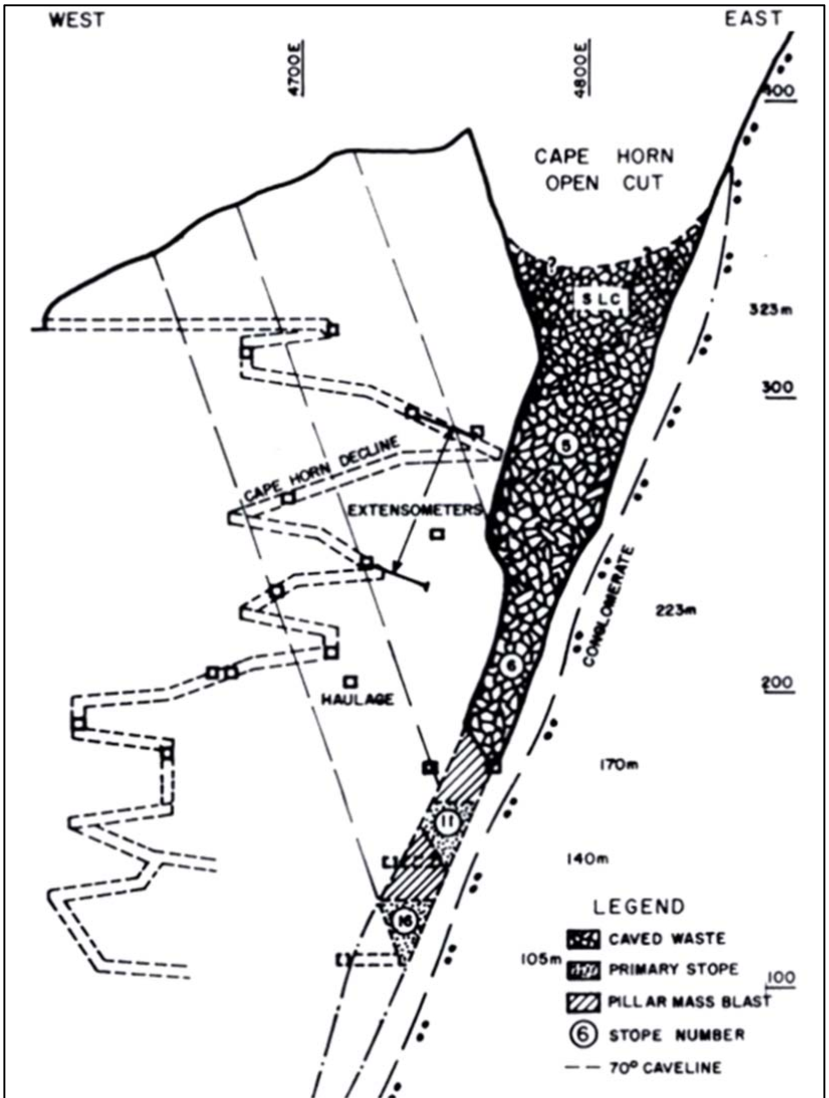

Fig. 4 - Cross section of the Cape Horn mine

Northparkes (Australia) – E26 Lift 1

Source: Duffield (2000)

Caving Period Reported: 1993-2000

Summary: The design of the second lift for the Northparkes' E26 mine is reported. Included in this description is a geological cross-section showing the outline of the mined out Lift 1 block cave. No direct data is provided in the form of subsidence measurements, but caving angles for Lift 1 can be approximated from the cross-section supplemented by subsidence-related information in the source paper. Caving of Lift 1 involved the collapse of the crown pillar into an air gap beneath the cave back, owing in part to a change in the geology related to a gypsum leached zone. As a result, the cave angles are near vertical. The lift also caved into the bottom of a small open pit; the caving zone measured does not include ground disturbed due solely to open pit mining.

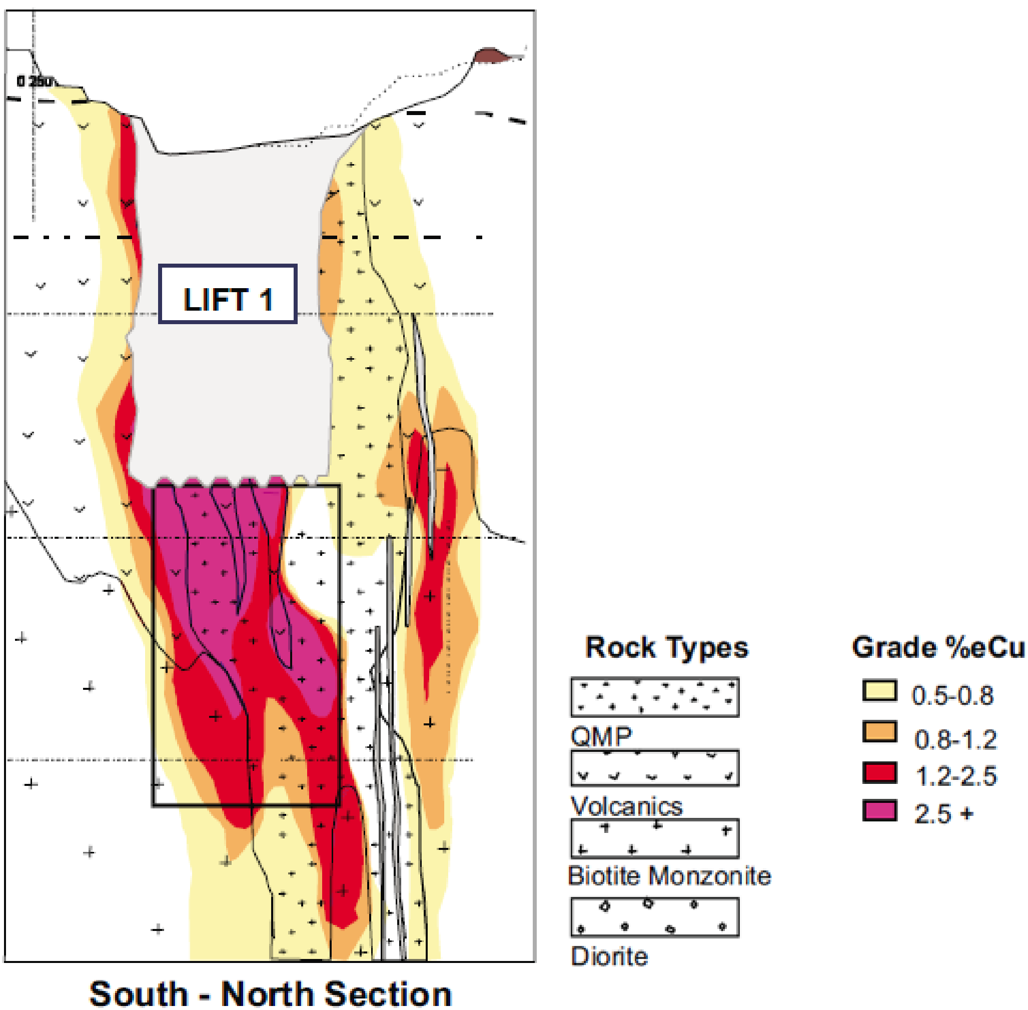

FIG 3 - E26 mine geology – Section.

Palabora (South Africa)

Source: Pretorius (2007)

Caving Period Reported: 2001-2007

Summary: The effects of dilution resulting from a 130 million ton pit wall failure above an active block cave are reported. The block cave undercut is approximately 400 m below the bottom of the 800 m deep pit at a depth of 1200 m. The source reports the caving angles originally projected to open up into the floor of the pit, and the unexpected caving-induced triggering of a large pit wall failure. Physical and numerical modeling predicted a loss of around 30% of the original ore reserve. The source paper reports the caving angle at 86-88 degrees. The fracture initiation angle is projected with respect to the location of the back scarp of the rockslide behind the crest on the north wall of the pit.

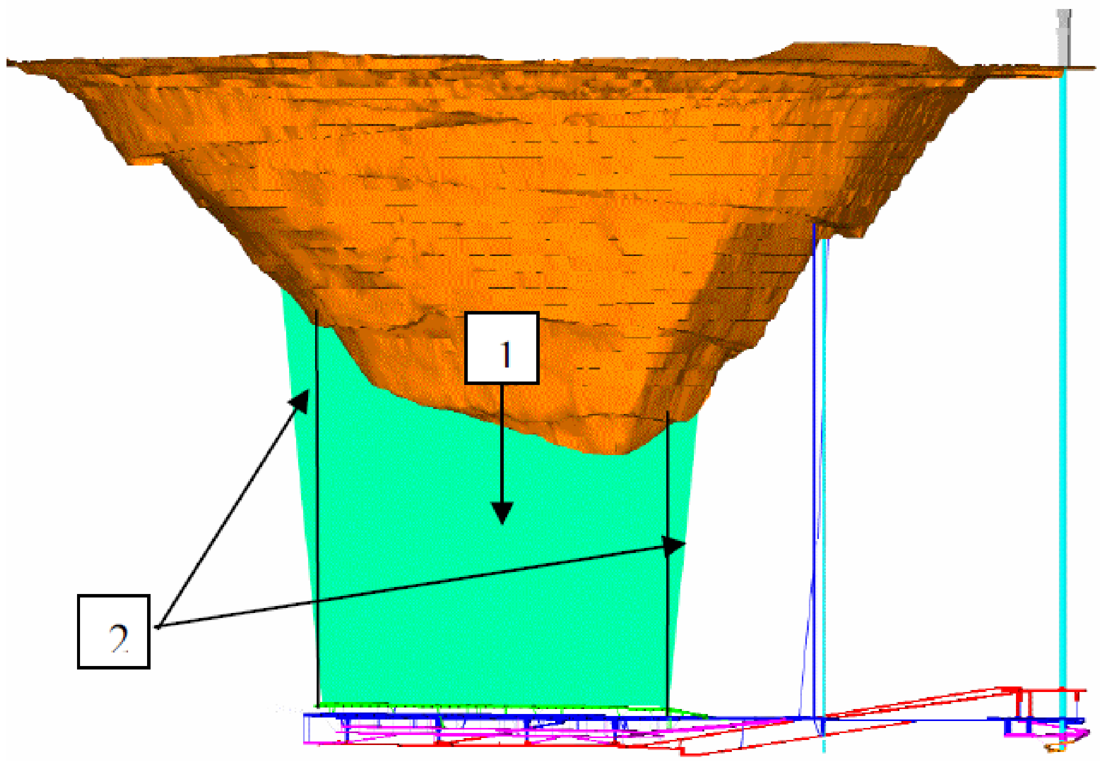

Figure 8: Ore Loss effects on the Palabora reserve from external dilution: 1 – Dilution entry, 2 – Replacement of ore by waste

Perseverance (WA, Australia) - 2000

Source: Jarosz et al. (2007)

Caving Period Reported: 1994-2000

Summary: A report is provided on the use of InSAR to measure mining-induced deformations above a sublevel caving operation. Included is a cross-section that shows the caving profile above the sublevel undercut at 640 m depth (9920 Level). These underground operations are located below a large open pit with caving on the hangingwall side extending beyond the pit. InSAR data is also presented, however, no indication is given as to how the monitored displacements relate spatially to the undercut sublevels.

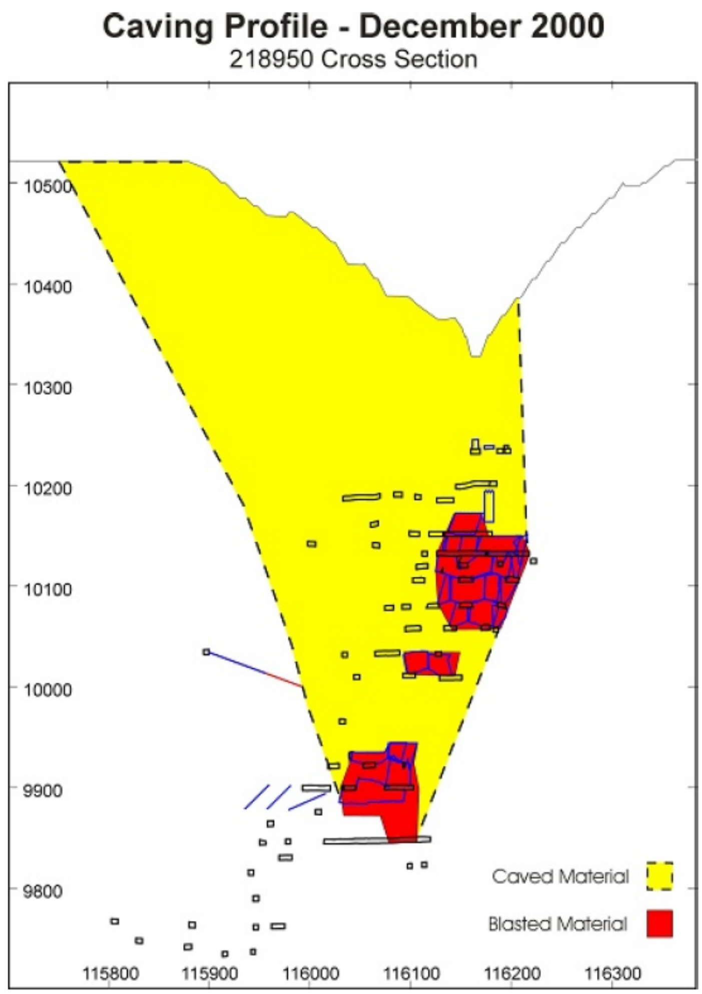

Perseverance (Australia) - 2004

Source: Tyler et al. (2004)

Caving Period Reported: 1994-2004

Summary: Subsidence above the Perseverance sub-level caving nickel mine is reported. Subsidence maps are provided for several different years and mining levels, showing the limits of caving and fracture initiation based on the interpretation of air photographs, walk-over surveys and GPS/prism data. Caving and fracture initiation angles calculated based on stated mining depths and outlines of the caving levels relative to the outlines of caving on surface. Caving occurs beneath a large open pit with caving on the hangingwall side extending beyond the pit limits.

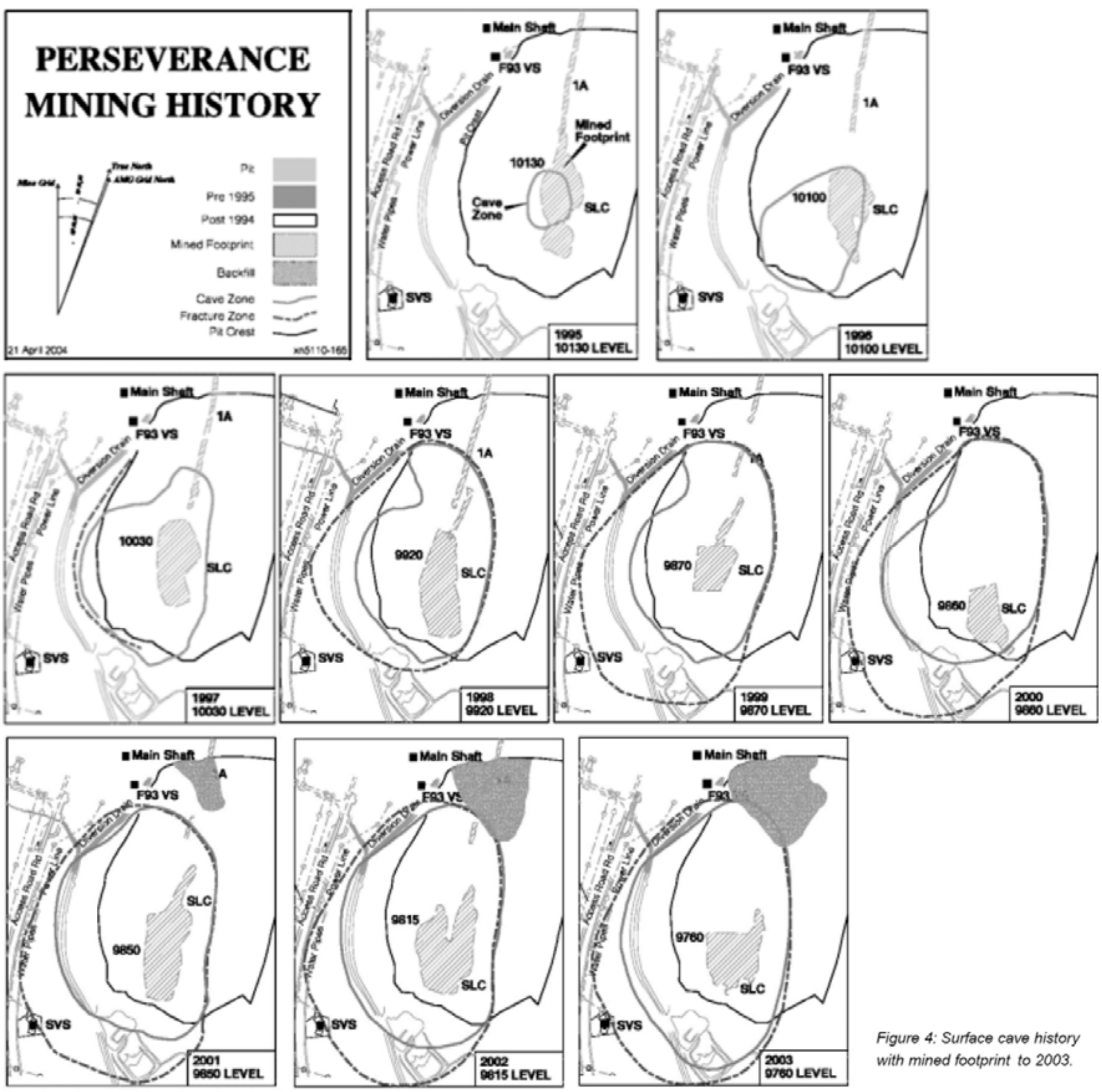

Figure 4: Surface cave history with mined footprint to 2003.

Questa (New Maxico,USA)

Source: Gilbride (2005)

Caving Period Reported: 1979-2005

Summary: Subsidence at the Questa mine related to historic block caving (Goathill orebody) and block caving of a new orebody ("D") is reported. Data is provided for the measured historic subsidence over the Goathill orebody in the form of an air photo outlining the caving and fracture initiation zones, and limits of ground deformation (i.e. continuous subsidence zone). The respective angles are reported with reference to the undercut level at 300 m depth. The limits depicted are based on field measurements and air photo analysis. Incorporated in the subsidence zone is a shallow-seated slide undercut at its toe by the caving zone. A subsidence contour map is provided for the ground deformations over the D orebody, Panel 1 undercut (600 m depth). Deformations were measured by surface surveys across a grid. At the time of reporting, subsidence over Panel 1 was not developed enough to allow the measurement of the caving or fracture initiation angles. The subsidence magnitudes, however, were large enough to initiate large-scale sliding of the hillside above. Subsidence above the D Orebody was first detected in April 2003, 30 months after caving was initiated. Caving propagated to surface through 550 m of overburden at an average rate of 0.21 m per day.

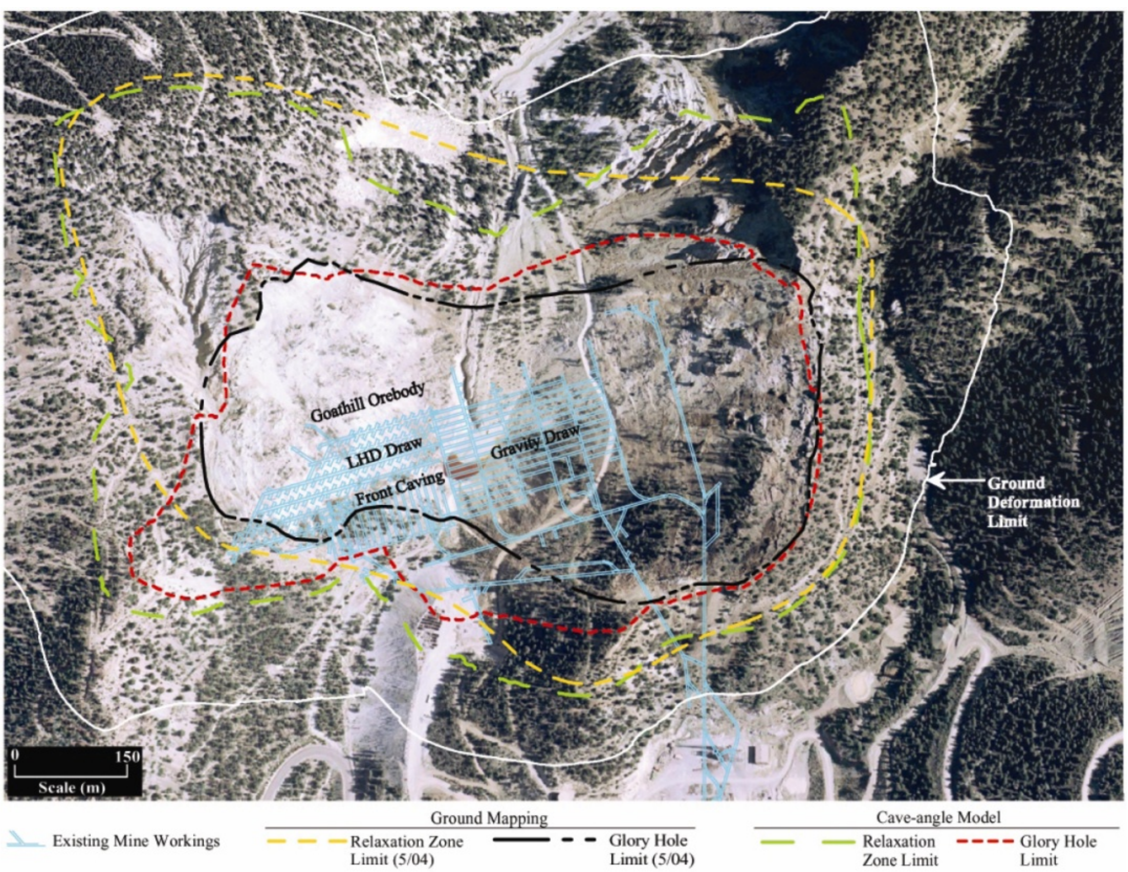

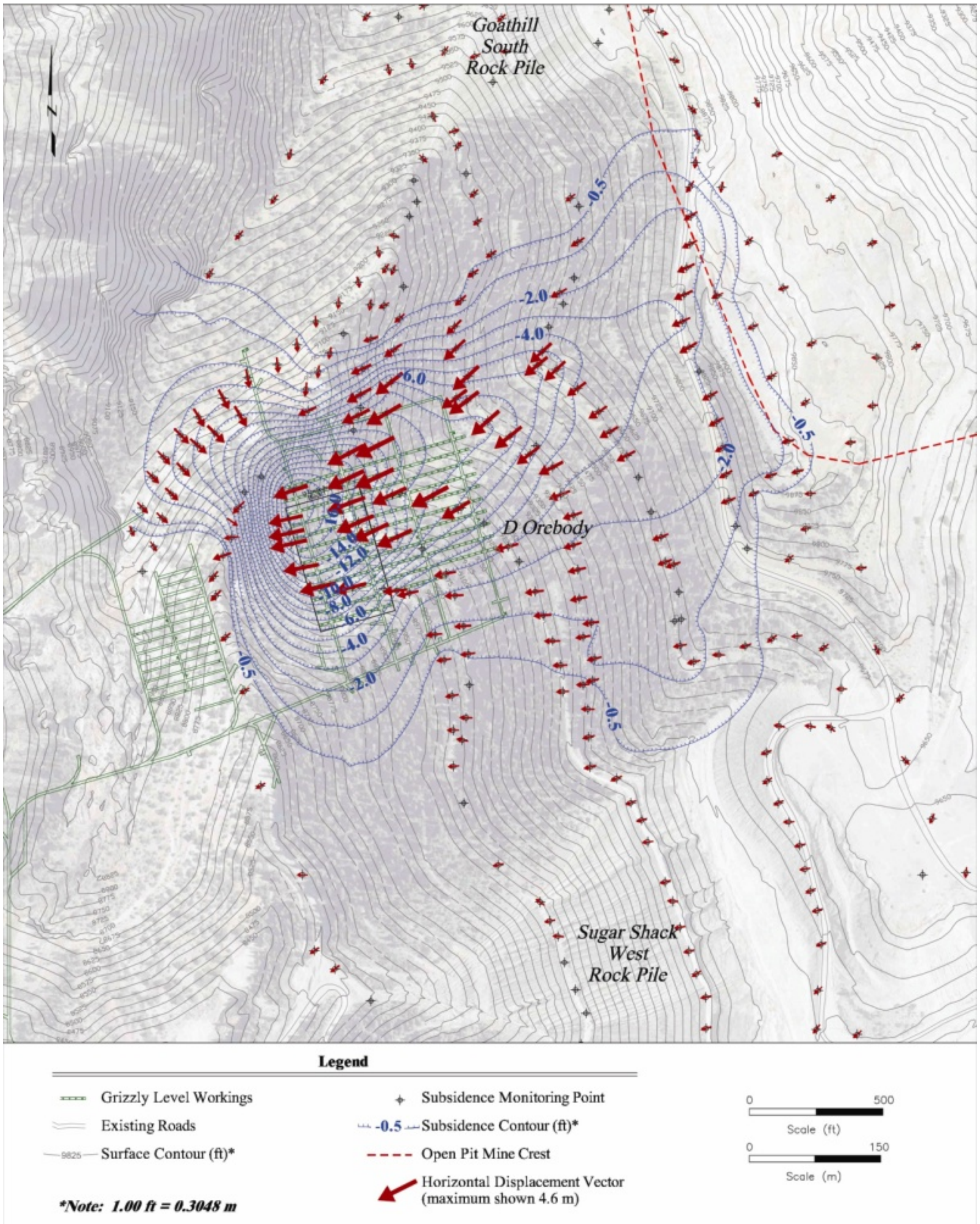
Goathill South Rock Pile
D Orebody
Sugar Shack West Rock Pile
-0.5
-2.0
-4.0
6.0
8.0
10.0
12.0
14.0
Legend
Grizzly Level Workings
Existing Roads
Surface Contour (ft)*
Subsidence Monitoring Point
-0.5 Subsidence Contour (ft)*
Open Pit Mine Crest
Horizontal Displacement Vector (maximum shown 4.6 m)
*Note: 1.00 ft = 0.3048 m
0 500 Scale (ft)
0 150 Scale (m)

Rajpura Dariba (India)

Source: Singh (1993)

Caving Period Reported: ?

Summary: Numerical modelling of progressive hangingwall failure is reported, including a brief description of a case history of the Rajpura Dariba sublevel caving mine. No direct data is reported but the caving and fracture initiation angles on the hangingwall side of the orebody are reported together with the mining depth. The respective angles on the footwall side are assumed to be aligned with the 70° dip of the footwall.

Salvador (Chile)

Source: Escobar & Tapia (2000)

Caving Period Reported: 1995-1999

Summary: The investigation into the 1999 air blast event at the Salvador panel cave operation is reported. This involved the sudden collapse of the cave back in the Inca West area after a stable arch had formed resulting in the development of a large void. No direct data is presented in the form of subsidence measurements, but a scaled cross-section showing the development of the collapse is provided which includes the outline of the caving zone and original topography relative to the undercut level (at 700 m depth).

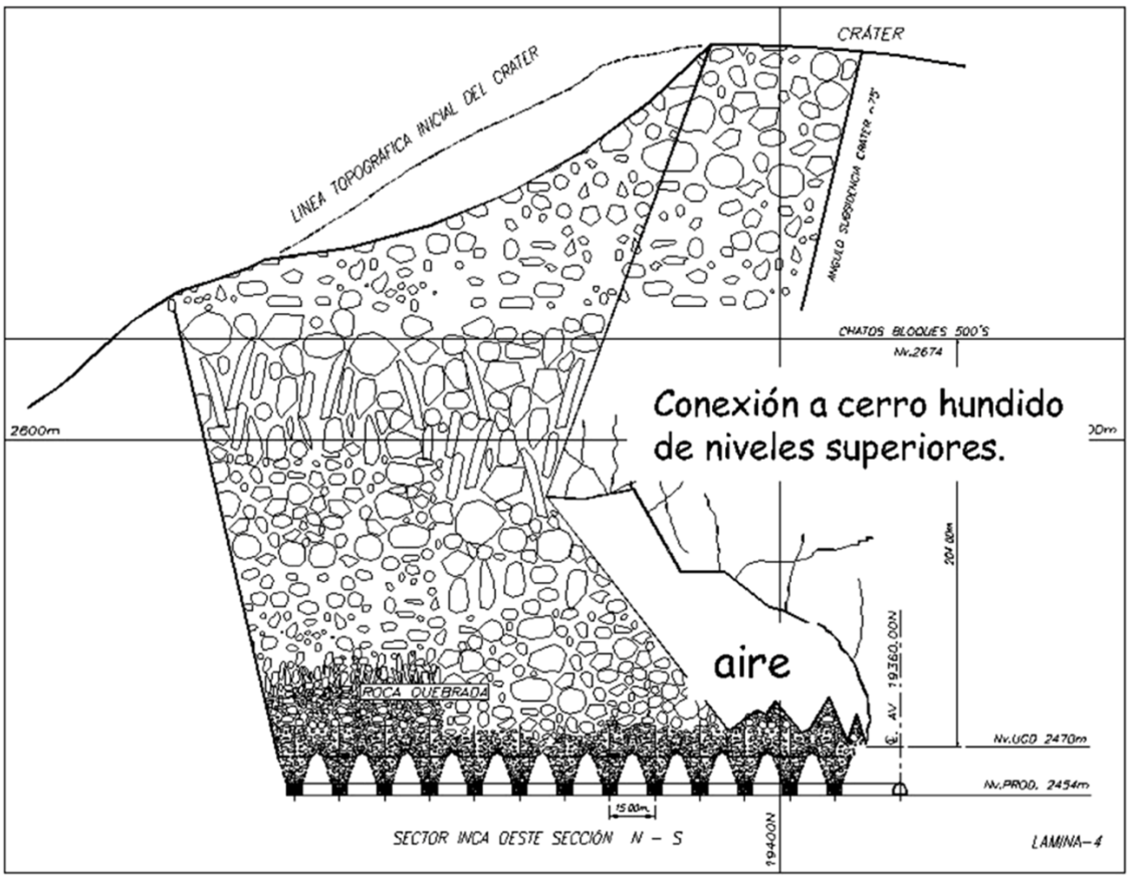

San Giovanni (Italy)

Source: Balia et al. (1990)

Caving Period Reported: 1985-1990

Summary: Analysis of progressive hangingwall failure is reported for the San Giovanni lead-zinc mine. The mining methods employed include cut and fill stoping in the lower levels, and sub-level caving and shrinkage stoping in the upper levels. The undercut depth for the lowermost sublevel caving level is at 100 m depth. Data is provided in the form of a longitudinal cross-section and subsidence map outlining the caving zone. The caving angle calculated for the footwall side of the orebody approximately coincides with the dip of the footwall at 75-80°.

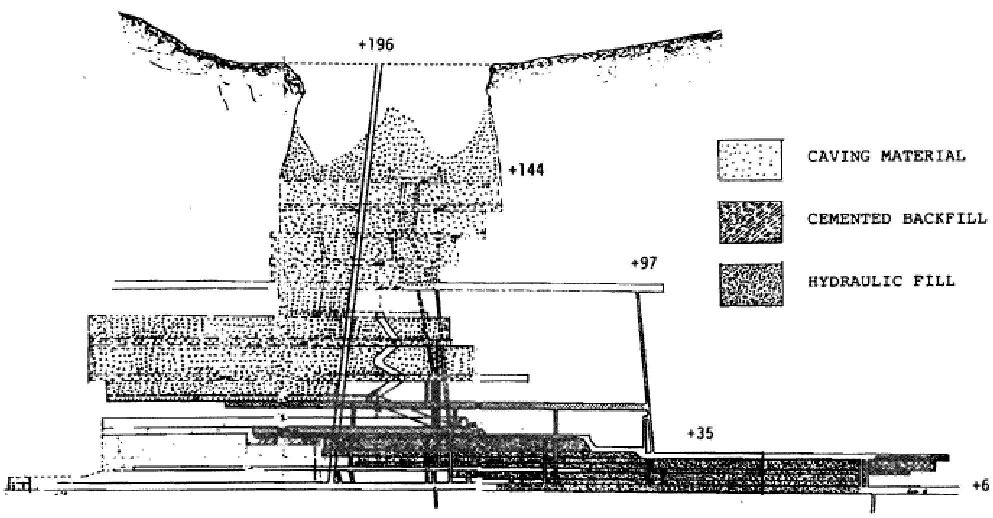

Figure 2 - Vertical longitudinal section of the "Contatto Ovest" orebody.

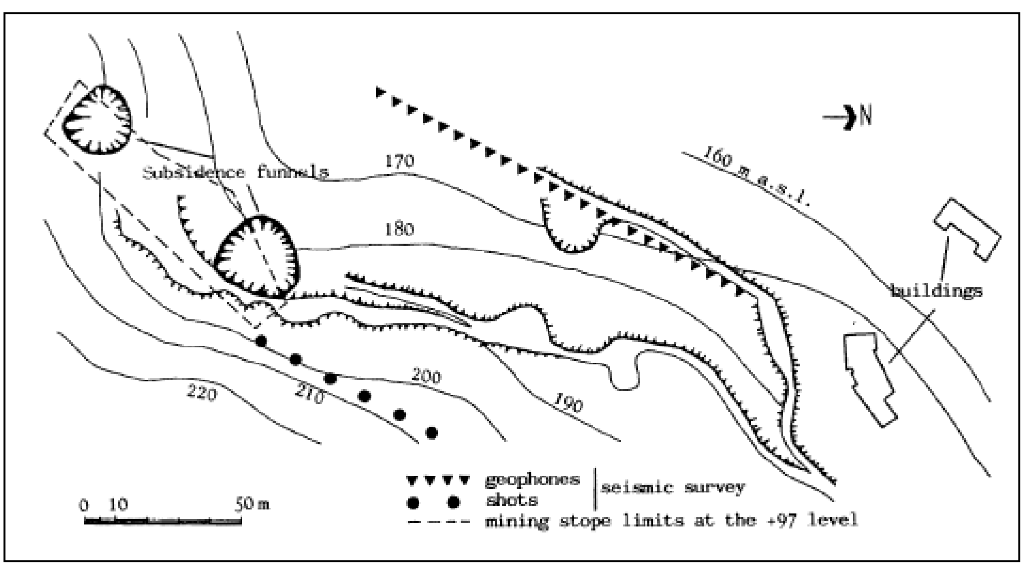

San Manuel (Arizona, USA)

Source: Buchanan & Buchella (1960); Johnson & Soulé (1963)

Caving Period Reported: 1956-1960

Summary: Data is reported for the block caving of the South orebody, Lift 1 (1450 Level undercut) from two different sources. The South ore body is the largest of the three ore bodies at San Manuel. The data from Johnson & Soulé (1963) provides more detail at a higher resolution and is the primary source used here. The undercut for Lift 1 is at a depth of 420 m with a block height of 180 m. At the time of reporting, only the central third of the ore zone has been caved. Surface subsidence data is provided in the form of a cross-section showing the subsidence profile for different intermediate stages of caving, several cross-sections showing the caving angle and angle of subsidence for different profiles above the undercut, and a subsidence contour map (with 25' contour intervals) showing the limits of scarp development and surface cracking. Note that the definitions from Kantner (1934) are used with angle of subsidence referring to the limits of caving on surface and break angle being applied to the limit of visible cracking in the same section. These are interpreted here as referring to the caving and fracture initiation angles, respectively. A general recommendation was provided to assume a setback distance of 230 m of lateral distance on surface for each 300 m of depth mined in order to protect structures and ensure safety.

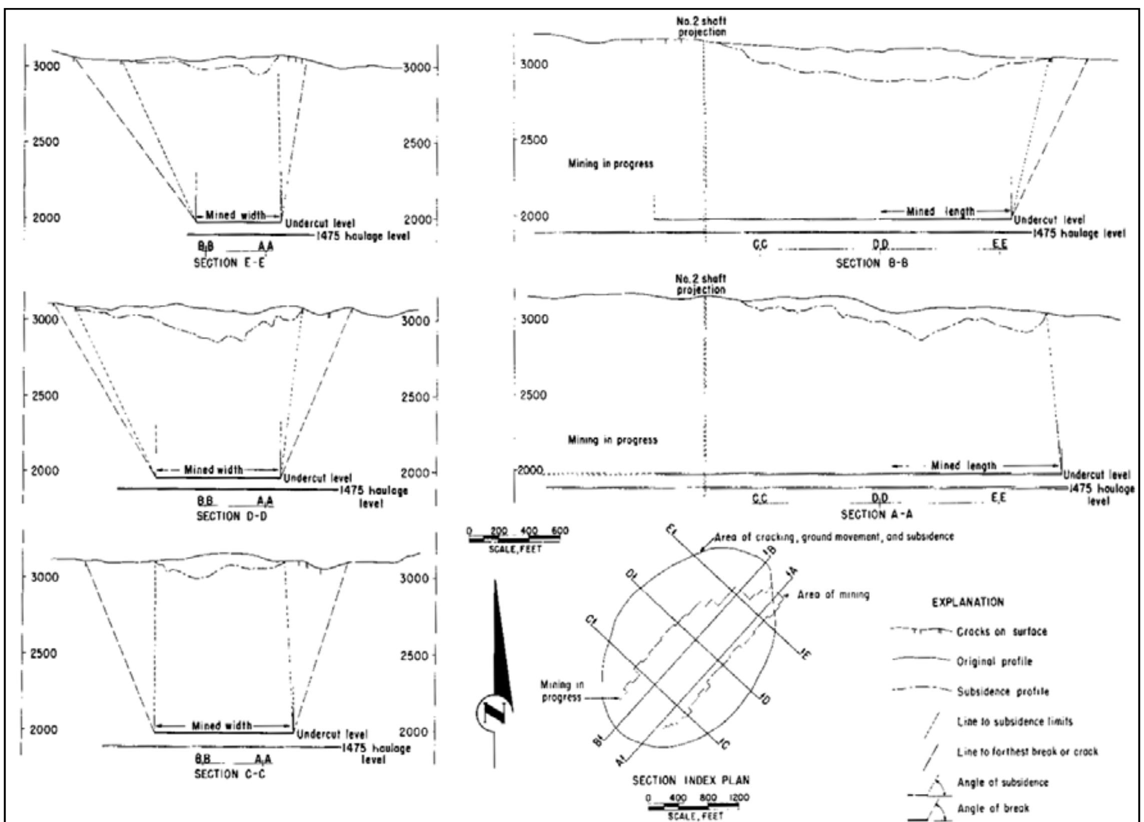

FIGURE 26. - Angles of Subsidence and Break.

San Manuel (Arizona, USA)

Source: Thomas (1971)

Caving Period Reported: 1956-1970

Summary: Data is provided summarizing that previously reported for the South orebody, Lift 1 (Johnson & Soulé 1963), subsequent data for its completion in mid-1962, data for the mining of Lift 2 (2015 Level), and data for the mining of the North orebody, Lift 1, which is comprised of two blocks, West and East, separated by a 200 m pillar. The undercut for Lift 1 (1450 Level) was at 420 m depth, whereas the undercut for Lift 2 (2015 Level) was at 605 m depth. Lift 2 for the South orebody was mined by block caving, although the method was gradually modified to follow a panel caving type sequencing. A similar panel caving approach was applied to the North orebody, although the small size of the West and East undercuts effectively resulted in block being caved. Surface subsidence data is provided in the form of several subsidence contour maps (with 50' contour intervals) showing the extension of the caving zone with time, together with scaled cross-sections showing the subsidence profiles. Active subsidence for the South orebody, Lift 2, is primarily contained within well established boundaries for Lift 2, with only minor activity outside this periphery. The increased depth of Lift 2 therefore results in a steepening of the caving angles. The caving zones for the North orebody, West and East, remained separate.

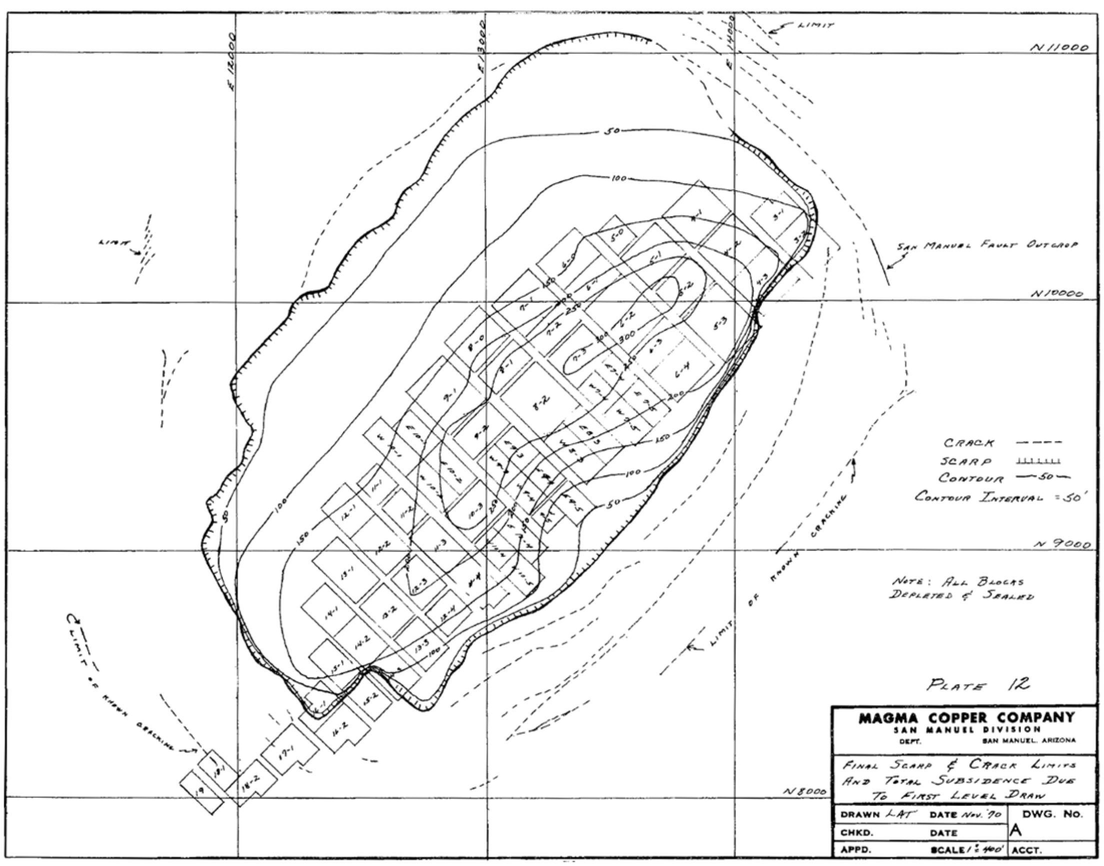

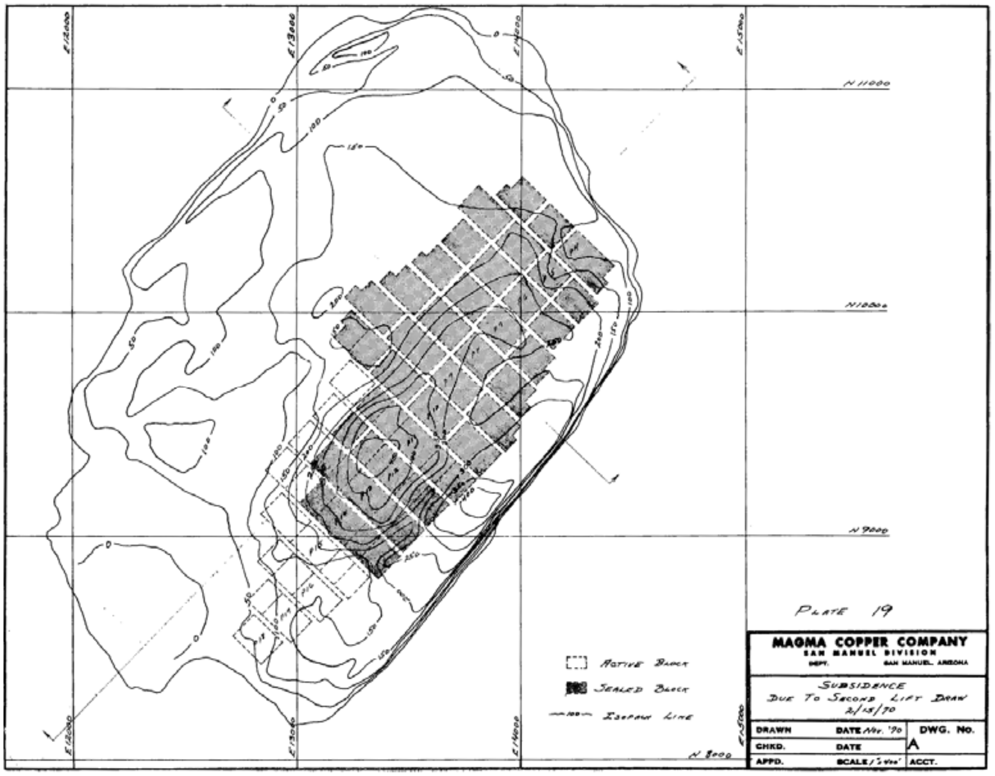
E 12000
E 13000
E 14000
E 15000
N 11000
N 10000
N 9000
N 8000
Active Block
Sealed Block
Isopach Line
PLATE 19
MAGMA COPPER COMPANY
SAN MANUEL DIVISION
DEPT.
SAN MANUEL, ARIZONA
SUBSIDENCE
DUE TO SECOND LIFT DRAW
2/15/70
DRAWN
DATE Nov. '70
DWG. No.
CHKD.
DATE
A
APPD.
SCALE 1"=400'
ACCT.

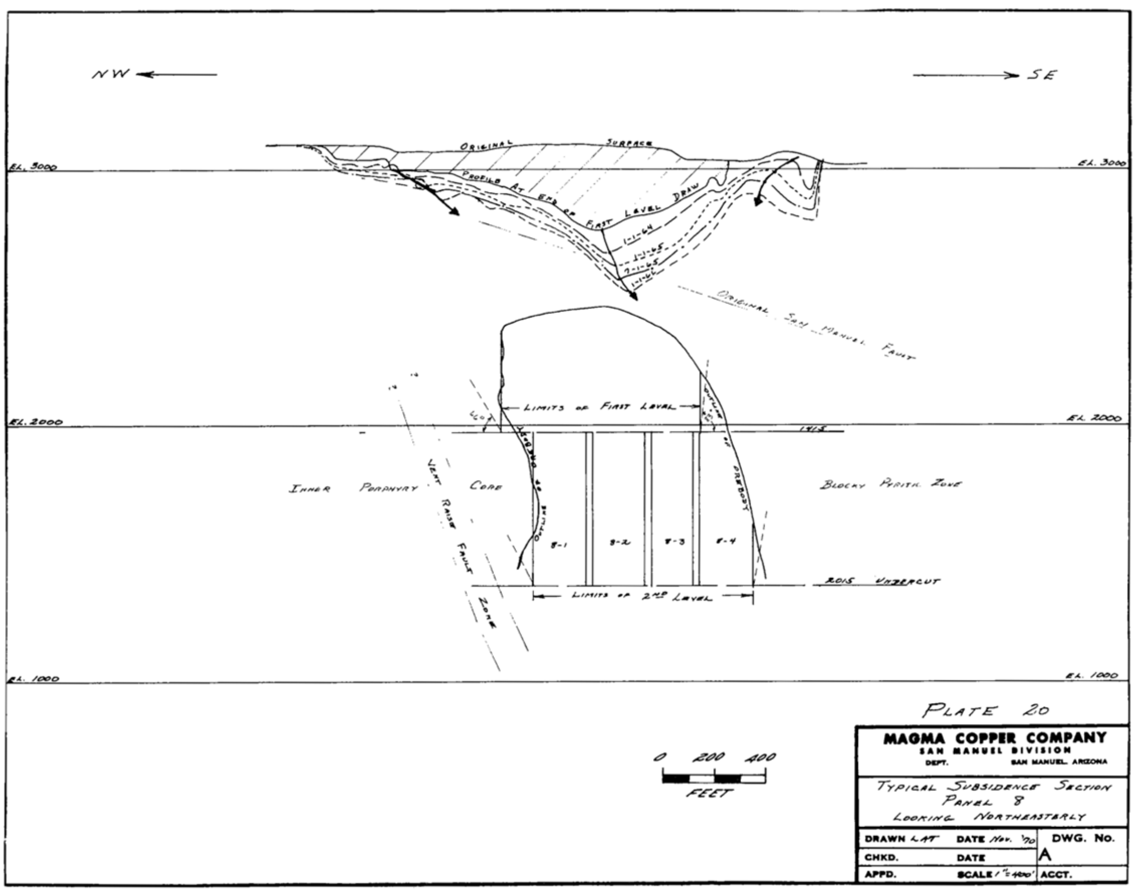
NW
SE
EL. 3000
ORIGINAL SURFACE
PROFILE AT END OF FIRST LEVEL DRAW
ORIGINAL SAN MANUEL FAULT
LIMITS OF FIRST LEVEL
EL. 2000
1415
INNER PORPHYRY CORE
VENT RAISE FAULT ZONE
BLOCKY PYRITIC ZONE
8-1
8-2
8-3
8-4
2015 UNDERCUT
LIMITS OF 2ND LEVEL
EL. 1000
PLATE 20
0 200 400
FEET
MAGMA COPPER COMPANY
SAN MANUEL DIVISION
DEPT.
SAN MANUEL, ARIZONA
TYPICAL SUBSIDENCE SECTION
PANEL 8
LOOKING NORTHEASTERLY
DRAWN LAT
DATE Nov. '70
DWG. No.
CHKD.
DATE
A
APPD.
SCALE 1"=400'
ACCT.

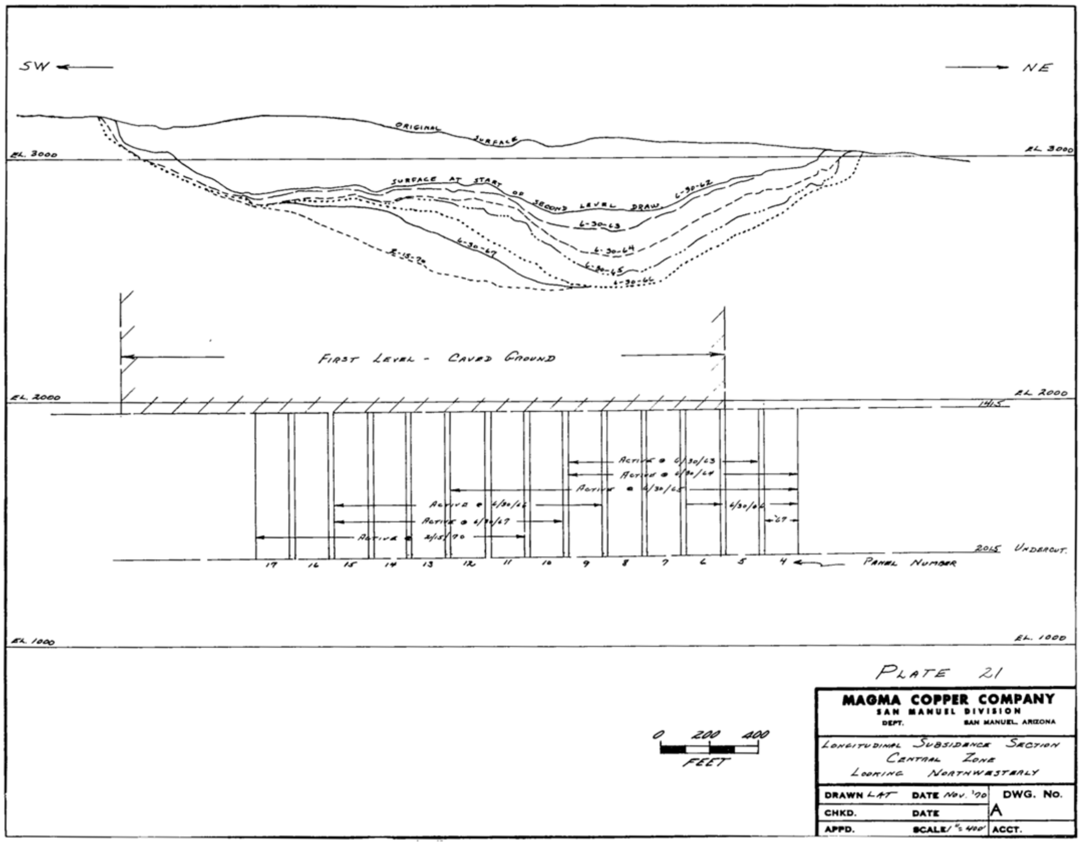

SW
NE
ORIGINAL SURFACE
EL. 3000
SURFACE AT START OF SECOND LEVEL DRAW 6-30-62
6-30-63
6-30-64
6-30-65
6-30-66
6-30-67
8-15-70
FIRST LEVEL - CAVED GROUND
EL. 2000
1415
2015 UNDERCUT
PANEL NUMBER
EL. 1000
PLATE 21
MAGMA COPPER COMPANY
SAN MANUEL DIVISION
DEPT.
SAN MANUEL, ARIZONA
LONGITUDINAL SUBSIDENCE SECTION
CENTRAL ZONE
LOOKING NORTHWESTERLY
0 200 400
FEET
DRAWN LAT DATE Nov. '70 DWG. No.
CHKD. DATE A
APPD. SCALE 1" = 400' ACCT.

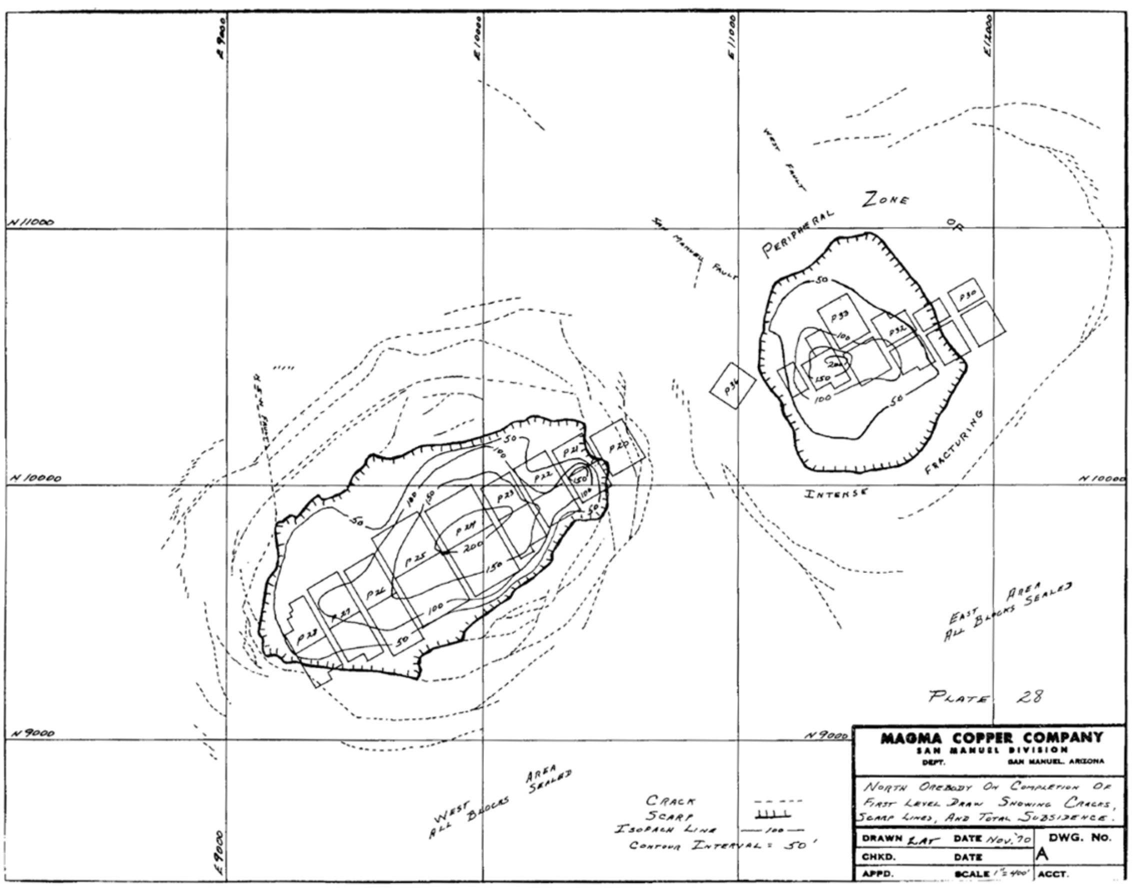

E 9000
E 10000
E 11000
E 12000
N 11000
N 10000
N 9000
WEST FAULT
SAN MANUEL FAULT
PERIPHERAL ZONE OF INTENSE FRACTURING
EAST AREA
ALL BLOCKS SEALED
WEST AREA
ALL BLOCKS SEALED
PLATE 28
CRACK
SCARP
ISOPACH LINE — 100 —
CONTOUR INTERVAL = 50'
MAGMA COPPER COMPANY
SAN MANUEL DIVISION
DEPT.
SAN MANUEL, ARIZONA
NORTH OREBODY ON COMPLETION OF FIRST LEVEL DRAW SHOWING CRACKS, SCARP LINES, AND TOTAL SUBSIDENCE.
DRAWN LAT DATE Nov. '70 DWG. No.
CHKD. DATE A
APPD. SCALE 1" = 400' ACCT.

Shabani (Zimbabwe)

Source: Wilson (2000)

Caving Period Reported: - 1999

Summary: Block caving and ground support practices at the Shabani asbestos mine are reported. Caving involves an inclined undercut dipping at an angle of approximately 30° from horizontal, with blocks being developed to target discrete, elongated pods of ore. No direct data is provided in the form of subsidence measurements, but a scaled cross-section is included that outlines the caving zone above two mined blocks (52 and 58) relative to the undercut level. An average depth of 630 m is shown for the dipping undercut.

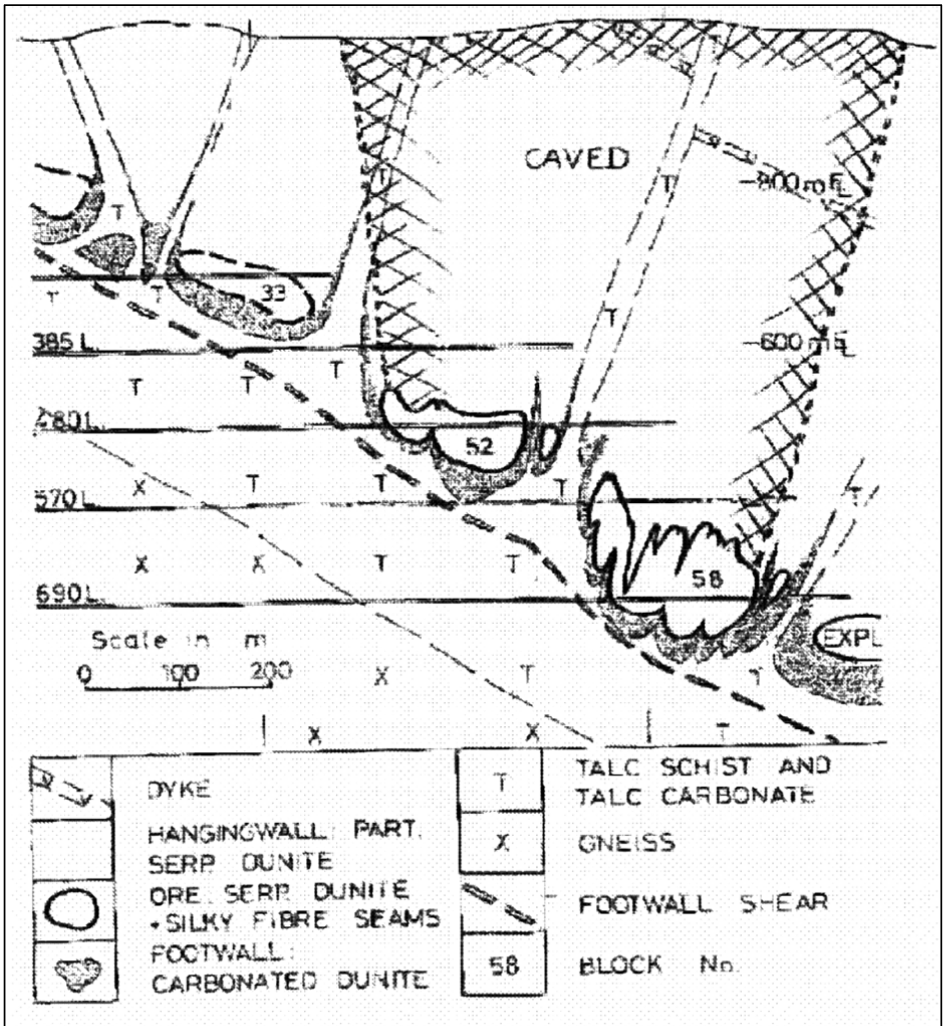

FIG 2 - Generalised cross-section through Shabanie mine.

Urad (Colorado, USA)

Source: Kendrik (1970)

Caving Period Reported: 1967-1969

Summary: Data is reported for panel caving from the 1100 Level of the Urad deposit. The height of the ore varies from 60 to 210 m and the overall depth varies from 120 to 300 m due to its position under a steep slope. Considerable pre-splitting and induction blasting was required to aid the caving process. A schematic drawing is provided from which the caving angle can be estimated assuming the sketch is to scale. Vertical boundary cut-off stopes were mined (shrinkage stoping) to limit the extent of the caving zone.

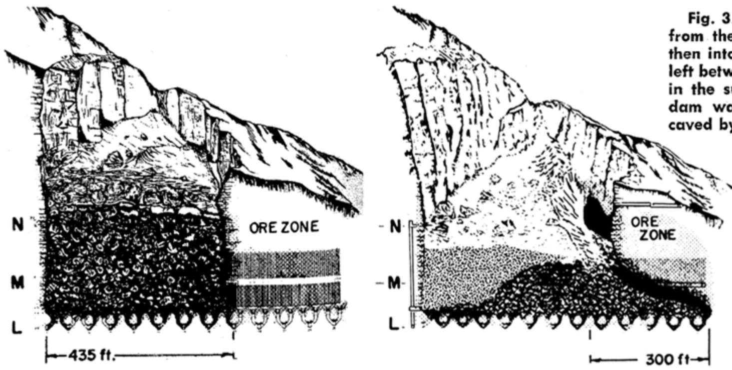

Fig. 3. In April 1969, to guard against dilution by waste from the top of the mountain into the subsided area and then into the undercut area, a dam of undrawn stopes was left between the old cave area and the new. This left a hump in the subsided area and stopped dilution. By August the dam was no longer effective and the unbroken ore was caved by a shot using 25,000 lb of ammonium nitrate